University of KwaZulu-Natal

Structural and kinetic studies of the ring opening polymerization of lactides and ε-caprolactone by (Benzimidazolylmethyl)amine Zn(II) and Cu(II) complexes

Nelson Worlanyo Attandoh

Structural and kinetic studies of the ring opening polymerization of lactides and ε-caprolactone by (Benzimidazolylmethyl)amine Zn(II) and Cu(II) complexes

By

Nelson Worlanyo Attandoh

BSc (Hon) Chemistry, (University of Ghana)

A thesis submitted in fulfilment of the requirement of the degree of

Master of Science

in

Chemistry

in the

School of Chemistry and Physics

University of KwaZulu-Natal

Supervisor: Dr Stephen O. Ojwach

March, 2014

DECLARATION

I hereby declare that this work, Structural and kinetic studies of the ring opening polymerization of lactides and ε-caprolactone by (Benzimidazolylmethyl)amine Zn(II) and Cu(II) complexes, is my original work and has never been submitted for the award of any form of degree in any university or institution and that all sources of information in the form of references and other sources used have been duly acknowledged.

Nelson Worlanyo Attandoh

(212561511)

……Date……

I hereby confirm that this thesis has been submitted for examination with my approval as a university supervisor.

……Date……

Dr Stephen O. Ojwach

(Supervisor)

DEDICATIONS

To my family and my sweetheart

ABSTRACT

The syntheses and structural characterization of Zn(II) and Cu(II) carboxylate complexes supported on benzimidazolyl amine ligands and their application in the ring opening polymerization of lactides and ε-caprolactone are reported. Synthesized derivatives of benzimidazole, N-(1H-benzimidazol-2-ylmethyl)aniline (**L1**), N-(1H-benzimidazol-2-ylmethyl)-2-methoxyaniline (**L2**), N-(1H-benzimidazol-2-ylmethyl)-2-bromoaniline (**L3**) and N-(1H-benzimidazol-2-ylmethyl)-2-aminothiophenol (**L4**) were reacted with Zn(II) and Cu(II) carboxylates to generate bimetallic complexes $[Zn_2(\mathbf{L1})_2(OBn)_4]$ (**1**), $[Zn_2(\mathbf{L2})_2(OBn)_4]$ (**2**), $[Zn_2(\mathbf{L3})_2(OBn)_4]$ (**3**), $[Zn_2(\mathbf{L4})_2(OBn)_4]$ (**4**), $[Cu_2(\mathbf{L1})_2(OBn)_4]$ (**5**), $[Cu_2(\mathbf{L3})_2(OBn)_4]$ (**6**), $[Cu_2(\mathbf{L1})_2(OAc)_2]$ (**9**) and monometallic complexes $[Zn(\mathbf{L1})_2(OAc)_2]$ (**7**) and $[Zn(\mathbf{L3})_2(OAc)_2]$ (**8**) in good yields. The complexes were characterized by mass spectrometry, IR spectroscopy, elemental analysis and single crystal X-ray diffraction for **3**, **6** and **8**. In addition, Zn(II) complexes (**1**-**4**, **7** and **8**) were characterized by NMR spectroscopy while the copper complexes (**5**, **6** and **9**) were characterized by magnetic moment measurements due to their paramagnetic nature. The magnetic moments measured for the copper complexes **5**, **6** and **9** were obtained as 1.85 BM, 1.86 BM and 2.12 BM respectively. The molecular structures of complexes **3**, **6** and **8** as established by single-crystal X-ray crystallography revealed ligands **L1**-**L4** are monodentate, binding *via* the N-atom of the benzimidazole. EPR spectra of the copper complexes **5** and **6** revealed that the paddle-wheel dimeric structures are retained in solution.

The catalytic activities of the complexes in the ring opening polymerization of ε-caprolactone (ε–Cl), $_{D,L}$-lactide ($_{D,L}$-LA) and $_{L}$-lactide ($_{L}$-LA) were investigated. All the complexes tested were active in the polymerization of both ε-caprolactone and lactides. Generally, zinc complexes were more active than their analogous copper complexes. The nature of the

carboxylate group also influenced the catalytic activities of the initiators. The acetate complexes showed higher activities than the corresponding benzoates. Catalyst activities of mononuclear complexes were also observed to be relatively higher compared to the binuclear complexes. Ligand architecture also influenced the activities of the complexes. The complexes bearing electron-withdrawing groups on their ligand motif showed lower activities compared to their corresponding complexes containing electron-donating groups. The lactide monomers showed greater reactivity compared to ε-caprolactone. The polymerization of the monomers proceeded via a pseudo-first order reaction pathway with respect to the monomer. All the tested complexes gave rise to moderate molecular weight polymers in the range of 2 000 to 12 700 g/mol and broad polydispersity index in the range of 1.29-3.64. The methine region of the ^{1}H and ^{13}C NMR of the polylactides revealed the polymerization of $_{L}$-lactide yielded isotactic polylactide while $_{D,L}$-lactide afforded predominantly atactic polymers. The tacticity of poly($_{D,L}$-lactide) indicates that the ligand architecture does not regulate the stereoselectivity of the complexes. From the analysis of the ^{1}H NMR spectra and MS-ESI data of ε-caprolactone and lactide polymers, the polymerization reaction proceeded via an activated-monomer mechanism.

TABLE OF CONTENT

TABLE OF CONTENT

LIST OF TABLES

LIST OF FIGURES

ABBREVIATIONS

Ac	Acetate
Ar	Aromatic
d	doublet
dd	doublet of doublet
$_{D}$-LA	$_{D}$-lactide
$_{D,L}$-LA	$_{D,L}$-lactide
ε-CL	ε-caprolactone
EPR	Electron paramagnetic resonance
GPC	Gel permeation chromatography
HRMS-ESI	High Resolution Mass Spectroscopy-Electron spray Ionization
I	Initiator
J	Coupling constant
Mn	number average molecular weight
Mw	weight average molecular weight
m	multiplet
meso-LA	*meso*-lactide
MS	Mass spectroscopy
NMR	Nuclear magnetic resonance
OBn	Benzoate
PDI	Polydispersity index
PCL	Poly(ε-caprolactone)
PLA	Polylactide
s	singlet
t	triplet

ACKNOWLEDGEMENTS

I hated every minute of training, but I said, 'Don't quit. Suffer now and live the rest of your life as a champion.'….Muhammad Ali

I am very grateful to my supervisor, Dr Stephen O. Ojwach for his remarkable tutelage, mentoring and unflinching support throughout my research; indeed your touch has been felt. I am indebted to Prof Orde Munro for the single crystal X-ray diffraction analysis of my crystals and to Dr Alex Xulu for the electron paramagnetic resonance of my compounds. To you, ever-willing Craig, no amount of words can express my appreciations for your time, tutoring and assistance. All I can say is thank you and God bless you. To all the members of the catalysis research group, I say thank you for making the lab a home-away-from-home and research worth through our interactions and engagements. The assistance from staff and friends in the department are highly appreciated. Colins is not forgotten for initiating the process. Most importantly the financial support from the University of KwaZulu-Natal and the research-friendly environment created by staff and fellow researchers within the department of chemistry is highly appreciated. My gratitude also goes to my family and you, Dorinder, for your unflinching support and counsel throughout my study and pray for your continuous support as I prepare for the final stage. Last but not the least; I thank the Almighty God for His grace, guidance and protection throughout my study.

Chapter One

Synthesis, properties and applications of polylactides and polycaprolactones

1.1 General Introduction

Aliphatic polyesters obtained from renewable resources like beet and corn have attracted significant research interest from academia and industries due to their biodegradable, biocompatible and bioadsorbable properties.[1] These properties have given them an edge over conventional petroleum-based plastics which are non-degradable, hence drawing health and environmental concerns. For instance polyethylene and polypropylene used for commodity plastics are all derived from petroleum sources and persist in the environment for years after disposal. Gaseous and particulate emission during incineration as a waste management option only goes to worsen public health and also contribute to global warming.[2] Furthermore, the over dependence on dwindling fossil fuel reserves and the consequent rise in price of crude oil has stimulated the search for alternate and sustainable biodegradable polymeric materials that would mitigate these rising environmental and health concerns.[3]

Aliphatic polyesters have been identified as suitable substitutes due to the presence of ester linkers that can be cleaved hydrolytically and/ or enzymatically to yield smaller environmentally-friendly units containing carboxylic and hydroxyl chain ends.[4] In addition, the ease of handling and processing makes them attractive for structural fabrication.[5,6] Poly(lactides) (PLAs) and poly(ε-caprolactones) (PCLs) are amongst the few known aliphatic polyesters that are being considered as potential substitutes to the conventional plastics due to their properties. Over the years, the physical, mechanical and degradable properties of these polyesters have been considerably exploited in the area of tissue engineering to design scaffold materials that are combined with stem cells to grow tissues for organs under suitable

conditions.[2] They are also used for other biomedical related applications. Beside biomedical application, these polyesters have also witnessed extensive application in the pharmaceutical, agriculture, textiles and packaging fields.

1.2 Polylactides

Polylactides (PLAs) are mainly obtained from the ring opening polymerization of the monomer lactide. Lactides are dimeric compounds obtained from optically active lactic acids produced from the fermentation of starch and other polysaccharides available from corn, beets, sugar cane and other biomass. Lactic acid has two possible conformations depending on the arrangement of substituents on the chiral carbon atom. These different conformations give rise to the three different diastereomers of lactides (Figure 1-1). The most commercially available however is $_{L}$-lactide and *meso*-lactide.[7]

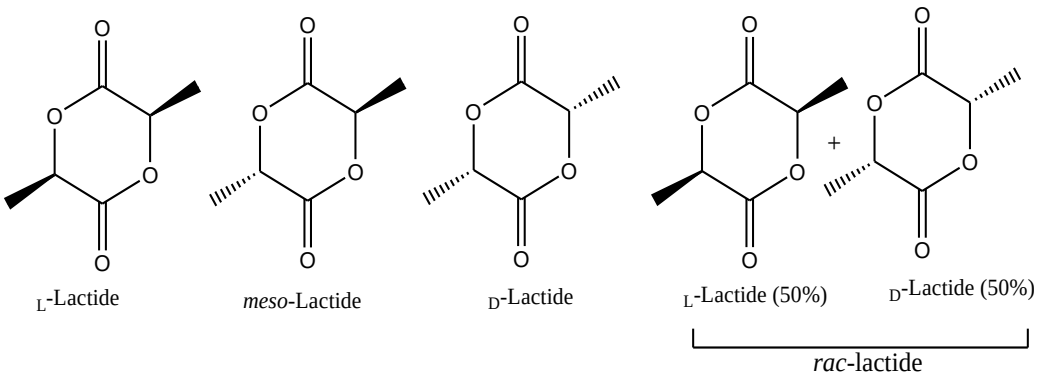

Figure 1-1 Diastereomers of lactides

Properties of PLAs depend on the stereochemistry within the polymer backbone and the molecular mass of the polymer.[8] Physical, thermal, solubility and other properties of PLAs vary depending on the enantiopurity of the monomers which also determine the stereochemical makeup of the polymer backbone. A typical PLA melts between 130 - 180 ^{o}C and their glass transition temperature ranges from 50 - 80 ^{o}C.[9] Amorphous poly(*meso*-lactide) has relatively lower melting and glass transition temperature while the analogous poly($_{L}$-

lactide) or poly($_D$-lactide) exhibit high glass transition and melting temperatures as a result of high crystallinity.[10] Most PLAs are soluble in dioxane, acetonitrile and chlorinated solvents like chloroform and dichloromethane but partially soluble in toluene, acetone and tetrahydrofuran at room temperature.[9]

1.2.1 Stereochemistry of Polylactides

The eventual applications of polylactides depend on their physical properties which rely principally on the sequence of the stereocenters. The stereochemistry also influences the rate of biological and chemical degradation. Besides the type of monomers, the nature of the polymerization catalyst as well as the chain end group contributes significantly in determining the stereosequence of the polymer.[11] The arrangement of repeat units in a stereosequence determines the tacticity of the polymer. For instance when the configuration of the repeat unit in a stereosequence are relatively similar, the microstructure of the polymer is described as isotactic while polylactides with syndiotactic microstructure exhibit chronologically opposite configuration in the stereosequence. Other possible microstructures observed in polylactides are presented in Scheme 1-1.

Over the past years, the high cost of PLA production limited their use to medical application but recent technological advances has lowered the production cost thereby diversifying their applications into packing sectors and other high polymer consuming fields. PLAs usage has increased over the years and is expected to further increase with an estimated annual growth rate of 19%.[12] This rise in production is based on the installation of 140,000 tonnes/year facility by Cargill Dow LLC and over 150,000 tonnes/year facility by Natureworks^{TM} LLC in the United States.[12]

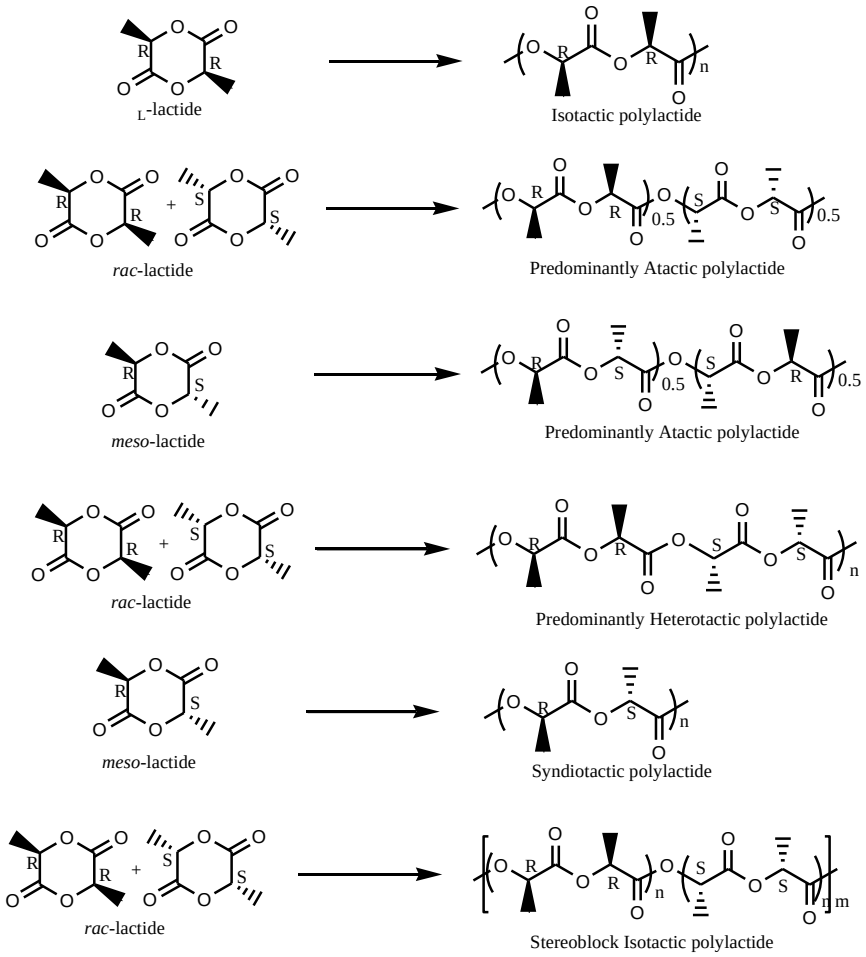

Scheme 1-1

1.3 Polycaprolactone (PCL)

Polycaprolactones are another set of important biocompatible polyesters derived from the ring opening polymerization of the monomer, ε-caprolactone which is synthesized by the oxidation of cyclohexanone with hydrogen peroxide or peracetic acid in a Bayer-Villiger reaction process (Scheme 1-2).[13] There are also reports of synthesizing this monomer from renewable sources like starch.[14]

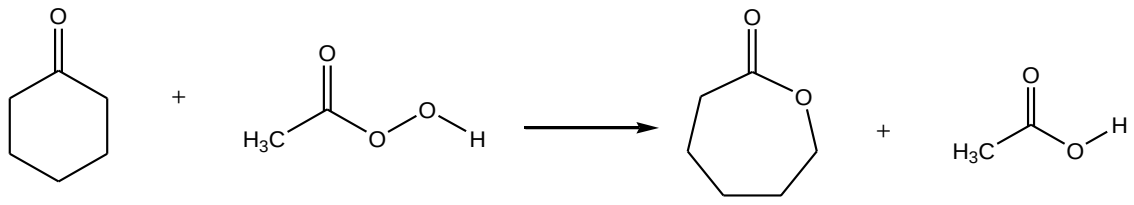

Scheme 1-2

PCLs are amorphous in nature, have a glass transition temperature of -60 ^{o}C and melts in the range of 59 – 64 ^{o}C. Like all other aliphatic polyesters, their physical and other properties are determined by the molecular structure thereby directing the usage of the polymer. PCLs have a waxy feel and tensile modulus similar to low density polyethylene due to the long methylene group in the monomer units.[15] They can also be easily blended with other biodegradable and non-degradable polymers to improve their properties for enhanced performance. For instance they are blended with polyvinyl chlorides (PVC), chlorinated polyethylene (PE) and bisphenol A polycarbonate to function as plasticizers.[16] PCLs are very soluble in chloroform, dichloromethane, carbon tetrachloride, benzene, toluene, cyclohexanone and 2-nitropropane at room temperature.[17] Though ε-caprolactone is synthesized from compounds sourced from crude oil the polymers, PCLs, are however biodegradable. They undergo thermal, hydrolytic and enzymatic degradation under favorable conditions which could take few months to several years depending on the molecular weight and degree of crystallinity. During thermal degradation for instance, high temperatures result in specific chains scission whilst random scission is observed at lower temperatures.[18]

1.4 Application of Polylactide (PLA) and Polycaprolactone (PCL)

Over the years, the biodegradability, biocompatibility, mechanical and physical properties of these polyesters have been exploited to provide relief for human in the area of biomedicine, pharmacy and environmental management. The more versatile of these two polyesters, PLAs, has attracted significant industrial and academic research interest; nonetheless, both polymers are produced on a commercial scale.[19]

These polyesters are used to produce biomaterials like tissue scaffolds, medical sutures, pins, screws and surgical sponges that are indispensable in biomedicine.[20]For instance, Saim *et*

al.[21] reported the successfully growth of autologous cells on polylactide scaffolds and used as implants for treating ear defects. Small intestine and bone tissues were also grown from stem cells incorporated into polymer scaffolds.[22]

Besides tissue regeneration, PLAs and PCLs play critical roles in the pharmaceutical sector as drug delivery vehicles/ agents. Drug delivery agents are biodegradable polymers that are used to deliver drugs to targeted cells in the body without affecting healthy cells in the body. They are normally permeable to cell membranes and not cytotoxic.[23] Liu *et al.*[24] reported the copolymerization of PLAs and PCLs with other biodegradable polymers to form polymersomes that are capable of encapsulating and delivering drugs or chemicals to target sites. In other spheres, anticancer drugs and non-toxic gene carriers have been successfully delivered to target sites using polymers serving as drug delivery agents.[25] PCLs and PLAs have also being used in the formulation of polymer nanoparticles that serve as drugs delivery agents in the body.[26]

PCLs and PLAs are being targeted for packaging materials to substitute synthetic plastics in an attempt to reduce the environmental crisis posed by continuous use of these non-degradable materials. Large volumes of plastic wastes are generated when short shelf-life products are packaged in commodity polymers which are currently managed by incineration or land filling. However, with the dwindling availability of land fill sites and release of toxins like dioxins into the atmosphere on incineration, the use of biodegradable polymers is a suitable alternative.[27] For instance PCLs are modified and used as films for packaging food to prevent oxidation and microbial growth thereby extending the shelf life of the food.[28] They are also blended with starch to produce refuse collection bags. PLAs are also used in forming containers and films for short-shelf-life products.[14]

1.5 Synthesis of PCLs and PLAs

PCLs and PLAs are synthesized mainly by metal-catalyzed ring-opening polymerization (ROP) of their respective monomers to form larger molecular weight aliphatic polymers. Besides this method, PLAs can also be synthesized through polycondensation polymerization under varying reaction conditions outlined below.

1.5.1 Direct polycondensation polymerization of lactides

This reaction is carried out in bulk or in solution using lactic acid and a Bronsted or Lewis acid catalyst under reduced pressure to produce PLA. The bulk polymerizations are preferred to solutions due to associated flammability of solvents, toxicity and difficulty in removal from the polymer. This synthetic approach results in low molecular weight polymers with inferior mechanical properties due to the lack of control over the stereochemistry of the lactic acids during the reaction.[29] However, these low molecular weight polymers can be modified to form high molecular weight polymers by reacting them with other monomers to form copolymers or by employing a chain-coupling agent to join the low/short polymer chains.[13]

1.5.2 Azeotropic condensation polymerization of lactides

Azeotropic condensation polymerization entails the conversion of lactic acid to polylactide in a low boiling point organic solvent using highly reactive Lewis acid catalysts. The condensation by-product, water, is removed from the system azeotropically to give high molecular weight polymers. The method gives relatively high molecular weight polymers with good molecular weight distribution due to the low temperatures that limit side reactions.

1.5.3 Solid state polymerization of lactides

Solid state polymerization involves the simultaneous heating of a solid or semi-crystalline pre-polymer below its melting point while removing by-products from the material under reduced pressure or blowing an inert gas. The reaction is carried out in bulk and the temperatures are adjusted to allow the chain growth. This mode of polymerization gives rise to relatively high molecular weight polymers and improved mechanical properties due to the control of polymer tacticity during the reaction. This is facilitated by the low temperatures under which the reactions preceded.[13]

Polycondensation reactions do not favor the synthesis of PCLs. The challenges encountered in the polymerization *via* this route make these less attractive.[30]

1.5.4 Ring opening polymerization (ROP) of lactide (LA) and ε-caprolactone (ε-CL)

ROP is the most convenient method for synthesizing polyesters from smaller cyclic esters such as LAs and ε-CLs[31] to yield high molecular weight polymers as a result of the non-generation of leaving groups that can limit monomer conversion or degree of polymerization.[32] The process is enthalpy-controlled and involves the opening of cyclic ester monomers to form linear polymers which relieves the angle-strain in the ring.[33] ROP has been found to give higher molecular weight polymers with low molecular weight distribution and also give rise to good stereoregular PLAs.[34] This mode of polymerization was first demonstrated by Carothers *et al*.[35] in 1932 when they attempted to analyze the reversible polymerization of cyclic esters. Since its discovery, a lot of research has gone into designing catalyst that could initiate and improve upon polymerization process *via* this mechanism.

The ROP of lactide and ε-caprolactone proceeds in four different ways and this classification has been based on the nature of the initiator and the reaction mechanism. The methods identified include anionic, cationic, enzymatic and coordination-insertion mechanism.

1.5.4.1 Anionic polymerization

The anionic ROP involves the attack of the carbonyl group of the monomer by a nucleophilic ion, an initiator, resulting in cleavage of the bond between the carbonyl carbon and the endocyclic oxygen. The cleavage transforms the endocyclic oxygen into an ion which initiates the propagation (Scheme 1-3).[36] The suitable initiators for anionic polymerization include alkali metal alkoxides, alkali metals, alkali metal naphthalenide complexes with crown ethers.[37] The polymerization reaction using these complexes could be living or non-living depending on the reaction conditions.[38]

Anionic mode of polymerization is saddled with drawbacks that make it unsuitable for synthesizing high molecular weight PLAs and PCLs. The highly nucleophilic propagating alkoxide has a tendency of deprotonating the monomer (lactides) in the α-position which leads to racemization.[23] Furthermore, the highly active propagating alkoxide at high temperatures could also attack the carbonyl of a growing chain, a process referred to as intra or intermolecular backbiting. Backbiting, racemization and other side reactions consequently affect the final molecular properties of the polymer.

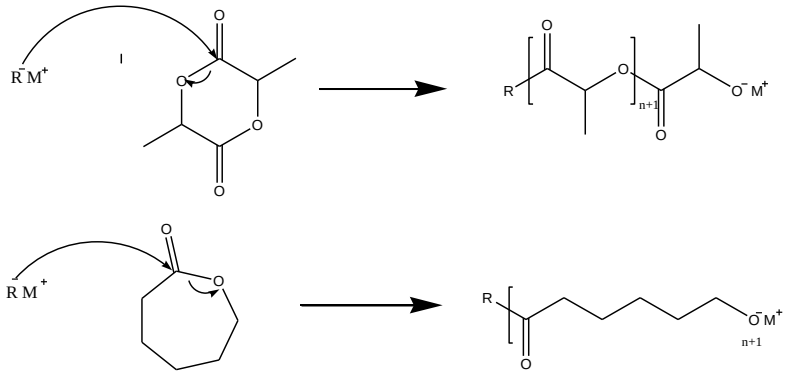

Scheme 1-3

1.5.4.2 Cationic polymerization

Cationic polymerization occurs with the initial transformation of a neutral monomer to cationic species and a subsequent attack by the carbonyl oxygen of another monomer to cleave the acyl–oxygen bond (Scheme 1-4). Suitable catalysts/initiators for cationic polymerization include strong acids and carbenium ion donors like triethyloxonium tetrafluoroborate, borontrifluoride, and trifluoroacetic acid.[39] Other organocatalysts that can polymerize LAs and ε-CLs include diphenylammonium triflate (DPAT), $HCl{\cdot}Et_2O$, phosphazene bases, Bredereck's reagents, pyridine-base organic compounds, phosphine compounds and N-heterocyclic carbenes.[40]

The polymerization begins with the initial protonation or alkylation of the carbonyl oxygen of a monomer by the catalyst to form a positively charged molecule. The resultant positively charged O–CH bond is then attacked by a second monomer to cleave this bond and form another carbanium (Scheme 1-4). The chain propagation is terminated by the presence of a monofunctional nucleophile like water.[41] Cationic polymerization of lactides at high temperatures results in racemization which affects the mechanical and physical properties of the polymer. However, this can be minimized at lower temperature conditions ($\leq 50\ ^{o}C$) but

lowering the temperature slows down the rate of reaction and gives rise to polymers with low molecular weight.[14]

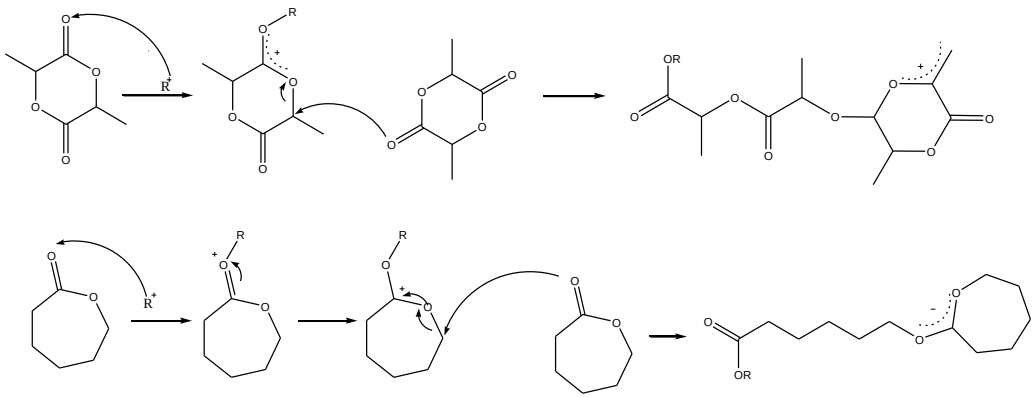

Scheme 1-4

1.5.4.3 Enzymatic polymerization

Enzymatic polymerization involves the use of biologically active microorganisms for the ring opening of cyclic ester monomers. This method was necessitated by the quest to synthesized metal-free polymers that are used in biological systems and also produce polymers that are difficult to synthesize using the conventional polymerization methods.[42]Furthermore, the high regio- and stereoselectivity of enzymes, their high activity under mild conditions and product purity makes them suitable for synthesizing polymers that are biodegradable and used for biological applications.[43] The enzyme Lipase has been identified as an efficient enzymatic catalyst for the ROP of lactones by hydrolyzing the ester group in the monomer.[44] For instance, the enzyme *Candida cylindracea* (lipase CC), *Pseudomonas cepacia* (lipase PC) and PPL were found to be active in the bulk polymerization of $_{D}$-lactide, $_{L}$-lactide and $_{D,L}$-lactide to afford polymers with molecular weight ranging between 8 000 to 270 000.[45] Other lipase enzymes include lipase CA (*Candida Antarctica*), lipase CC (*Candida cylindracea*), lipase PF (*Pseudomonas fluorescens)* and *Rhizopus japonicus* lipase (lipase RJ). Besides

lipase enzymes, there are other non-lipase enzymes like Humicola Insolens Cutinase (HIC) which are also active in the polymerization of cyclic esters.[20]

Lipase-catalyzed polymerization proceeds *via* a monomer-activated mechanism (Scheme 1-5), where the enzyme is attached to the monomer through its active site, serine residue, and open the ring to from an acyl-enzyme complex. The polymerization is initiated by a nucleophilic attacked on the acyl-enzyme complex by water molecule in the enzyme to form an oxyacid. The propagation stage involves the reaction of the intermediate with the terminal hydroxyl group of the polymer to form a polymer that is extended by a unit.[46] Though enzyme-catalyzed polymerization is able to give rise to pure and biodegradable polymers, the method is saddled with low molecular weight polymers, long reaction time and requires higher amount of enzymes to yield high molecular weight polymers.

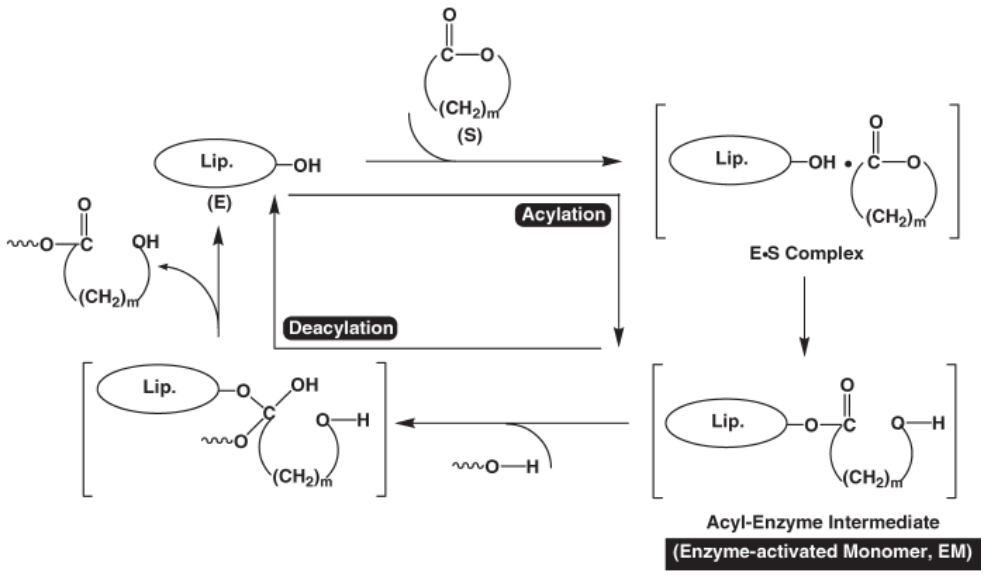

Scheme 1-5[30]

1.5.4.4 Monomer activated mechanism

Monomer activated ROP mechanism proceeds with the activation of the monomer through the attachment of a Bronsted acid, a proton or a nucleophile such as N-heterocyclic carbenes

to the carbonyl of the monomer. This renders the C-atom of the carbonyl group highly electrophilic and susceptible to a nucleophilic attack from a hydroxyl group (Scheme 1-6).[47]

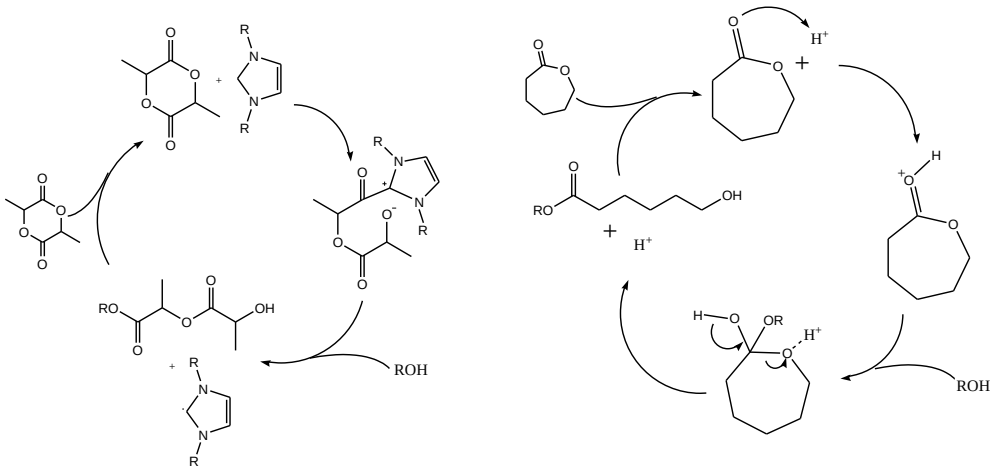

Scheme 1-6

1.5.4.5 Coordination insertion mechanism

Coordination insertion mechanism is the most common route for the ROP of lactides, ε-caprolactone and other cyclic ester monomers using metal alkoxides or carboxylates, as catalysts. In this method, the substrate or the monomer coordinates to the metal centre and the alkoxides or carboxylates serve as initiators. The coordination of the metal with a monomer is facilitated by the presence of empty *p, d* or *f* orbitals with favorable energy level.[17,26,48] The metal centre functions as a Lewis acid and bond weakly to the oxygen atom of the carbonyl. This enhances the electrophilicity of the carbonyl group on the monomer and nucleophilicity of the metal carboxylate or alkoxide on the initiator. The coordination is followed by the cleavage of the acyl–oxygen bond of the monomer and the chain formed is inserted into the metal–oxygen bond of the initiator (Scheme 1-7).[17,14,49,50] Polymerization through coordination insertion mechanism has been identified as one of the most efficient methods in synthesizing high molecular weight polymers with well controlled molecular weight distribution. The mechanism also results in stereoregular polymers (in the case of PLA) and

limits side reactions that are inevitable in the other routes.[51] However, long reaction time and high temperatures may result in intra- and intermolecular transesterification leading to broad molecular weight distribution index.[26]

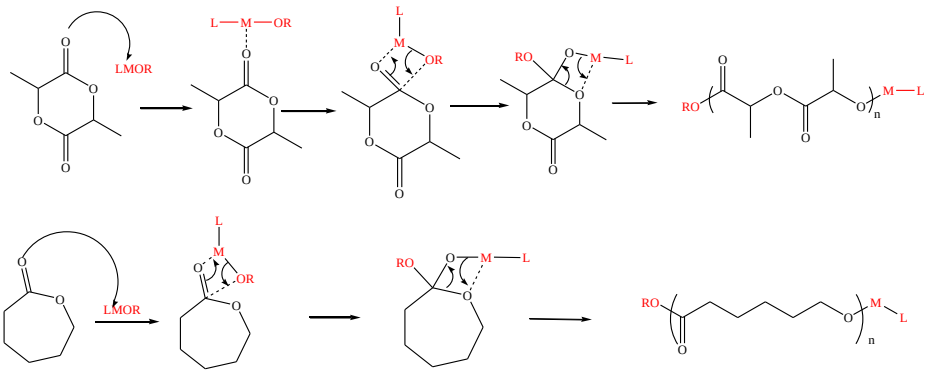

Scheme 1-7

1.6 Challenges of ROP of PLAs and PCLs

Transesterification is the major side reaction that saddle ROP of polyesters resulting in polymers with high polydispersity index (PDI) and low molecular weight. Transesterification is controlled by temperature, reaction time and the type and catalyst concentration.[52] The process can occur within a growing chain, intramolecular, or between chains, intermolecular esterification (Scheme 1-8).

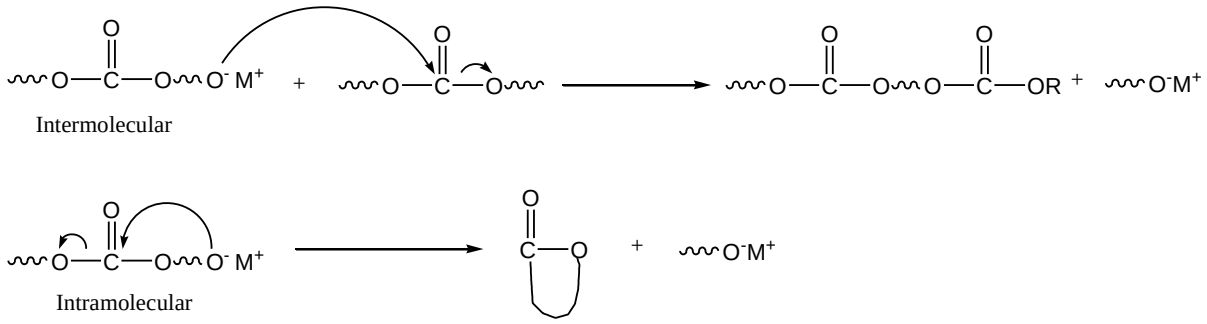

Scheme 1-8

References

[1] Wheaton, C.A.; Hayes, P.G.; Ireland, B.J. *Dalton Trans*. **2009**, 4832 – 4846.

[2] Rem, P. C.; Olsen, S.; Welink, J. H.; Fraunholcz, N. *Environ. Eng. Manage. J.* **2009**, *8*, 975-980.

[3] (a) Ragauskas, A. J.; Williams, C. K.; Davison, B. H.; Britovsek, G.; Cairney, J.; Eckert, C. A.; Frederick Jr., W. J.; Hallett, J. P.; Leak, D. J.; Liotta, C. L.; Mielenz, J. R.; Murphy, R. Templer, R.; Tschaplinski, T. *Science*, **2006**, *311*, 484 – 489. (b) Chen, G.-Q.; Patel, M.K. *Chem. Rev.* **2012,** *112*, 2082–2099.

[4] (a) Thomas, C. M.; Lutz, J.-F. *Angew. Chem., Int. Ed.* **2011**, *50*, 9244–9246. (b) Mochizuki, M.; Mukai, K.; Yamada, K.; Ichise, N. Murase, S.; Iwaya, Y. *Macromolecules* **1997,** *30*, 7403-7407.

[5] Lavik, E.; Langer, R. *Appl. Microbiol. Biotechnol*. **2004**, *65*, 1–8. (b) Seal B.L.; Otero, T.C.; Panitch, A. *Mater. Sci. Eng.* **2001,** *34*, 147-230.

[6] Drumright, R. E.; Gruber, P. R.; Henton, D. E. *Adv. Mater*. **2000**, *12*, 1841 - 1846.

[7] Kricheldorf, H.R. *Chemosphere* **2001**, *43*, 49-54.

[8] (a) Perego, G.; Cella, G.D.; Bastioli, C. *J. Appl. Polym. Sci.* **1996**, *59*, 37- 43. (b) Stoclet, G.; Seguela, R.; Lefebvre, J. M.; Li, S.; Vert, M. *Macromolecules* **2011**, *44*, 4961–4969.

[9] Auras, R.; Harte, B.; Selke, S. *Macromol. Biosci.* **2004**, *4*, 835–864.

[10] Garlotta, D. *J. Polym. Environ.* **2001**, *9*, 63–84.

[11] (a) Chamberlain, B. M.; Cheng, M.; Moore, D.R.; Ovitt, T.M.; Lobkovsky, E.B.; Coates, G.W. *J. Am. Chem. Soc.* **2001,** *123*, 3229-3238. (b) Kasperczyk, J.E. *Polymer* **1999**, *40*, 5455-5458.

[12] Leibfarth, F. A.; Moreno, N.; Hawker, A.P.; Shand, J.D. *J. Polym. Sci., Part A: Polym. Chem.* **2012**, *50*, 4814-4822.

[13] Flieger, M.; Kantorová, M.; Prell, A.; Řezanka, T.; Votruba, J. *Folia Microbiol.* **2003,** *48*, 27–44.

[14] Minami, M.; Kozaki, S. US patent 2003/6531615 B2, **2003.**

[15] Yoshito, I.; Hideto, T. *Macromol. Rapid Comm.* **2000**, *21*, 117 – 132.

[16] Albertsson, A.-C.; Varma, I. *Adv. Polym. Sci.* **2002**, *157*, 1- 40.

[17] Sinha, V. R.; Bansal, K.; Kaushik, R.; Kumria, R.; Trehan, A. *Int. J. Pharm.* **2004**, *278*, 1–23.

[18] Djonlagic, J.; Nikolic, M. S. 2011, *A Handbook of Applied Biopolymer Technology: Synthesis* **2011**, 149-196.

[19] Gross, R.A.; Kalra, B. *Science* **2002**, *297*, 803 -807.

[20] Middleton, J.C.; Tipton, A.J. *Biomaterials* **2000**, *21*, 2335-2346.

[21] Saim, A.B.; Cao, Y.L.; Weng, Y.L.; Chang, C.N.; Vacanti, C.A.; Vacanti, M.A.; Eavey, R.D. *Laryngoscope* **2000**, *110*, 1694-1697.

[22] (a) Hori, Y.; Nakamura, T.; Kimura, D.; Kaino, K.; Kurokawa, Y.; Satomi S.; Shimizu, Y.; *J. Surg. Res.* **2002**, *102*, 156–160. (b) Gao, J.; Dennis, J.; Solchaga, L.; Awadallah, A.; Goldberg, V.; Caplan, A.; *Tissue Eng.* **2001**, *7*, 363–371.

[23] Ikada, Y.; Tsuji, Y. *Macromol. Rapid Commun.* **2000**, *21*, 117–132.

[24] Liu, G.-Y.; Chen, C.-J.; Ji, J. *Soft Matter* **2012**, *8*, 8811–8821.

[25] (a) Hua, C.; Dong, C.-M.; Wei, Y. *Biomacromolecules* **2009**, *10*, 1140–1148. (b) Li, Y.; Cui, L.; Li, Q.; Jia, L.; Xu, Y.; Fang, Q.; Cao, A. *Biomacromolecules* **2007**, *8*, 1409-1416.

[26] Roger, M.; Clavreul, A.; Venier-Juliennea, M.C.; Passirani, C.; Montero-Menei, C.; Menei, P. *Biomaterials* **2011**, *32*, 2106-2116. (b) Bernardi, A.; Braganhol, E.; Jäger, E.; Figueiróa, F.; Edelweiss, M.I.; Pohlmannb, A.R., Guterres, S.S.; Battastini, A.M.O. *Cancer Letters* **2009**, *281*, 53–63.

[27] Luckachan,G.E; Pillai, C.K.S. *J Polym Environ* **2011**, *19*, 637–676.

[28] Joseph, C.S.; Prashanth, K.V.H; Rastogi N.K.; Indiramma, A.R.; Reddy, S.Y.; Raghavarao, K.S.M.S. *Food Bioprocess Technol*. **2011**, *4*, 1179–1185.

[29] Gupta, A.P.; Kumar, V. *Eup. Polym. J.* **2007**, *43*, 4053-4074.

[30] Djonlagi, J.; Nikolic, M.S. *RSC Green Chemistry* **2011**, *12*, 149-196.

[31] Strandman, S.; Gautrot, J.E.; Zhu, X. X. *Polym. Chem*. **2011**, *2*, 791–799.

[32] Arumugasamy, S.K.; Ahmad, Z. *Asia-Pac. J. Chem. Eng.* **2011,** *6***,** 398–405.

[33] O'Keefe, B.J.; Hillmyer, M.A.; Tolman, W.B. *J. Chem. Soc., Dalton Trans*. **2001**, 2215–2224.

[34] (a) Dechy-Cabaret, O.; Martin-Vaca, B.; Bourissou, D. *Chem. Rev*. **2004**, *104*, 6147–6176. (b) Thomas, C. M. *Chem. Soc. Rev.* **2010**, *39*, 165- 173. (c) Mazzeo, M.; Tramontano, R.; Lamberti, M.; Pilone, A.; Milione, S.; Pellecchia, C. *Dalton Trans.* **2013,** *42*, 9338-9351.

[35] Carothers, W.H.; Dorough, G.L.; Van Natta F.J. *J. Amer. Chem. Soc*. **1932**, *54*, 761-772.

[36] Stridsberg, K. M.; Ryner, M.; Albertsson, A.-C. *Adv. Polym. Sci*. **2002**, *157*, 41–65.

[37] Kricheldorf, H.R.; Kreiser-Saunders, I. *Makromol. Chem.* **1990**, *191*, 1057 - 1066.

[38] Albertsson, A.-C.; Varma, I.K. *Biomacromolecules* **2003**, *4*, 1466 – 1486.

[39] Tang, Z.; Chen, X.; Liang, Q.; Bian, X.; Yang, L.; Piao, L.; Jing, X. *J. Polym. Sci. Part A: Polym. Chem.* **2003**, *41*, 1934 – 1941.

[40] Kamber, N.E.; Jeong, W.; Waymouth, R.M.; Pratt, R.C.; Lohmeijer, B. G. G.; Hedrick, J. L. *Chem Rev.* **2007**, *107*, 5813 – 5840.

[41] Kricheldorf, H. R.; Dunsing, R. *Makromol. Chem.* **1986**, *187*, 1611–1625.

[42] Kobayashi, S.; Uyama, H. ; Namekawa, S.; Hayakawa, H. *Macromolecules* **1998,** *31*, 5655–5659.

[43](a) Matsumura, S.*; Macromol. Biosci.* **2002**, *2,* 105-126. (b) Panova, A.A.; Kaplan, D.L. *Biotechnol. Bioeng.* **2003**, *84*, 103 -113.

[44]Kobayashi, S.; *Macromol. Symp.* **2006**, *240*, 178–185.

[45](a) Matsumura, S.; Mabuchi, K.; Toshima, K. *Macromol. Rapid Commun.* **1997**, *18*, 477-482. (b) Matsumura, S.; Mabuchi, K.; Toshima, K. *Macromol. Symp.* **1998**, *130*, 285 - 304.

[46](a) Kobayashi, S.; Takeya, K.; Sudu, S.; Uyama, H. *Macromol. Chem. Phys.* **1998**, *199*, 1729-1736. (b) Kobayashi, S. *J. Polym. Sci. Part A: polym. Chem.* **1999**, *37*, 3041–3056.

[47] (a) Platel, R.H.; Hodgson, L.M.; Williams, C.K. *Polym. Rev.* **2008,** *48*, 11-63. (b) Kim, M. S.; Seo, K. S.; Khang, G.; Lee, H. B. *Macromol. Rapid Commun.* **2005**, *26*, 643–648.

[48] Kowalski, A.; Duda, A.; Penczek, S. *Macromolecules* **2000**, *33*, 7359–7370.

[49] Thomas, C. M. *Chem. Soc. Rev.* **2010**, *39*, 165–173.

[50] Stridsberg, K.M.; Ryner, M.; Albertsson, A.-C.; *Adv. Polym. Sci.* **2002,** *157*, 42-65.

[51] Arbaoui, A.; Redshaw, C. *Polym. Chem.* **2010**, *1*, 801 – 826.

[52] Dubois, P.; Ropson, N.; Jerome, R.; Teyessie, P. *Macromolecules* **1996**, *29*, 1965 -1970.

Chapter Two

Literature review of metal catalyzed ROP of lactide and ε-caprolactone

2. 1 Introduction to metal complexes (Organometallics)

Metal complexes are the most convenient and preferred catalyst systems for the ROP of lactides and ε-caprolactones following their discovery by Kleine.[1] Their attractiveness is due to their high rates of reaction, good degree of polymerization, better control of polymer stereochemistry (lactide polymerization) and their ability to favor block and co-polymer productions.[2] This group of catalysts has been transformed over the years from homoleptic form (MOR) to heteroleptic form (L_nMOR) with the inclusion of well defined ligand systems. This has resulted in better selectivity and enhanced catalytic activities for the polymerization reactions.[3] Though homoleptic complexes form more active catalysts, they normally lack control over the molecular weight distribution due to the many initiating groups that are capable of attacking the growing chain. They also lack stereocontrol and exhibit complex kinetics making characterization difficult. The many alkoxide groups also result in the initiation and growing of multiple chains per metal centre.[4] One example of homoleptic complex is the tin(II) bis(ethylhexanoate), $Sn(Oct)_2$, widely used as an industrial catalyst for PLA, PCL and other polyester syntheses.[5] Other examples include alkali metal alkoxides[6] and alkyls[7], aluminum alkoxide,[8] tin(II) alkoxide[9] and lanthanide alkoxides.[10]

Consequently, heteroleptic complexes in the form of well-defined single-site catalysts capable of controlling polymer molecular weight and distribution and the stereochemistry have been the focus of current research. These compounds have their metal centers coordinated by single or multidentate ligands containing nitrogen and/ or oxygen donor atoms to control the stability and reactivity of the metal complexes; eventually, improving the polymerization products. Mazzeo *et al.*[11] demonstrated this by introducing suitable ligands

on some group three metal alkoxides to form their corresponding heteroleptic complexes. These complexes were observed to reduce inter and intramolecular transesterification and improve the molecular weight distribution in the polyesters.

2.1.1 Alkali and Alkaline earth complexes as ROP initiators

Complexes of these metals have recently attracted research interest due to their low toxicity, high reactivity and low cost. Despite their high activity, they do not control the molecular weight distribution of the resultant polymers. Nonetheless, Lu *et al.*[12] prepared sodium and lithium complexes using series of Schiff bases as supporting ligands (Scheme 2-1a). These complexes were observed to be active towards the polymerization of lactides, yielding 99% lactide conversion within 1 min at 100:1 monomer-catalyst ratio and polymer dispersity index (PDI) of 1.48. Chang and Liang also reported the synthesis of alkali metals anchored on bis(phenolate)phosphine ligand that gives a 91% conversion at ε-caprolactone-catalyst ratio of 300:1 within 12 h at 80 ^{o}C. Though the yield was high, there was evidence of transesterification reaction from the high polydispersity index recorded.[13] Multinuclear alkali metals supported by bulky tetraphenol ligands were also reported to be very efficient in the ROP of lactides.[14] Other efficient alkali metal complexes reported have BHT ligand system on the metal centre (Scheme 2-1b),[15] salen ligand[16] and polydentate amine ligand system (Scheme 2-1c).[17]

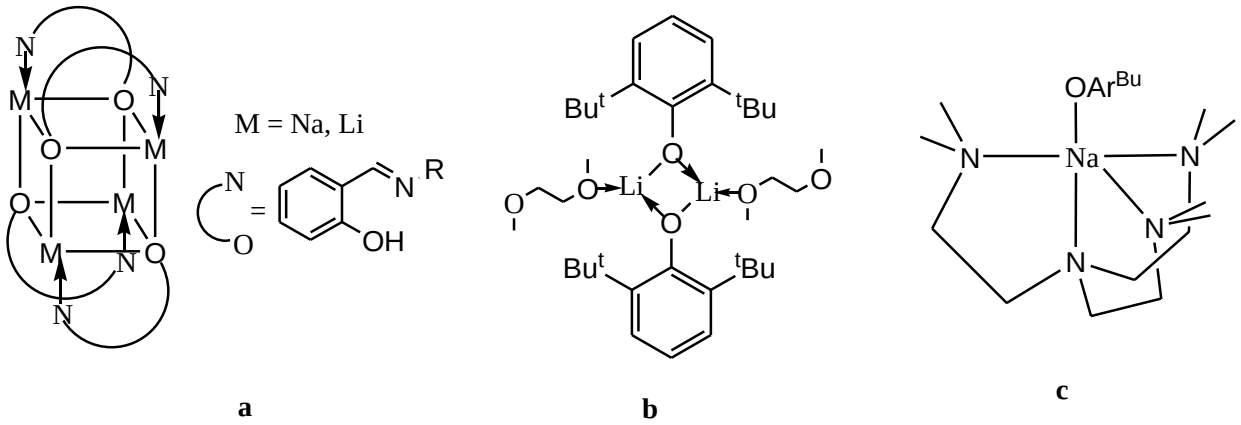

a **b** **c**

Scheme 2-1

Alkaline earth metal complexes of calcium and magnesium are the commonly used initiators for the polymerization of LA and ε-CL.[18] For instance the magnesium complex synthesized by Lee and co-workers using ketiminate ligands were relatively active in converting 98% of the monomer, ε-caprolactone, at 70 ^{o}C within 3 h at 200: 1 monomer: metal ratio.[19] Sanchez *et al.*[20] also synthesized mononuclear magnesium complex using a heteroscorpionate ligand system to afford a complex that is very efficient in the ROP of both lactides and ε-caprolactone. Active binuclear magnesium complexes anchored on NNO-tridentate ligand system (Scheme 2-2a) polymerized lactides at a rate ranging from 0.24 – 1.57 min^{-1} at 20 ^{o}C. These active complexes were also selective hence produce polymers with narrow polymer distribution ($1.07 \leq PDI \geq 1.26$).[21]

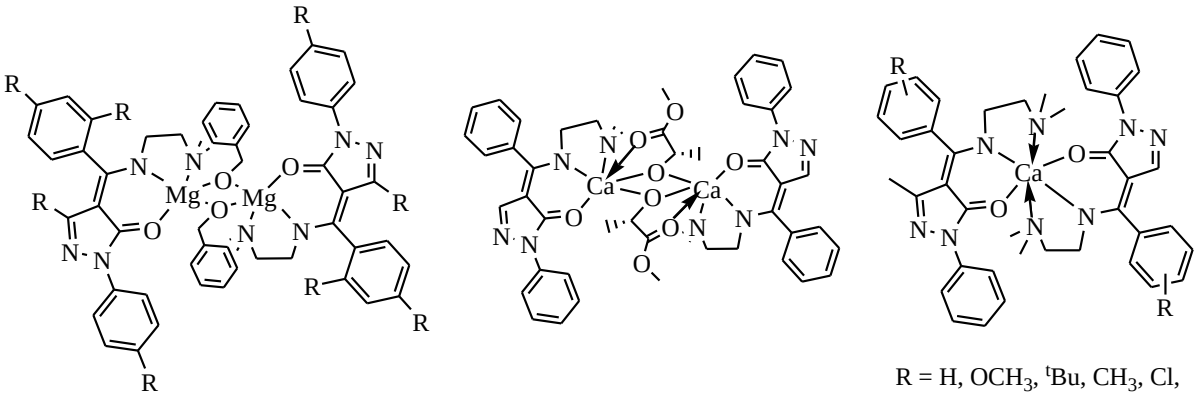

Scheme 2-2

Besides calcium and magnesium, strontium also demonstrates high catalytic activity toward the polymerization of cyclic esters. Strontium coordinated to polyether formed a chiral complex that polymerized *meso*-lactide at room temperature to yield 95% conversion after 30 min ([M]/[I]=100). The complex also exhibited high stereoselectivity to produce a heterotactic polylactide.[22]

Alkali and alkaline earth metal complexes have been observed to be active and efficient catalysts for the ROP of lactides and lactones but lack control over the reaction process and the distribution of molecular weight.

2.1.2 Rare earth metal-based catalysts

Rare earth metal-based catalysts are relatively new compounds that have attracted research interest due to their moderate Lewis acidity, good polymerization activity and most important, their low toxicity.[23] Their homoleptic forms are found to be very reactive but produce polymers with broad molecular weight due to lack of control on transesterification. Homoleptic yttrium alkoxide for instance remains one of the fastest initiators for lactides. It

was prepared by reacting yttrium isopropoxide with an alcohol to form $Y(OCH_2CH_2NMe_2)_3$. This complex showed a zero order dependence on lactide concentration.[24] Yttrium and other rare earth metal alkoxides were also found to efficiently initiate ε-caprolactone polymerization.[25] Control of molecular weight distribution was improved with introduction of bulky ligands on the metal centre to create a single-site type of catalyst. Some ligands used include cyclopentadienyl-based ligands[26] and bulky aryloxide.[27] Mazzeo *et al.*[11] recently synthesized very active heteroleptic yttrium and scandium complexes supported on phenoxy-thioether ligands for the polymerization of lactides and ε-caprolactone (Scheme 2-3a) and demonstrated moderate control over the molecular weight distribution. The polymerizations proceeded *via* a pseudo-first order dependency with respect to the monomers. The k_{obs} for lactide and ε-caprolactone polymerization by the yttrium complex was 0.0592 min^{-1} and 0.0161 s^{-1} respectively and the recorded k_{obs} for the scandium complex was 0.0105 min^{-1} and 0.00238 s^{-1} respectively. Several other heteroleptic rare earth metal-based catalysts used exhibited moderate control over the lactide and ε-caprolactone polymerization.[28]

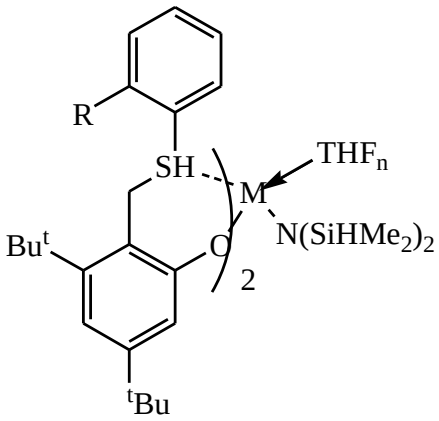

M = Y, Sc
R = H, CF_3

a

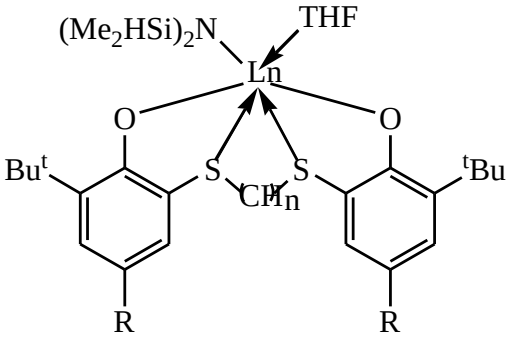

R = Me, ^{t}Bu

b

Scheme 2-3

2.1.3 Group 13 and 14 metal-based catalysts.

Aluminum complexes are common group 13 metals used in the polymerization of lactides and ε-caprolactones.[29] They are comparatively less active but are able to control the reaction process when supported on a ligand.[23, 30] For instance a well controlled molecular weight and good molecular weight distribution were observed when methyl aluminum diphenolate-alcohol system (Scheme 2-4a) [31] and biphenolate aluminum alkoxides (Scheme 2-4b)[32] were employed in the polymerization of ε-CL. In another study, Spassky *et al.*[33] demonstrated that the coordination of binaphthyl Schiff base ligand to aluminum methoxide resulted in a stereocontrolled PLA. Recent studies by Li *et al.*[34] using aluminum alkyl bearing N,N-substituted β-diketiminate (Scheme 2-4c) to polymerised ε-CL displayed high activity (k_{obs} = 0.218 min^{-1}) with narrow PDI values (1.04 ≤ PDI ≥ 1.36), however, the complex was not active in the polymerization of lactides. Active dinuclear aluminum complexes supported on N,O-chelate ligands exhibited good activity towards the polymerization of lactide in the presence of BnOH.[35] A 100:1 monomer:catalyst ratio led to 93% lactide conversion within 21 h. There was control over the polymer molecular weight and the molecular weight distribution was narrow. Other group 13 metals used as catalysts for ROP of cyclic esters are outlined in the work of Hillmyer *et al.*[36] and a review by Dagorne *et al.*[37]

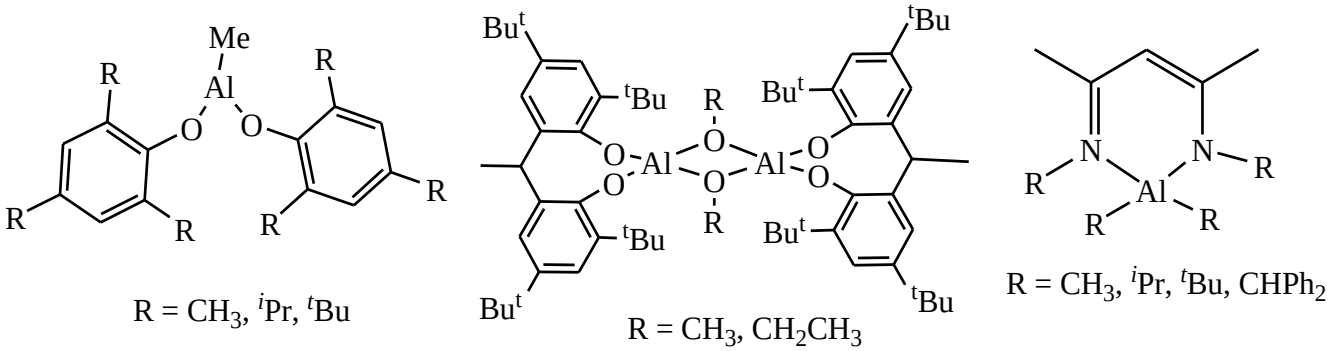

a **b** **c**

Scheme 2-4

The dominant metal complexes of group 14 used as catalysts are tin complexes. The most widely used is tin(II) octanoate (Scheme 2-5a). It is used industrially for cyclic ester polymerization due to their high catalytic activities, easy to handle and solubility in most organic solvents as well as molten lactides and lactones. However, the high temperatures at which catalyst efficiency is achieved also favor transesterification.[38] In other studies, Nimitsiriwat *et al.*[39] synthesized active imine ligated tin(II) complex (Scheme 2-5b) which consumed 100 equivalents of lactides within 4 h in toluene at 60 ^{o}C. Though high molecular weight polymers were obtained, the molecular weight distribution was broad (PDI = 1.48). In recent studies, tin(II) complex bearing quinoline-base N,N,O-tridentate ligands (scheme 2-5c) was observed to be moderately active in the polymerization of ε-caprolactone. Yielding 79% ε-caprolactone conversion within 4 h at 110 ^{o}C.[40]

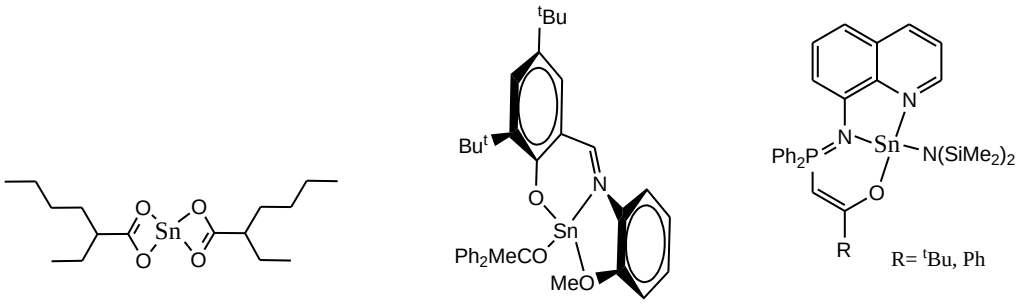

a **b** **c**

Scheme 2-5

The cytotoxicity of the tin compounds has become the major setback for the continuous use of tin complexes for lactide polymerization.

2.1.4 Early transition metal-based catalysts as ROP initiators

The predominant early transition metals used as catalysts are titanium[41] and zirconium[42] complexes with the later showing comparatively higher activity. These early transition metals bear ancillary ligands consisting series of nitrogen atom donors or combination of nitrogen,

oxygen and/or sulphur atom donors. Recent studies by Azor *et al.*[43] on the polymerization of lactide by titanium and zirconium complexes bearing biphenolate ligands revealed the complexes demonstrated a moderate activity with good control over the molecular weight and molecular weight distribution. The zirconium complexes were active, exhibiting 80-90% conversion within 10-12 h with a PDI between (1.13-1.18). In other studies, zirconium complex with NHC ligand (Scheme 2-6a) synthesized by Romain *et al.*[44] is active under mild conditions, stable and highly stereoselective and produce narrowly dispersed molecular weight (1 < PDI > 1.11) PLAs. Sauer *et al.*[45] also reported series of well coordinated zirconium and hafnium complexes (Scheme 2-6b) that are active towards the ROP of lactide. In the work of Gowda *et al.*[46], dimeric hafnium alkoxide complexes were found to exhibit high catalytic activity towards ROP of ε-caprolactone. Polymerization by the complexes were completed within 1 h at 80 ^{o}C for [M]/[I]=200 and the resultant polymer had high molecular weight with narrow molecular weight distribution. Similarly, titanium complexes of tridentate aminebiphenolate ligands (Schem2-6c) were observed to be active in the polymerization of ε-caprolactones. The propagation rates at room temperatures in toluene using different monomer:initiator ratio ranges from $2.84x10^{-5}$ - $2.23x10^{-4}$ s^{-1}. The molecular weight distribution was controlled and conversion was high (>99% conversion at room temperature within 24 h).[47]

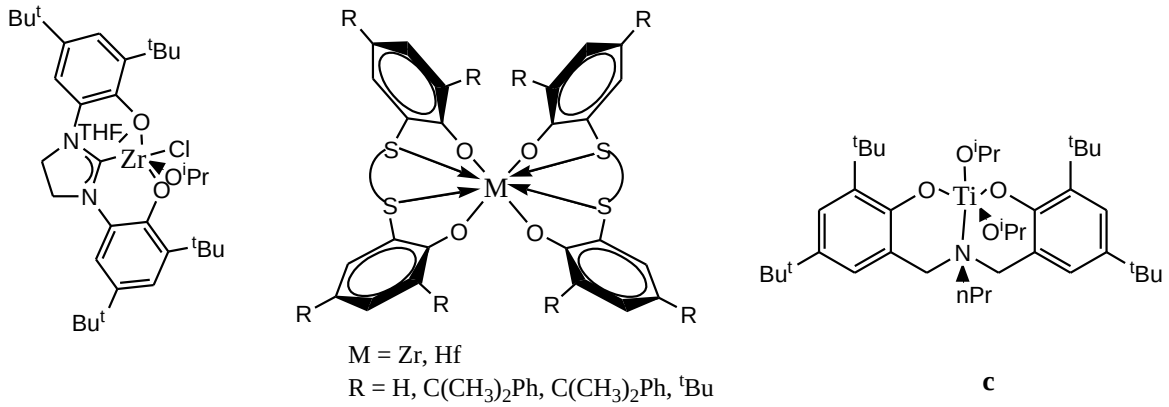

a **b** **c**

Scheme 2-6

Besides these early transition metal complexes, some mid-transition metal complexes tested for the polymerization of lactide are vanadium and molybdenum. They exhibited poor catalytic activity as evident in the work of Mahha *et al.*[48] Other heteroleptic early transition metal explored as catalyst for ROP of these cyclic esters is hafnium.[49]

2.1.5 Late transition metal complexes as ROP initiators

Late transition metal complexes have also been exploited as potential initiators for cyclic ester polymerization. Among them, nickel,[50] ruthenium[51] and iron[52] have been tested and shown to exhibit good catalytic activity. O'keefe *et al.*[53] used dinuclear iron complex ($Fe_2(OCHPh_2)_6$ to polymerize ε-CL in a well controlled process to produce PCLs with narrow molecular weight distribution. The polymerization at 25 ^oC in toluene proceed at a rate of 3.8 x 10^{-4} s^{-1} when [M]/[I] = 550.

The late transition metal that has witnessed significant research output is zinc. Zinc complexes have been exploited over the years as potential substitute for tin(II) octanoate due to their low toxicity, relatively high activity and stability.[54,55] Coate *et al.*[56] reported a series of β-diiminate zinc complexes that act as single-site during the ROP of lactides. The complexes of the type **a** and **b** (Scheme 2-7) exhibited high catalytic activity (k_{obs} = 0.037 min^{-1}, [LA]/[Zn] = 494 at 25 ^oC in CH_2Cl_2) and selectivity in the polymerization of lactide ($1.02 \leq PDI \geq 1.18$).

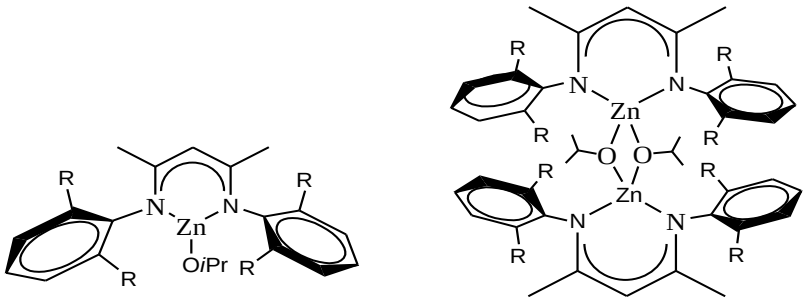

R = nPr, *i*Pr

a

R = *i*Pr

b

Scheme 2-7

Chen *et al.*[57] also reported a homoleptic zinc complex and a trinuclear zinc alkoxide complex (Scheme 2-8) supported on similar ligand used by Coates *et al.* This system forms a highly efficient initiator for the ROP of lactide and ε-caprolactone. Polymerization of $_{L}$-lactide with the trinuclear complex at room temperature when [LA]/[Zn] = 300 yielded a 95% conversion within 10 min. The measured polydispersity index is 1.02. However, the complexes were less active in the polymerization of ε-caprolactone.

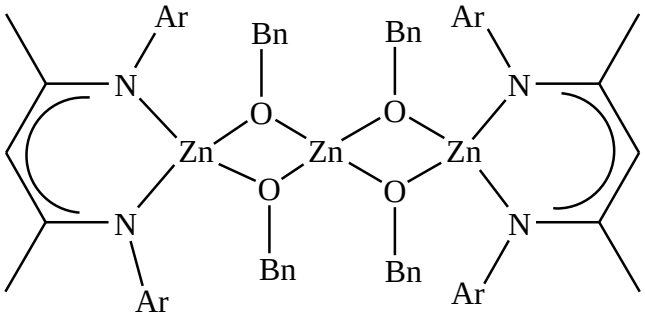

Ar = 2-methoxyphenyl

Scheme 2-8

In other recent studies, Sung *et al.*[58] polymerized lactides with zinc complexes bearing N,N,O-tridentate ligand systems. The conversions went to completion within 3 h for [M]/[Zn] ranging from 25-300 in 9-anthracenemethanol solvent at 30 ^{o}C. The molecular weight

distribution was moderate ($1.05 \leq PDI \geq 1.41$). Also, zinc complexes of the type **b** (Scheme 2-9) demonstrate high efficiency (k_{obs} = 0.651 min^{-1}) and immortality in the polymerization of cyclic esters in the presence of other external transfer agent. About 97% conversion of 1000 equivalent of lactide in toluene at 60 ^{o}C was attained within 8 min. The polydispersity index was 1.08.[59]

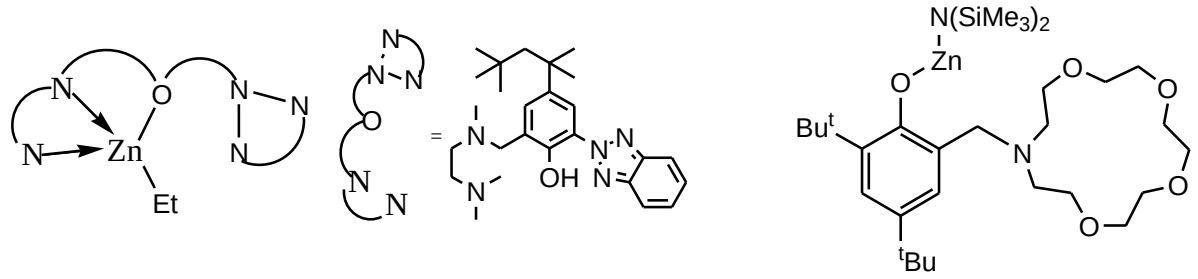

a **b**

Scheme 2-9

Copper on the other hand is one of the late transition metals that has few reports on their catalytic activities on the ROP of cyclic polyesters.[60] Most of the reported complexes exhibit low activity whiles in some cases lack control on stereochemistry of the polymers. However, Li *et al.*[61] reported on the syntheses of stable copper complexes supported by derivatives of benzotriazole phenoxide ligand (Scheme 2-10). The complexes produced high molecular weight polymers with moderately narrow polydispersity index between 1.09 - 1.29.

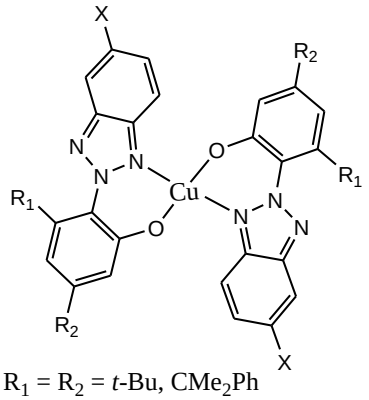

$R_1 = R_2 = t$-Bu, CMe_2Ph
X = H, Cl

Scheme 2-10

In another study, copper metal supported on phenoxy-ketimine ligands were employed in a melt polymerization of lactide at 160 ^{o}C for different [M]/[I] ratios. The observed percentage conversion after 4 h were between 50 -75% depending on the ligand structure. However, the molecular weight distributions were between 1.10 to 1.50.[50] Recently, Whitehorne and Schaper[62] reported the polymerization of *rac*-lactide with dibenzyl diketiminate copper alkoxide (Scheme 2-11) at room temperature with very high activity to form predominantly atactic polylactide. The recorded molecular weight distribution was in the range of 1.04 and 1.08 which signify the absence of transesterification reactions.

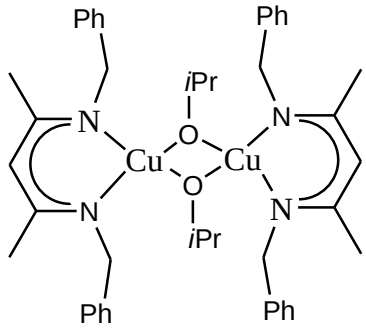

Scheme 2-11

The catalytic activity of zinc and copper acetate anchored on di- and monodentate nitrogen donor ligand (Scheme 2-12) was investigated in the polymerization of ε-CL. The complexes **a** and **b** were observed to exhibited a rate constant of 0.096 h^{-1} and 0.031 h^{-1} respectively.[63]

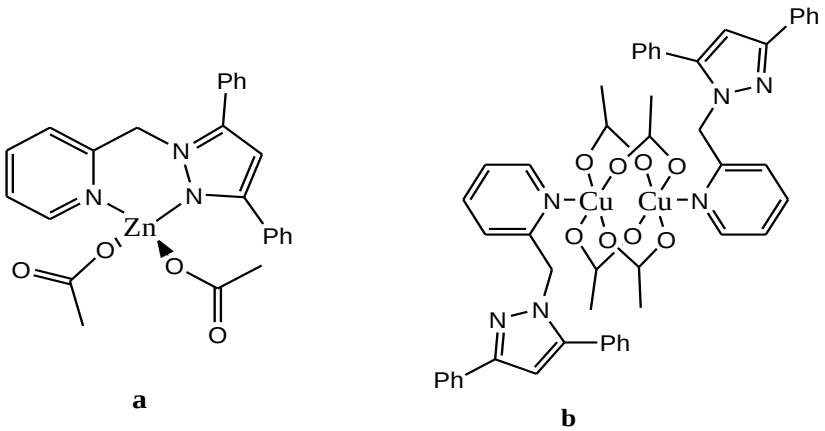

a **b**

Scheme 2-12

Zinc and copper metals are very crucial metals that can mark a significant milestone in the syntheses of biocompatible and environmentally friendly polymers. Residues of these metals in polymers do not pose problems of cytotoxicity because they are essential for human growth and development due to their therapeutic as well their enzymatic roles in the body.[64] They are also essential for plant growth. For instance, the enzyme carbonic anhydrase consist of zinc coordinated to histidine and is essential for the hydration of carbon dioxide in the body.[64a]

In the polymerization of LA and ε-CL, zinc and copper complexes containing well defined ligand systems have demonstrated moderate to high catalytic potentials with increase in control over the polymerization process. The variations in catalytic activity have been observed to depend on the type of ligand system as well as the initiating group on the metal centre.

The efficient production of quality and environmentally friendly PLAs and PCLs depends on very active but virtually non-toxic metal-based catalysts containing good ligand motif. In this regard, the current project aims at producing active non-toxic catalysts that can polymerize lactides and ε-caprolactone with high efficiency.

2.2 Rationales and Justification of the study

The use of metal-based catalysts for the ROP of biodegradable cyclic esters such as lactides and ε-caprolactones is the most convenient method for the syntheses of the respective polymers. The polymers are targeted as potential substitutes to current traditional plastics which persist in the environment for many years before degrading, hence posing environmental nuisance. Furthermore, these polyesters play essential role in health delivery

as they are used for tissue engineering, biomedical materials and as drug delivery polymers. Currently, the tin-based catalyst being used is highly toxic and difficult to remove from the synthesized polymer hence non-essential. The design of homogenous catalysts that are less toxic is thus very critical. Catalytic amount of zinc and copper metals have been identified as less toxic to the body since some enzymes in the body are made up of these metals. Moreover, some complexes of these metals have been identified as very active in the polymerization of lactides and ε-caprolactones.

This project therefore aims to build on the search for more active and less toxic catalysts for the ROP of LA and ε-CL. Zinc and copper complexes supported by nitrogen-donor benzimidazolyl derivative have been synthesized and investigated as initiators for the polymerization reaction of lactides and ε-caprolactones. Chapter 3 reports the synthesis and structural characterization of the zinc and copper complexes while Chapter 4 presents results of the polymerization and kinetics of lactides and ε-caprolactones using the metal complexes.

2.3 Objectives

The specific objectives of this study can thus be formulated as follows:

1. To synthesize and structurally characterize new (benzimidazolylmethyl) aniline derivatives and their corresponding Zn(II) and Cu(II) complexes.
2. To investigate the ability of the isolated Zn(II) and Cu(II) complexes to catalyze the ROP of lactides and ε-caprolactones.
3. To study the kinetics and mechanism of these polymerization reactions.

References

[1] Kleine, J.; Kleine, H. H. *Makromol. Chem.* **1959**, *30*, 23-38.

[2] Dechy-Cabaret, O.; Martin-Vaca, B.; Bourissou, D. *Chem. Rev.* **2004**, *104*, 6147−6176

[3] Tschan, M. J.-L.; Brule, E.; Haquette, P.; Thomas, C. M. *Polym. Chem.* **2012**, *3*, 836–851.

[4] Gupta, A.P.; Kumar, V. *Eur. Polym. J.* **2007**, *43*, 4053-4074.

[5] Storey, F.R.; Sherman, J.W.; *Macromolecules* **2002,** *35*, 1504-1512.

[6] Kasperczyk, J. E. *Macromolecules* **1995**, *28*, 3937–3939 (b) Kurcok, P.; Penczek, J.; Franek, J.; Jedlidski, Z. *Macromolecules* **1992**, *25*, 2285-2289.

[7] Kasperczyk, J.; Bero, M. *Polymer* **2000**, *41*, 391-395.

[8] (a) Duda, A.; Florjanczyk, Z.; Hofman, A.; Slomkowski, S.; Penczek, S. *Macromolecules* **1990**, *23*, 1640–1646. (b) Tina, M.; Ovitt, T.M.; Geoffrey, W.; Coates, G.W. *J. Polym. Sci. Part A: Polym. Chem.* **2000**, *38*, 4686–4692.

[9](a) Kricheldorf, H. R.; Fechner, B. *Biomacromolecules* **2002**, *3*, 684-690. (b) Finne, A.; Albertsson, A.-C. *Biomacromolecules* **2002**, *3*, 691–695.

[10](a) McLain, S.J.; Drysdale, N. E. *Polym. Prepr., Am. Chem. Soc.* **1992**, *33*, 174-180. (b) Penczek, S.; Cypryk, M.; Duda, A.; Kubisa, P.; Slomkowski, S. *Prog. Polym. Sci.* **2007**, *32*, 247–282.

[11] Mazzeo, M.; Tramontano, R.; Lamberti, M.; Pilone, A.; Milione, S.; Pellecchia, C. *Dalton Trans.* **2013**, *42*, 9338–9351.

[12] Lu, W.-Y.; Hsiao, M.-W.; Hsu, S.C.N.; Peng, W.-T.; Chang, Y.-J.; Tsou, Y.-C.; Wu, T.-Y.; Lai, Y.-C.; Chen, Y.; Chen, H.-Y. *Dalton Trans.* **2012**, *41*, 3659-3667.

[13] Chang, Y.-N.; Liang, L.-C. *Inorg. Chim. Acta.* **2007**, *360*, 136–142.

[14] Zhang, J.; Jian, C.; Gao, Y.; Wang, L.; Tang, N.; Wu, J. *Inorg. Chem.* **2012**, *51*, 13380–13389.

[15] Chen, H.-Y.; Mialon, L.; Abboud, K. A.; Miller, S.A. *Organometallics* **2012**, *31*, 5252−5261.

[16] Yao, L.; Wang, L.; Pan, X.; Tang, N.; Wu, J. *Inorg. Chim. Acta* **2011,** *373*, 219–225.

[17] Calvo, B.; Davidson, M.G.; García-Vivo, D. *Inorg. Chem.* **2011**, *50*, 3589–3595.

[18] (a) Chisholm, M.H.; Gallucci, J. C.; Phomphrai, K. *Inorg. Chem.* **2004**, *43*, 6717–6725. (b) Zhong, Z.; Schneiderbauer, S.; Dijkstra, P. J.; Westerhausen, M.; Feijen, J. *Polym. Bull.* **2003**, *51*, 175–185.

[19] Lee, L.-Y.; Hsieh, H.-H.; Hsieh, C.-C.; Lee, H. M.; Lee, G.-H.; Huang, J.-H.; Wu, T.-C.; Chuang, S.-H. *Organomet. Chem.* **2007**, *692*, 1131–1137.

[20] Sanchez-Barba, L. F.; Garces, A.; Fajardo, M.; Alonso-Moreno, C.; Fernandez-Baeza, J.; Otero, A.; Antinolo, A.; Tejeda, J.; Lara-Sanchez, A.; Lopez-Solera, M. I. *Organometallics* **2007,** *26*, 6403-6411.

[21] Chuang, H.-J.; Chen, H.-L.; Ye, J.-L.; Chen, Z.-Y.; Huang, P.-L.; Liao, T.-T.; Tsai, T.-E.; Lin, C.-C. *J. Polym. Sci., Part A: Polym. Chem.* **2013**, *51*, 696–707

[22] Davin, J. P.; Buffet , J.-C.; Spaniol, T. P.; Okuda, J *Dalton Trans.* **2012**, *41*, 12612-12618.

[23] Platel, R.H; Hodgson, L.M.; Williams, C.K. *Polym. Rev.* **2008**, *48*, 11-63.

[24] McClain, S. J.; Ford, T. M.; Drysdale, N. E. *Polym. Prep.* **1992**, 463–464.

[25] (a) Shen, Z.Q.; Shen, Y.Q.; Sun, J.Q.; Zhang, F.Y.; Zhang, Y.F. *Polym. J.* **1995**, *27*, 59-64. (b) Nomura, N.; Taira, A.; Nakase, A.; Tomioka, T.; Okada, M. *Tetrahedron* **2007**, *63*, 8478–8484. (c) Deng, X. M.; Zhu, Z.; Xiong, C.; Zhang, L. *J. Appl. Polym. Sci.* **1997**, *64*, 1295–1299.

[26] (a) Zhou, S.; Wang, S.; Yang, G.; Li, Q.; Zhang, L.; Yao, Z.; Zhou, Z.; Song, H.-B. *Organometallics* **2007**, *26*, 3755-3761. (b) Zhou, S. L.; Wang, S. W.; Sheng, E. H.; Zhang, L. J.; Yu, Z. Y.; Xi, X. B.; Chen, G. D.; Luo, W.; Li, Y. *Eur. J. Inorg. Chem.* **2007**, 1519-1528.

(c) Wang, S. W.; Tang, X. L.; Vega, A.; Saillard, J. Y.; Zhou, S. L.; Yang, G. S.; Yao, W.; Wei, Y. *Organometallics* **2007**, *26*, 1512-1522.

[27] (a) Zhang, L. F.; Niu, Y. H; Wang, Y.; Wang, P.; Shen, L. J.; *J. Mol. Catal. A: Chem.* **2008**, *287*, 1-4.

[28] (a) Ma, H.; Spaniol, T. P.; Okuda, J. *Dalton Trans.* **2003**, 4770-4780. (b) Ma, H.; Spaniol, T. P.; Okuda, J. *Inorg. Chem.* **2008**, *47*, 3328-3339. (c) Luo, Y.; Li, W.; Lin, D.; Yao, Y.; Zhang, Y.; Shen, Q. *Organometallics* **2010**, *29*, 3507-3517. (d) Lin, W.; Sun, W. L.; Shen, Z. Q. *Chin. Chem. Lett.* **2007**, 18, 1133–1136.

[29] (a)Wu, J.; Pan, X.; Tang, N.; Lin, C.-C. *Eur. Polym. J.* **2007**, *43*, 5040–5046. (b) Zhong, Z.; Dijkstra, P. J.; Feijen, J. *Angew. Chem., Int. Ed.* **2002,** *41*, 4510–4513.

[30] Atwood, D. A. *Coord. Chem. Rev.* **1997**, *165*, 267–296.

[31] Akatsuka, M.; Aida, T.; Inoue, S. *Macromolecules* **1995**, *28*, 1320–1322.

[32] Liao, T.-C.; Huang, Y.-L.; Huang, B.-H.; Lin, C.-C. *Macromol. Chem. Phys.* **2003**, *204*, 885-892.

[33] Spassky, N.; Wisniewski, M.; Pluta, C.; Le Borgne, A. *Macromol. Chem. Phys.* **1996**, *197*, 2627–2637.

[34] Li, D.; Peng, Y.; Geng, C.; Liu, K.; Kong, D. *Dalton Trans.* **2013**, *42*, 11295–11303.

[35] Yu, X.-F.; Wang, Z.-X. *Dalton Trans*. **2013**, *42*, 3860–3868.

[36] Pietrangelo, A.; Hillmyer, M. A.; Tolman, W. B. *Chem. Commun.* **2009**, 2736–2737.

[37] Dagornea, S.; Normand, M.; Kirillov, E.; Carpentier, J.-F. *Coord. Chem. Rev.* **2013**, 1869–1886.

[38] (a)Moller, M.; Kange, R.; Hedrick, J. L. *J. Polym. Sci., Part A: Polym. Chem*. **2000**, *38*, 2067–2074. (b) Albertsson, A.-C.; Varma, I.K. *Biomacromolecules* **2003**, *4*, 1466-1486.

[39] Nimitsiriwat, N.; Gibson, V.C.; Marshall, E.L.; Elsegood, M.R.J. *Inorg. Chem.* **2008,** 5417-5424

[40] Ma, W.-A.; Wang, Z.-X. *Dalton Trans.* **2011**, *40*, 1778–1786.

[41] (a) Kricheldorf, H. R.; Berl, M.; Scharnagl, N. *Macromolecules* **1988**, *21*, 286-293. (b) Patel, D.; Liddle, S. T.; Mungur, S. A.; Rodden, M.; Blake, A. J.; Arnold, P. L. *Chem. Commun.* **2006**, *3*, 1124–1126. (c) Broomfield, L. M.; Wright, J. A.; Bochmann, M. *Dalton Trans.* **2009**, 8269-8279. (d) Postigo, L.; Sanchez-Nieves, J.; Royo, P.; Mosquera, M.E.G. *Dalton Trans.* **2009**, 3756-3765. (e) Cayuela, J.; Bounor-Legare, V.; Cassagnau, P.; Michel, A. *Macromolecules* **2006**, *39*, 1338-1346. (f) Chmura, A.J.; Davidson, M.G.; Jones, M.D.; Lunn, M.D.; Mahon, M.F. *Dalton Trans.* **2006**, 887-889.

[42] (a) Schwarz, A. D.; Herbert, K. R.; Paniagua, C.; Mountford, P. *Organometallics* **2010**, *29*, 4171-4188. (b) Whitelaw, E. L.; Jones, M. D.; Mahon, M. F. *Inorg. Chem.* **2010**, *49*, 7176-7181. (c) Gendler, S.; Segal, S.; Goldberg, I.; Goldschmidt, Z.; Kol, M. *Inorg. Chem.* **2006**, *45*, 4783-4790. (d) Wang, H.; Chan, H.-S.; Okuda, J. *Organometallics* **2005**, *24*, 3118 - 3124. (e) Munha, R.F.; Alves, L.G.; Maulide, N.; Duarte, M.T.; Marko, I.E. Fryzuk, M.D.; Martins, A.M. *Inorg. Chem. Commun.* **2008**, *11*, 1174–1176.

[43] Azor, L.; Bailly, C.; Brelot, L.; Henry, M.; Mobian, P.; Dagorne, S. *Inorg. Chem.* **2012**, *51*, 10876-10883.

[44] Romain, C.; Heinrich, B.; Laponnaz, S.B.; Dagorne, S. *Chem. Commun.* **2012**, *48*, 2213–2215.

[45] Sauer, A.; Kapelski, A.; Fliedel, C.; Dagorne, S.; Kol, M.; Okuda, J. *Dalton Trans.* **2013**, *42*, 9007–9023.

[46] Gowda, R.R.; Chakraborty, D.; Ramkumar, V. *Polymer*, **51**, 4750-4759.

[47] Liang, L.-C.; Lin, S.-T.; Chien, C.-C. *Inorg. Chem.* **2013,** *52*, 1780-1786.

[48] Mahha, Y.; Atlamsani, A.; Blais, J.-C.; Tessie, M.; Bregeault, J.-M.; Salles, L. *J. Mol. Catal. A: Chem.* **2005,** *234*, 63–73.

[49] Hu, M.; Wang, M.; Zhu, H.; Zhu, L.; Zhang, H.; Sun, L. *Dalton Trans.* **2010**, *39*, 4440-4446.

[50] John, A.; Katiyar, V.; Pang, K.; Shaikh, M. M.; Nanacati, H.; Hemant, G.; Ghosh, P. *Polyhedron* **2007**, *26*, 4033-4044.

[51] Mata-mata, J.L.; Gutierrez, J.L.; Paz-Sandoval, M.A.; Madrigal, A.R.; Martinez-Richa, A. *J. Polym. Sci., Part A: Polym. Chem.* **2006**, *44*, 6926-6942.

[52] (a) Stolt, M.; Södergard, A. *Macromolecules* **1999**, *32*, 6412-6417. (b) Gibson, V. C.; Marshall, E. L.; Navarro-Llobet, D.; White, A. J. P.; Williams, D. J. *J. Chem. Soc., Dalton Trans.* **2002**, 4321-4322. (c) Gorczynski, J. L.; Chen, J.; Fraser, C. L. *J. Am. Chem. Soc.* **2005**, *127*, 14956-14957.

[53] O'Keefe, J.B.; Breyfogle, L.E.; Hillmeyer, M.A.; Tolman, W.B. *J. Am. Chem. Soc.* **2002**, *124*, 4384-4393.

[54] Kowalski, A.; Duda, A.; Penczek, S. *Macromol. Rapid Commun.* **1998**, *19*, 567–572.

[55] Sarazin, Y.; Schormann, M.; Bochmann, M. *Organometallics* **2004**, *23*, 3296–3302.

[56] Chamberlain, B. M.; Cheng, M.; Moore, D. R.; Ovitt, T. M.; Lobkovsky, E. B.; Coates, G. W. *J. Am. Chem. Soc.* **2001**, *123*, 3229–3238 (b) Rieth, L. R.; Moore, D. R.; Lobkovsky, E. B.; Coates, G. W. *J. Am. Chem. Soc.* **2002,** *124*, 15239–15248.

[57] Chen, H.-Y. Huang, B.-H.; Lin, C.-C. *Macromolecules* **2005,** *38*, 5400-5405.

[58] Sung, C.-Y.; Li, C.-Y.; Su, J.-K.; Chen, T.-Y.; Lin, C.-H.; Ko, B.-T. *Dalton Trans.*, **2012**, *41*, 953–961.

[59] Poirier, V.; Roisnel, T.; Carpentier, J.-F.; Sarazin, Y. *Dalton Trans.* **2011**, *40*, 523–534.

[60] (a) Bhunora, S.; Mugo, J.; Bhaw-Luximon, A.; Mapolie, S.; Van Wyk, J.; Darkwa, J.; Nordlander, E. *Appl. Organometal. Chem.* **2011**, *25*, 133–145. (b) Gowda, R. R.; Chakraborty, D. *J. Mol. Catal. A, Chem.* **2011**, *349*, 86-93.

[61] Li, C.-Y.; Hsu, S.-J.; Lin, C.-L.; Tsai, C.-Y.; Wang, J.-H.; Ko, B.-T.; Lin, C.-H.; Huang, H.-Y. *J. Polym. Sci., Part A: Polym. Chem.* **2013**, *51*, 3840-3849.

[62] Whitehorne, T.J.J.; Schaper, F. *Chem. Commun.* **2012**, *48*, 10334–10336.

[63] Ojwach, S.O.; Okemwa, T. T.; Attandoh, N.W.; Omondi, B. *Dalton Trans.* **2013**, *42*, 10735–10745.

[64] (a) Parkin, G. *Chem. Rev.* **2004,** *104*, 699-767. (b) Desai, V.; Kaler, S.G. *Am. J. Clin. Nutr.* **2008,** *88*, 855-858.

Chapter Three

Synthesis of (Benzoimidazolylmethyl)amine Zinc(II) and Copper(II) complexes

3. 1 Introduction

Over the years, many metal complexes of the form $M_x(R)_y$ or $M_xL_z(R)_y$ (x, z ≥ 1, y ≤ 2), M= metal centre (main group, transition, lanthanide or actinides metals), L= ancillary ligand, R= alkyl, alkoxy, phenoxy or carboxylate, have been employed as catalysts/ initiators for the ROP of monomers.[1] However, much emphasis has been given to $M_xL_z(R)_y$ type of complexes due to the significant role of the ancillary ligand. The coordination of ancillary ligands which are normally characterized by their bulky nature to the active metal centers provide steric barriers and prevent the growing polymer chain from accessing the active catalyst site, thereby preventing backbiting/ transesterification reaction[2]. They also contribute to the electronic properties of the complex thereby influencing the efficiency of the catalyst.[3] Besides the structural and electronic effects, some ligands are also capable of imposing chirality on the complex thereby making the complex stereoselective.[4] These tendencies have led to the design and fine tuning of several ligands containing single or multiple unsaturated nitrogen, oxygen and/or sulphur atoms that are monodentate, bidentate or multidentate depending on the ligand architecture and the identity of the metal atom.[5]

In this report, derivatives of benzimidazole were exploited as potential N-atom donors to Zn(II) and Cu(II) metal ions. These ligands have attracted research interest due to their highly nucleophilic imide N-atom, their tendency to form aggregation with transition metal ions[6] and their biocompatibility.[7] In addition to ligand design, the choice of the metal centre has become very important as a result of the applications of the catalyst/ initiators. The use of more biocompatible metals which are equally active and versatile as compared to the widely

used tin-based catalysts[8] and other heavy metals is directing current research trends. Besides Ca,[9] Mg,[10] Fe,[1a] and alkali metals,[11] Zn(II) and Cu(II) metals are attractive for the design of catalysts/initiators for ROP of lactides and lactones due to their low toxicity.[12] Furthermore, complexes of these metals have been found to exhibit good activity towards ROP of cyclic monomers as a result of their good Lewis acidity.[3,13] Besides, they are relatively inexpensive and easy to handle. For example Williams *et al.*,[14] Drouin *et al.*,[15] Garces *et al.*,[16] have reported zinc-base catalysts used for the polymerization of ε-caprolactone and lactides, while John *et al.*,[17] Bhunora *et al.*[18] and Sun *et al.*[19] examined the catalytic activity of copper complexes in the polymerization of these cyclic monomers.

In this Chapter, we herein describe the coordination chemistry of Zn(II) and Cu(II) carboxylate complexes with benzoimidazolyl derivatives. The ability of these complexes to initiate the ring-opening polymerization of lactides and ε-caprolactone would be discussed in Chapter four.

3. 2 Experimental

3.2.1 Materials and Instrumentation

The chemicals, aniline (≥99.5%), 2-aminothiophenol (≥99%), 2-bromoaniline (98%), 2-methoxyaniline (≥99%), benzoic acid (99.5%) and 2-chloromethylbenzimidazole were purchased from Sigma Aldrich and were used as received. $Zn(CH_3COO)_2{\cdot}2H_2O$ (≥99.5) and $Cu(CH_3COO)_2{\cdot}2H_2O$ (≥99.5) were sourced from Saarchem and BHD respectively. Potassium iodide (KI), sodium hydroxide (NaOH) and potassium hydroxide were obtained from Merck chemicals. The solvents, absolute ethanol (~99.5%$^{V}/_{V}$), methanol (~99.5%$^{V}/_{V}$) and DMSO-d_6 were purchased from Merck while deuterated chloroform ($CDCl_3$) was purchased from Sigma Aldrich.

NMR spectra were recorded on Bruker 400 UltraShield NMR (400 MHz for ^{1}H and 100 MHz for ^{13}C) spectrometer. All the chemical shifts were recorded in δ ppm relative to tetramethylsilane. The ^{1}H and ^{13}C spectra are referenced using residual $CDCl_3$ and DMSO-d_6 solvent peaks and the coupling constants (*J*) are reported in hertz (Hz). Elemental analyses were carried out on Flash 2000 thermoscientific analyser. IR spectra were recorded using Perkin-Elmer spectrum 100 series FT-IR spectrometer while the mass spectra of the analytes were obtained using micromass LCT premier mass spectrometer. The magnetic moments of paramagnetic copper complexes were determined using Evans balance while electron paramagnetic resonance (EPR) spectra of the complexes were recorded on a Bruker EMX/Premium-240 653 instrument operating at X-band (9 GHz) frequency.

Crystallographic data were collected on a Bruker APEXII diffractometer with Mo Kα radiation (λ = 0.7107 Å). All the reflections were successfully indexed by an automated indexing routine built in the APEXII program suit.[20] Direct method was used to solve for structures and refined by full-matrix least-squares procedures against F^2 using SHELXS97. All non-hydrogen atoms were refined with anisotropic displacement coefficient.[21]

3.2.2 Syntheses of ligands and their Zn(II) and Cu(II) complexes.

3.2.2.1 Synthesis of N-(1H-benzoimidazol-2-ylmethyl)aniline (L1).

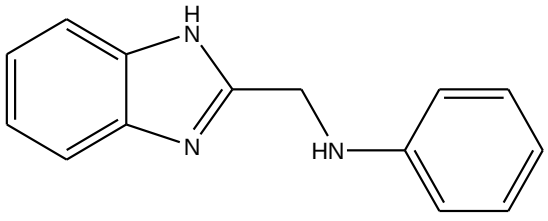

This ligand was prepared by dissolving 2-chloromethylbenzoimidazole (1.67 g, 10.00 mmol), KI (1.66 g, 10.00 mmol) and aniline (0.94 g, 0.92 ml, 10.00 mmol) in ethanol (40 ml) and

refluxed for 6 h at 80 ^{o}C. This was followed by addition of KOH (0.40 g, 10.00 mmol) and refluxed further for 2 h. The reaction mixture was allowed to cool to room temperature and poured into ice-cold water to give a pale yellow precipitate which was filtered and dried to afford **L1** as a pale yellow solid (1.59 g, 71%). ^{1}H NMR (400 MHz, $CDCl_3$,): δ 7.53 (dd, 2H, $^{3}J_{HH}$ = 3.2, ArH), 7.23 (dd, 2H, $^{3}J_{HH}$ = 3.1, ArH), 7.12 (dd, 2H, $^{3}J_{HH}$ = 7.6, ArH), 6.73 (t, 1H, $^{3}J_{HH}$ = 7.3, ArH), 6.60 (d, 2H, $^{3}J_{HH}$ = 7.7, ArH), 4.62 (s, 2H, CH_2). ^{13}C NMR (100 MHz, $CDCl_3$): δ 153.2 (C), 147.2 (C), 137.9 (C), 129.5 (CH), 122.8 (CH), 118.9 (CH), 114.9 (C), 113.2 (CH), 43.0 CH_2). IR (KBr) ν (cm^{-1}): 3405 s,3050 w, 1604 s, 1510 s, 1455 m, 1421 s, 1347 w, 1318 s, 1269 s, 1183 w, 1153 w, 1106 w, 1075 w, 1011 w, 996 w, 928 w, 875 w, 875 w, 838 w, 745 s, 692 m. HRMS-ESI ([M-H^{+}]): m/z calcd: 223.111; found: 222.104.

3.2.2.2 Synthesis of N-(1H-benzoimidazol-2-ylmethyl)-2-methoxyaniline (L2).

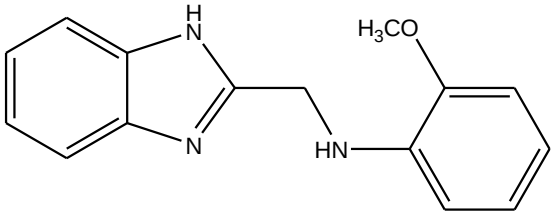

The procedure adopted was similar to **L1.** 2-chloromethylbenzoimidazole (1.23 g, 7.39 mmol), 2-methoxyaniline (0.83 ml, 7.39 mmol), KI (1.23 g, 7.39 mmol) and KOH (0.42 g, 7.39 mmol) yielded a brick red precipitate. Purification by column chromatography on silica gel using diethyl ether and dichloromethane (2:1) solvent system as the eluent afforded **L2** as an analytically pure pale yellow solid (0.95 g, 51 %). ^{1}H NMR (400 MHz, $CDCl_3$): δ 7.55 (dd, 2H, $^{3}J_{HH}$ =3.2, ArH), 7.23 (dd, 2H, $^{3}J_{HH}$ =3.2, ArH), 6.84-6.73 (m, 3H, ArH), 6.53 (dd, 2H, $^{3}J_{HH}$ =2.0, ArH), 4.69 (s, 2H, CH_2), 3.89 (s, 3H, CH_3). ^{13}C NMR (100 MHz, $CDCl_3$): δ 153.6 (C), 147.0 (C), 138.3 (C), 137.2 (CH), 122.5 (CH), 121.4 (CH), 118.2 (CH), 114.9 (C), 110.5 (CH), 109.6 (CH), 55.4 (CH_3), 42.9 (CH_2). IR (KBr) ν (cm^{-1}): 3427 s, 3006 w, 2955 w,

2835 w, 1603 m, 1545 w, 1514 m, 1440 m, 1457 m, 1432 m, 1422 m, 1360 w, 1330 m, 1303 m, 1260 m, 1224 s, 1179 m, 1144 w, 1130 m, 1053 m, 1026 s, 906 w, 836 w, 812 w, 771 s, 743 s, 656 w. HRMS-ESI ([M + Na^+]): m/z calcd: 276.289; found: 276.112.

3.2.2.3 Synthesis of N-(1H-benzoimidazol-2-ylmethyl)-2-bromoaniline (L3).

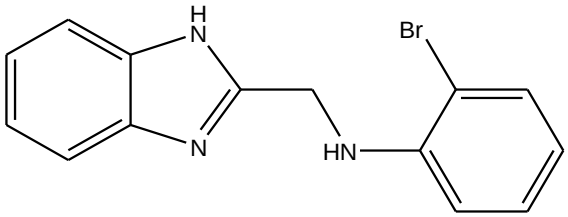

This ligand was also prepared following the procedure in **L1**. 2-chloromethylbenzoimidazole (1.52 g, 9.14 mmol), KI (1.52 g, 9.14 mmol), 2-bromoaniline (1.57 g, 1.03 ml, 9.14 mmol) and KOH (0.52 g, 9.14 mmol) afforded a pale yellow solid (1.77 g, 64%). ^{1}H NMR (400 MHz, DMSO-d_6): δ 7.44 (dd, 3H, $^3J_{HH}$ = 1.7, ArH), 7.14-7.11 (m, 3H, ArH), 6.66 (dd, $^3J_{HH}$ = 1.5, 1H, ArH), 6.57-6.53 (m, 1H, ArH), 4.59 (d, 2H, $^3J_{HH}$ =5.7, CH_2). ^{13}C NMR (100 MHz, $CDCl_3$): δ 153.3 (C), 145.2 (C), 132.7 (CH), 129.1 (CH), 118.3 (CH), 112.1 (CH), 109.3 (C), 42.2 (CH_2). IR (KBr) ν (cm^{-1}): 3426 m, 2916 w, 1595 m, 1510 m, 1456 m, 1424 m, 1399 w, 1324 w, 1311 m, 1271 m, 1220 m, 1163 w, 1097 w, 1021 m, 997 w, 929 w, 903 w, 845 w, 772 s, 736 s, 665 w. HRMS-ESI ([M^+]): m/z calcd: 302.169; found: 302.029.

3.2.2.4 Synthesis of N-(1H-benzoimidazol-2-ylmethyl)-2-thioaniline (L4).

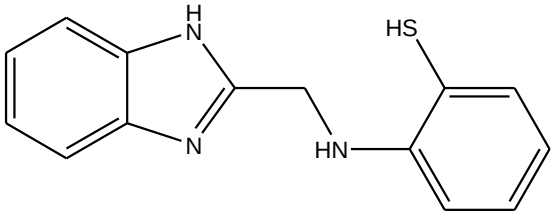

This ligand was prepared in a similar manner as **L1**. 2-chloromethylbenzimidazole (1.26 g, 7.55 mmol), 2-aminothiophenol (0.81 ml, 7.55 mmol), KI (1.25 g, 7.55 mmol) and KOH

(0.43 g, 7.63 mmol) yielded **L4** as a pale yellow solid (1.20 g, 62.3%). ^{1}H NMR (400 MHz, $CDCl_3$): δ 7.52 (dd, 2H, $^{3}J_{HH}$ = 3.2, ArH), 7.31 (dd, 1H, $^{3}J_{HH}$ = 1.5, ArH), 7.23 (dd, 2H, $^{3}J_{HH}$ = 3.2, ArH), 7.14-7.10 (m, 1H, ArH), 6.72 (dd, 1H, $^{3}J_{HH}$ = 1.2, ArH), 6.66-6.63 (m, 1H, ArH), 4.21 (s, 2H, CH_2). ^{13}C NMR (100 MHz, $CDCl_3$): δ 151.7 (C), 148.4 (C), 138.5 (C), 136.3 (CH), 130.8 (CH), 122.6 (CH), 119.1 (CH), 116.6 (C), 115.4 (CH), 115.0 (CH), 32.9 (CH_2). IR (KBr) ν (cm^{-1}): 3358 w, 3053 w, 2743 w, 1604 s, 1531 w, 1477 s, 1432 s, 1308 m, 1272 s, 1227 m, 1139 w, 1023 m, 999 w, 909 w, 841 w, 768 m, 737 s. HRMS-ESI ([M-H^+]): m/z calcd: 255.338; found: 255.078.

3.2.2.5 Synthesis of $[Zn_2(L1)_2(OBn)_4]$ (1)

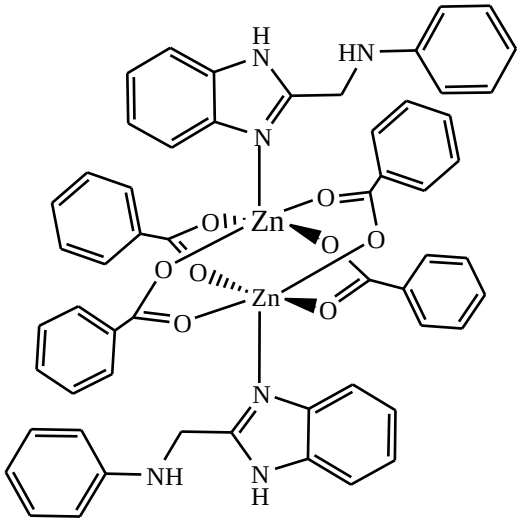

A solution of $Zn(Ac)_2{\cdot}2H_2O$ (0.312 g, 1.42 mmol) and C_6H_5COOH (0.348 g, 2.85 mmol) in methanol (30 ml) was refluxed at 80 ^{o}C for 5 h followed by drop-wise addition of **L1** (0.317 g, 1.42 mmol) in methanol (10 ml). The solution was refluxed for additional 24 h. The reaction mixture was cooled to room temperature, filtered and the solvent removed under reduced pressure to afford sticky yellow precipitate. The resulting yellow precipitate was dissolved in dichloromethane and the solvent remove *in vacuo* to yield a pale yellow solid (0.577 g, 38 %). ^{1}H NMR (400 MHz, DMSO-d_6): δ 7.96 (d, 7H, $^{3}J_{HH}$=*7.4*, ArH), 7.50-7.39

(m, 13H, ArH), 7.20 (br, 4H, ArH), 7.01 (br, 2H, ArH), 6.62-6.56 (m, 3H, ArH), 6.36 (br, 1H, ArH), 4.65 (s, 2H, CH_2). ^{13}C NMR (100 MHz, $CDCl_3$): δ 174.0 (CO), 148.3 (C), 134.5 (C), 131.8 (CH), 129.9 (CH), 129.3 (CH), 128.5 (CH), 123.2 (C), 122.4 (C), 117.5 (C), 113.1 (C), 22.0 (CH_2). IR (KBr) ν (cm^{-1}): 3034 w, 1700 br, 1602 w, 1558 br, 1403 m, 1317 w, 1220 s, 1176 w, 1070 w, 1025 w, 935 w, 841 w, 755 s, 714 m, 687 m. Anal. Calcd for $C_{56}H_{46}N_6O_8Zn_2 \cdot 0.5CH_2Cl_2$: C, 61.45; H, 4.29; N, 7.61. Found: C, 61.69; H, 4.40; N,7.17.

Synthesis of complexes 2-4. These compounds were prepared following the procedure outlined for the synthesis of **1**.

3.2.2.6 Synthesis of $[Zn_2(L2)_2(OBn)_4]$ (2)

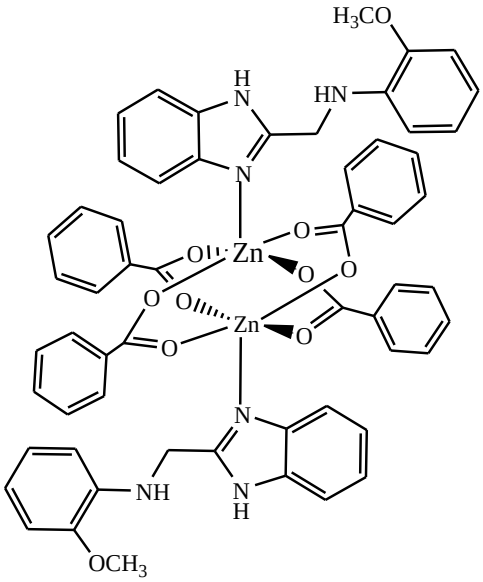

$Zn(Ac)_2 \cdot 2H_2O$ (0.362 g, 1.65 mmol), C_6H_5COOH (0.404 g, 3.31 mmol) and **L2** (0.418 g, 1.65 mmol). Pale yellow solid (0.572 g, 31%). ^1H NMR (400 MHz, $CDCl_3$): δ 7.98-7.96 (m, 2H, ArH), 7.64 (s, 1H, ArH), 7.49-7.39 (m, 4H, ArH), 7.14 (d, 2H, $^3J_{HH}$ = 4.0, ArH), 6.83 (d, 1H, $^3J_{HH}$ = 7.3, ArH), 6.66-6.64 (m, 1H, ArH), 6.56 (t, 1H, ArH), 6.49 (d, 1H, $^3J_{HH}$ = 7.3, ArH), 5.70 (s, 1H, NH), 4.58 (d, 2H, $^3J_{HH}$ = 3.9, CH_2), 3.81 (s, 3H, CH_3). ^{13}C NMR (100 MHz, $CDCl_3$): δ 207.0 (CO), 155.5 (C), 147.1 (C), 137.8 (C), 131.5 (CH), 129.9 (CH), 128.4 (CH),

122.5 (CH), 121.4 (CH), 117. 1 (CH), 110.3 (CH), 110.0 (CH), 41.9 (CH_2), 31.1 (CH_3). IR (KBr) ν (cm^{-1}): 3050 w, 1604 s, 1567 m, 1516 m, 1457 m, 1427 w, 1415 w, 1371 s, 1335 m, 1303 w, 1278 w, 1249 m, 1222 m, 1177 w, 1134 m, 1068 w, 1036 m, 1004 w, 842 w, 749 m, 743 s, 683 m. Anal. Calcd for $C_{58}H_{50}N_6O_{10}Zn_2 \cdot 0.5C_6H_{14}$: C, 62.89; H, 4.93; N, 7.21. Found: C, 63.94; H, 4.63; N, 10.16

3.2.2.7 Synthesis of $[Zn_2(L3)_2(OBn)_4]$ (3)

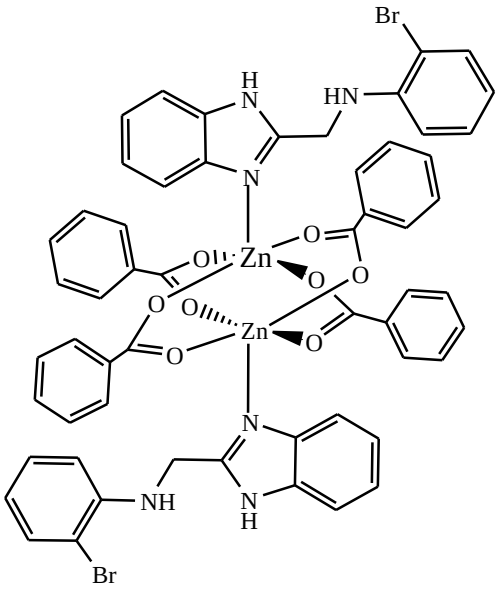

$Zn(Ac)_2 \cdot 2H_2O$ (0.091 g, 0.415 mmol), C_6H_5COOH (0.101 g, 0.826 mmol) and **L3** (0.125 g, 0.415 mmol). Pale yellow solid (0.319 g, 63%). Slow evaporation of methanol solution of **3** at room temperature yielded pale yellow crystals for X-ray diffraction analysis. ^{1}H NMR (400 MHz, DMSO): δ 7.98-7.96 (m, 2H, ArH), 7.64 (s, 1H, ArH), 7.50-7.39 (m, 5H, ArH), 7.15 (s, 2H, ArH), 7.06(s, 1H, ArH), 6.65 (d, 2H, $^3J_{HH}$ = 7.9, ArH), 6.53 (t, 1H, $^3J_{HH}$ = 7.1, ArH), 5.99 (t, 1H, NH), 4.69 (s, 2H, CH_2). ^{13}C NMR (100 MHz, DMSO-d_6): δ 145.1 (C), 132.8 (CH), 129.9 (CH), 129.0 (CH), 128.4 (CH), 118.4 (CH), 112.1 (CH), 109.4 (C), 42.2 (CH_2). IR (KBr) ν (cm^{-1}): 3034 w, 1687 w, 1597 w, 1558 w, 1509 w, 1453 w1383 br, 1220 s, 1022 w, 931 w, 843 w, 772 s, 710 w, 684 w. Anal. Calcd for $C_{56}H_{44}Br_2N_6O_8Zn_2$: C, 55.15; H, 3.64; N, 6.89. Found: C, 55.43; H, 3.83; N, 9.06.

3.2.2.8 Synthesis of $[Zn_2(L4)_2(OBn)_4]$ (4)

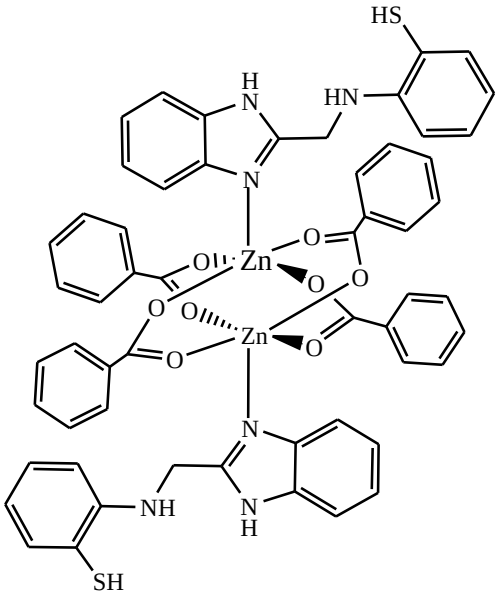

$Zn(Ac)_2{\cdot}2H_2O$ (0.095 g, 0.433 mmol), C_6H_5COOH (0.105g, 0.859 mmol) and **L4** (0.110 g, 0.431 mmol). Pale green solid (0.425 g, 87%). ^{1}H NMR (400 MHz, $CDCl_3$): δ 8.07 (d, H, $^3J_{HH}$ =7.3, ArH), 7.49 (t, H, $^3J_{HH}$ =7.4, ArH), 7.36 (t, H, $^3J_{HH}$ = 7.4, ArH), 7.19-7.13 (m, H, ArH), 6.98 (t, H, $^3J_{HH}$ = 5.6, ArH), 6.73-6.70 (m, H, ArH), 6.58 (ddd, H, $^3J_{HH}$ = 1.3, 1.4, 1.4, ArH), 6.52 (s, 1H, NH), 4.41 (s, 2H, CH_2). ^{13}C NMR (100 MHz, $CDCl_3$): δ 173.4 (CO), 148 .6 (C), 136.8 (CH), 132.6 (CH), 132.3 (C), 131.6 (CH), 130.3 (CH), 128.2 (CH), 124.0 (C), 118.8 (C), 118.3 (CH), 115.3 (CH) 22.1 (CH_2). IR (KBr) ν (cm^{-1}): 3061br, 1705 m, 1600 s, 1559 s, 1478 w, 1448 m, 1400 s, 1314 m, 1281 m, 1250 m, 1175 m, 1158 m, 1070 m, 1048 m, 1024 m, 936 w, 916 w, 842 m, 820 w, 772 m, 747 m, 684 m. Anal. Calcd for $C_{56}H_{46}Zn_2N_6O_8S_2{\cdot}CH_2Cl_2$: C, 56.54; H, 4.00; N, 6.94. Found: C, 56.48; H, 4.34; N, 6.02.

3.2.2.9 Synthesis of $[Cu_2(L1)_2(OBn)_4]$ (5)

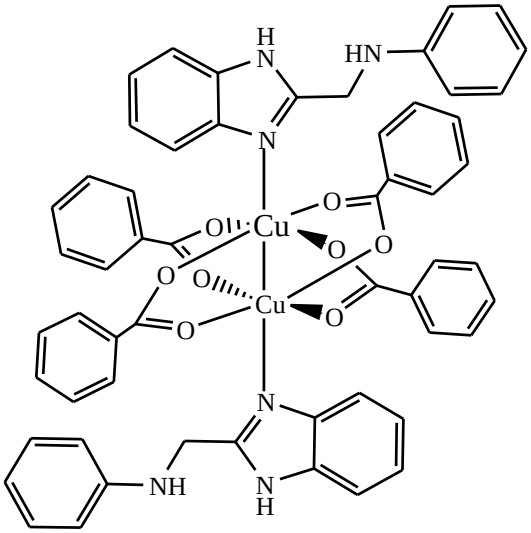

$Cu(Ac)_2{\cdot}2H_2O$ (0.282 g, 1.41 mmol) was added to a solution of C_6H_5COOH (0.345 g, 2.82 mmol) in methanol (40 ml) and refluxed for 5 h at 80^{o}C. This was followed by drop-wise addition of **L1** (0.315 g, 1.41 mmol) in methanol (5 ml) and further refluxed for additional 24 h. The reaction mixture was cooled to room temperature and filtered. The filtrate was dried under reduced pressure to yield sticky green precipitate. The resulting precipitate was recrystallized in dichloromethane/hexane solvent mixture to afford a green solid (0.417 g, 28%). IR (KBr) ν (cm^{-1}): 2830 br, 2555 w, 1917 br, 1682 s, 1602 m, 1583 m, 1497 w, 1453 m, 1419 m, 1324 m, 1290 s, 1220 s, 1180 m, 1128 m, 1101 w, 1073 m, 1001 w, 933 s, 805 m, 706 m, 684 m, 667 m. Anal. Calcd for $C_{56}H_{46}Cu_2N_6O_8{\cdot}0.5C_6H_{14}$: C, 64.35; H, 4.85; N, 7.63. Found: C, 64.72; H, 4.68; N, 1.46. μ_{eff} = 1.85 BM.

3.2.2.10 Synthesis of $[Cu_2(L3)_2(OBn)_2]$ (6)

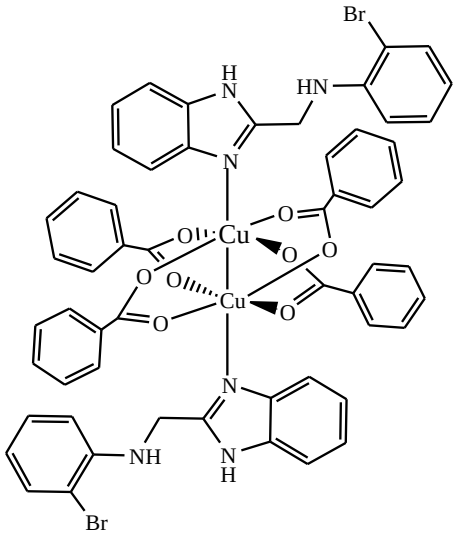

This compound was prepared following a similar procedure outlined for **5**. **L3** (0.308 g, 1.02 mmol), $Cu(Ac)_2{\cdot}2H_2O$ (0.205 g, 1.03 mmol) and C_6H_5COOH (0.250 g, 2.05 mmol). Pale green solid (0.512 g, 41%). Slow evaporation of methanol solution of **6** at room temperature yielded pale green crystals suitable for X-ray diffraction analysis. IR (KBr) ν (cm^{-1}): 2831 w, 2554 w, 1684 s, 1601 m, 1573 m, 1496 w, 1453 m, 1400 s, 1324 m, 1291 s, 1178 m, 1128 w, 1072 w, 1026 w, 933 m, 843 w, 805 w, 745 m, 684 m, 667 m. Anal. Calcd for $C_{56}H_{44}Br_2Cu_2N_6O_8{\cdot}0.5CH_2Cl_2$: C, 53.93; H, 3.60; N, 6.68. Found: C, 54.07; H, 4.10; N, 6.51. μ_{eff} = 1.86 BM.

3.2.2.11 Synthesis of [Zn(L1)$_2$(OAc)$_2$] (7)

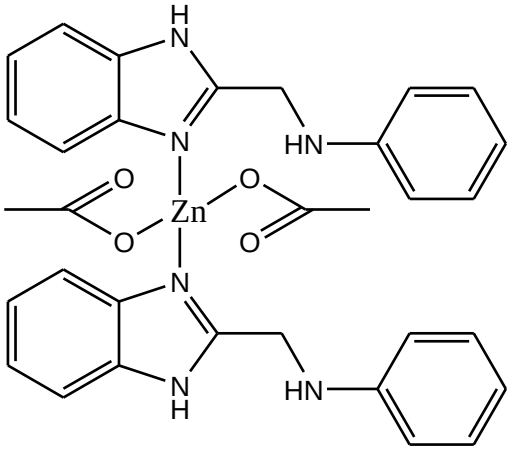

To a solution of **L1** (0.24 g, 1.08 mmol) in methanol (5 ml) was added $ZnAc_2 \cdot 2H_2O$ (0.24 g, 1.08 mmol) and stirred at room temperature for 24 h. After the reaction period, the solution was evaporated under vacuum and the crude product recrystallized from dichloromethane/hexane solvent mixture to afford **7** as a pale yellow solid (0.27 g, 62 %). ^{1}H NMR (400 MHz, DMSO-d_6, ppm): 6.3-7.7 (m, 9H, Ar-H); 4.4 (s, 2H, CH_2); 1.8 (s, 6H, CH_3). (ESI-MS) m/z (%): 405 (M^+, 5); 346.04 (M^+-$C_2H_3O_2$, 60); 223.11 (M^+- $C_4H_6O_4Zn$, 15). Anal. Calcd. for $C_{32}H_{32}N_6O_4Zn \cdot 1.75CH_2Cl_2$: C, 52.06; H, 4.60; N, 10.79. Found: C, 52.12; H, 4.83 N, 16.17.

3.2.2.12 Synthesis of [Zn(L3)$_2$(OAc)$_2$] (8)

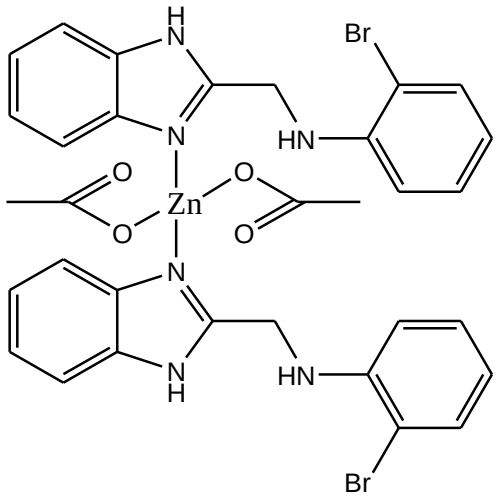

To a solution of **L3** (0.13 g, 0.42 mmol) in methanol (5 ml) was added $ZnAc_2{\cdot}2H_2O$ (0.092 g, 0.42 mmol) and stirred at room temperature for 24 h. After the reaction period, the solution was evaporated under vacuum and the crude product recrystallized from dichloromethane/hexane solvent mixture to afford complex **8** as a pale yellow solid (0.13 g, 62 %). Slow evaporation of dichloromethane solution of **8** at room temperature yielded pale yellow crystals for X-ray diffraction analysis.^{1}H NMR (400 MHz, $CDCL_3$, ppm): 7.6 (s, 2H, Ar-H); 7.4 (s, 2H, Ar-H); 7.3(s, 2H, Ar-H); 7.0 (s, 1H, Ar-H); 6.5 (s, 2H, Ar-H) 4.7 (s, 2H, CH_2); 2.0 (s, 6H, CH_3). ^{13}C NMR (100 MHz, DMSO): δ 176.3, 145.2, 132.6, 128.9, 121.9, 118.5, 109.6, 23.1. Anal. Calcd. for $C_{32}H_{30}N_6O_4Br_2Zn{\cdot}CH_2Cl_2$: C, 45.41; H, 3.70; N, 9.63. Found: C, 45.92; H, 3.73 N, 9.67.

3.2.2.13 Synthesis of $[Cu_2(L1)_2(Ac)_4]$ (9)

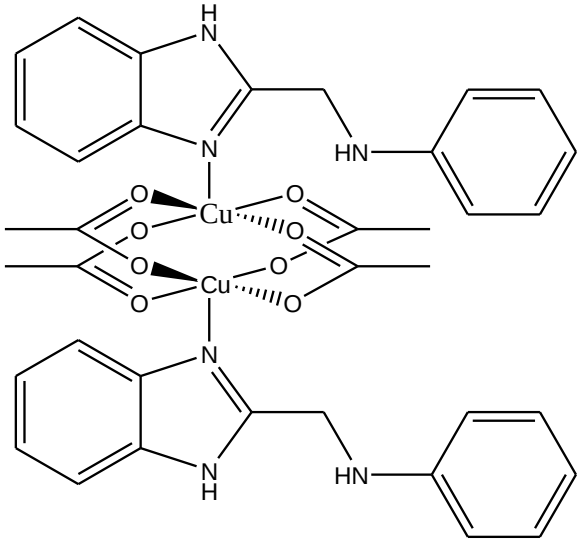

This complex was prepared by dissolving **L1** (0.18 g, 0.82 mmol) and $CuAc_2{\cdot}2H_2O$ (0.16 g, 0.82 mmol) in methanol (10 ml) and stirred for 24 h at room temperature. The resulting precipitate was collected by filtration, washed with methanol to give **9,** a pale blue solid (0.22 g, 66 %). (ESI-MS) m/z (%): 404 (M^+, 20); 345 (M^+-$C_2H_3O_2$, 10). Anal. Calcd for $C_{36}H_{38}N_6O_8Cu_2{\cdot}0.25CH_2Cl_2$: C, 53.39; H, 4.73; N, 10.38. Found: C, 52.16; H, 3.99; N, 11.45. μ_{eff} = 2.12 BM

3.3 Results and discussion

3.3.1 Ligands and complexes syntheses

The benzoimidazolyl amine ligands, **L1-L4**, were synthesized using a modified literature procedure[22] by reacting equimolar amounts of 2-chloromethylbenzimidazole with potassium iodide followed by the addition of the appropriate aniline. The reaction proceeded in a two-step single pot process where the chlorine atom on the 2-chloromethylbenzimidazole was first replaced by iodide, I⁻, before the aniline molecule was introduced to form the respective compounds (Scheme 3-1). The ligands were obtained in moderate to good yields (51-71 %) as pale yellow solids.

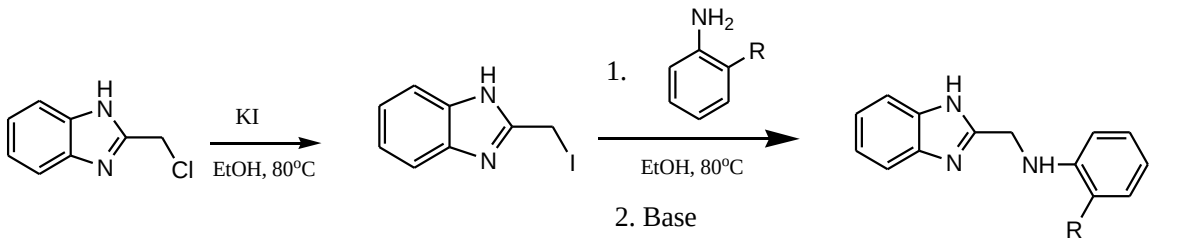

R = H **(L1)**; R = OCH_3 **(L2)**
R = Br **(L3);** R= SH **(L4)**

Scheme 3-1

The Zn(II) and Cu(II) benzoate complexes, **1**-**6**, were synthesized by a one-pot two step reaction process. The initial step involved the formation of the metal benzoate salt by reacting the appropriate metal acetate with benzoic acid in a 1:2 stoichiometric ratio respectively. This was followed by the *in situ* addition of the appropriate ligands, **L1**-**L4,** to form the corresponding binuclear compounds in low to good yield (21–87 %) (Scheme 3-2). The zinc complexes were pale yellow in color while the copper complexes were pale blue. All the complexes were soluble in polar organic solvents such as DMSO.

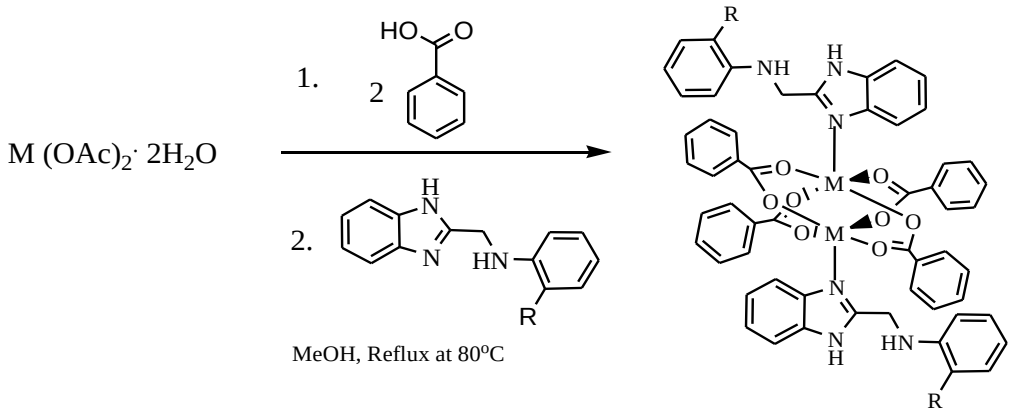

M=Zn, R=H (**1**); M=Zn, R=OCH3 (**2**); M=Zn, R=Br (**3**);
M=Zn, R=SH (**4**); M=Cu, R=H (**5**); M=Cu, R=Br (**6**)

Scheme 3-2

The Zn(II) and Cu(II) acetate complexes on the other hand were synthesized *via* a single step process by reacting the respective metal acetates with the corresponding ligand in a 1:1 ratio. The complexes were isolated in good yields (62-66 %) (Scheme 3-3).

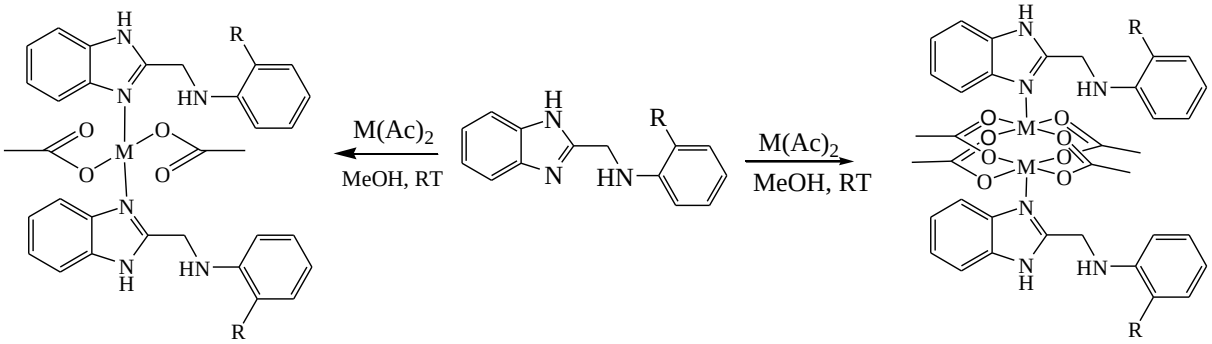

M, R
M= Zn, R= H (**7**)
M= Zn, R= Br (**8**)

M, R
M= Cu, R= H (**9**)

Scheme 3-3

The formation and identity of the ligands were established by analyzing the chemical shift of the diagnostic methylene protons of the benzimidazole from the ^{1}H NMR spectra. For instance in **L1**, the methylene protons (CH_2) shifted upfields from 4.94 ppm in the starting material, 2-chloromethylbenzimidazole, to 4.62 ppm in the product (Figure 3.1). Similarly, the methylene peaks were observed at 4.69 ppm, 4.59 ppm and 4.21 ppm for **L2**, **L3** and **L4** respectively. The methylene

protons appeared as a singlet in all the ligands except **L3** where it was observed as a doublet, hence, the quest to establish the source of the coupling.

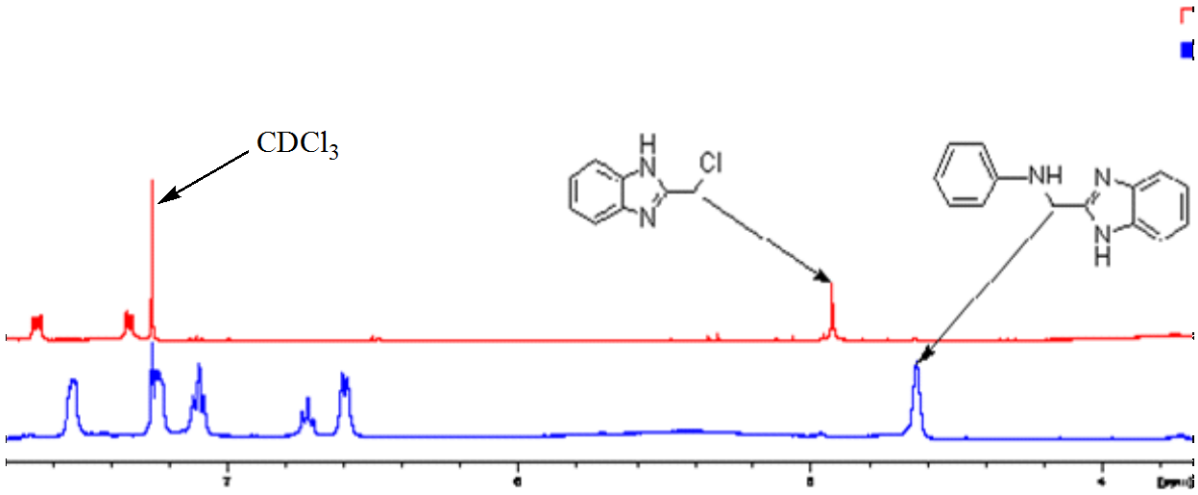

Figure 3.1: ^{1}H NMR of **L1** showing the CH_2 linker

This observation could be ascribed to the coupling of the methylene protons with the proton on the adjacent amine group as a result of the slow rate of exchange of the N–H protons in the presence of an electron withdrawing molecule(s) at the *ortho* position.[23] The ^{1}H–^{1}H COSY of **L3** was used to establish this coupling between the two adjacent protons (Figure 3.2). The off diagonal spots *a* and *b* in the spectrum confirms the coupling of the N–H and CH_2 protons.

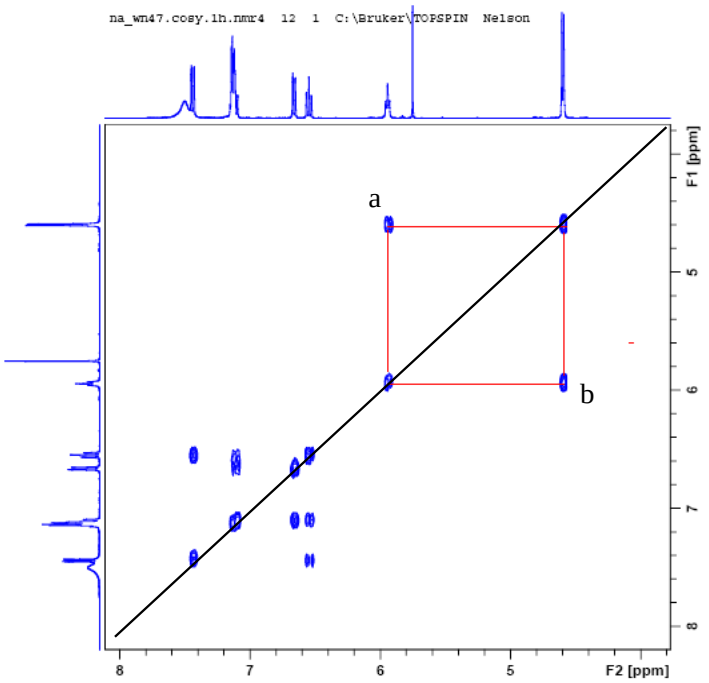

Figure 3.2: ^{1}H–^{1}H COSY spectra of **L3** confirming the coupling of the CH_2 and NH protons

The identity of the ligands, **L1**-**L4**, was also confirmed by HR-MS. For instance, the mass spectrum of **L4** (Figure 3.3) showed *m/z* peaks at 254.0753 corresponding to the base peak, [**L4**–H]$^{+}$, and *m/z* peak at 255.0784 representing the molecular ion.

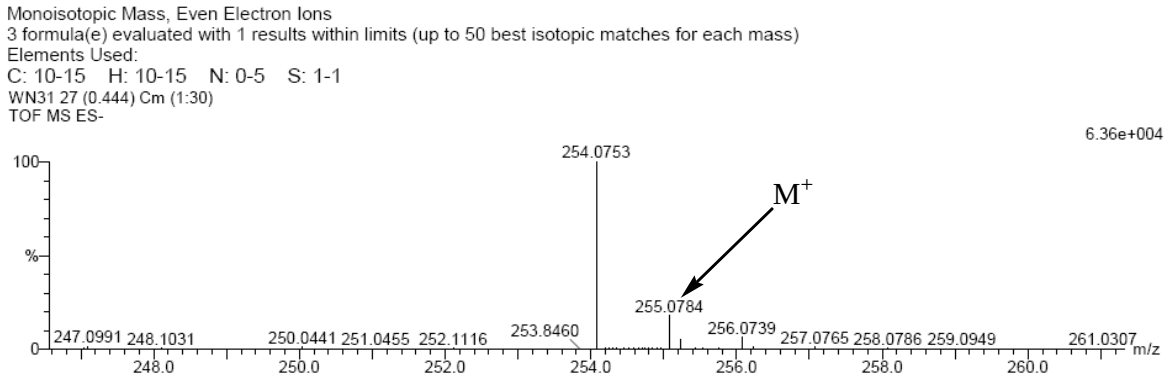

Figure 3.3: HR-MS spectrum of L4 showing the molecular ion and base peak.

All the zinc complexes (**1-4, 7** and **8**) were characterized by NMR spectroscopy while the copper complexes (**5**, **6** and **9**) were not due to their paramagnetic nature. The NMR spectra

of all the complexes were in conformity to the proposed structure. For instance, in the ^{1}H NMR spectrum of **3**, a slight shift in the methylene proton (CH_2 linker) from 4.59 ppm in the ligand (**L3**) to 4.69 ppm was indicative of complexation. This slight chemical shift observed could be due to the proximity of the coordination site from the CH_2 protons. In addition, significant shifts were observed for the protons on the benzimidazole ring (Figure 3.4).

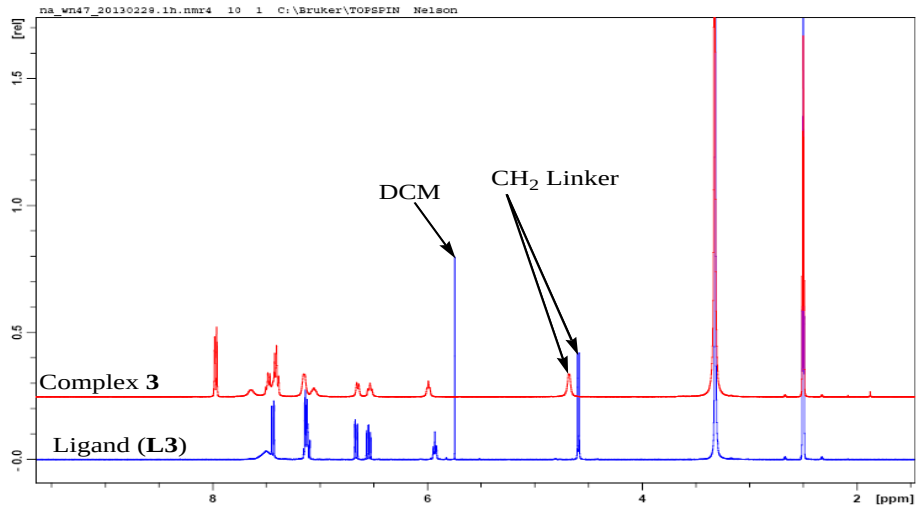

Figure 3.4: Overlay of **L3** and **3** ^{1}H NMR spectra showing shift in the CH_2 linker from 4.59 ppm to 4.69 ppm

^{13}C NMR was also used to diagnose complex formation as well as the mode of binding of the carboxylate group. Typical ^{13}C NMR chemical shifts for the CO group in metal carboxylates are within 160-192 ppm depending on the electronic properties of the complex, the binding fashion of the carboxylate group and the state in which the sample was analyzed.[24] For instance, the chemical shifts of bridging carbonyl carbons are normally observed downfield while monodentate carbonyl carbons are observed upfields due to increase in deshielding effect as the carbonyl carbon becomes more positively charged.[25] The monodentate carbonyl carbons are normally observed between 166 to 178 ppm while the carbonyl carbons in bridging mode are normally observed above 180 ppm.[25] ^{13}C NMR spectrum of **8** displayed the carbonyl carbon peak at about 176 ppm indicative of monodentate coordination mode which is also supported by the solid state structure in Figure 3.10. However, the spectrum of

3 was poorly resolved possibly due to poor dissolution and the bulky nature of the complex hence unable to identify the carbonyl carbon.

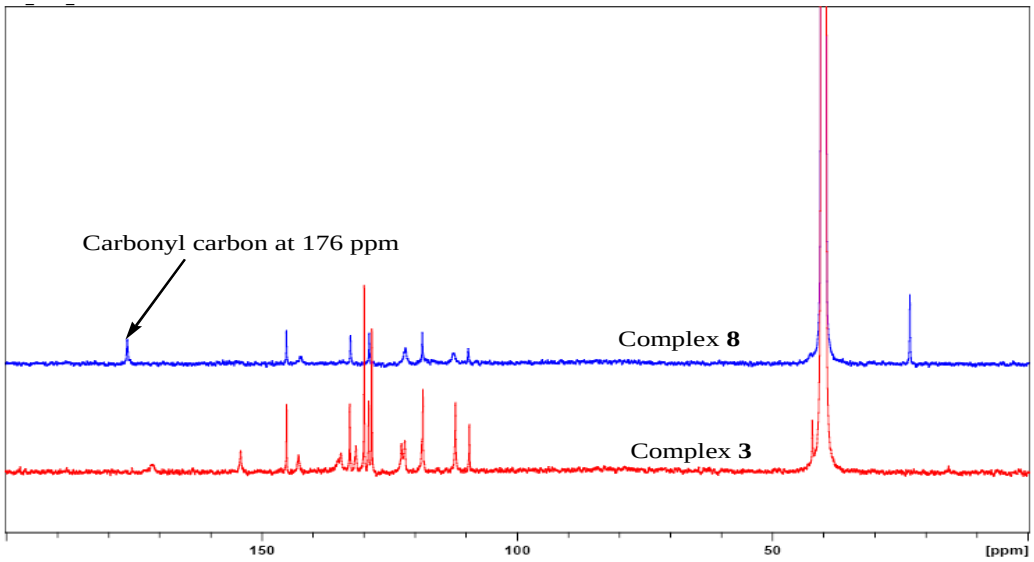

Figure 3.5: ^{13}C NMR spectra of **3** and **8**. The peak at 176 ppm in **8** is indicative of monodentate binding mode of the carboxylate however the spectrum of **3** displayed no peak downfield.

The complexes were also characterized by mass spectrometry. For example, the ESI-MS spectrum of **7** showed *m/z* peaks at 405 and 346 corresponding to $[M\text{-}C_{14}H_{13}N_3]^+$ and $[M\text{-}C_{16}H_{16}N_3O_2]^+$ respectively (Figure 3.6). Besides these peaks, the *m/z* peak at 223 was assigned to $[M\text{-}C_{18}H_{19}N_3O_4Zn]^+$. However, the fragmentation pattern of the other complexes did not show a clear trend. This could be due to compound instability under the operating conditions as several *m/z* peaks could not be related to specific complex fragments.

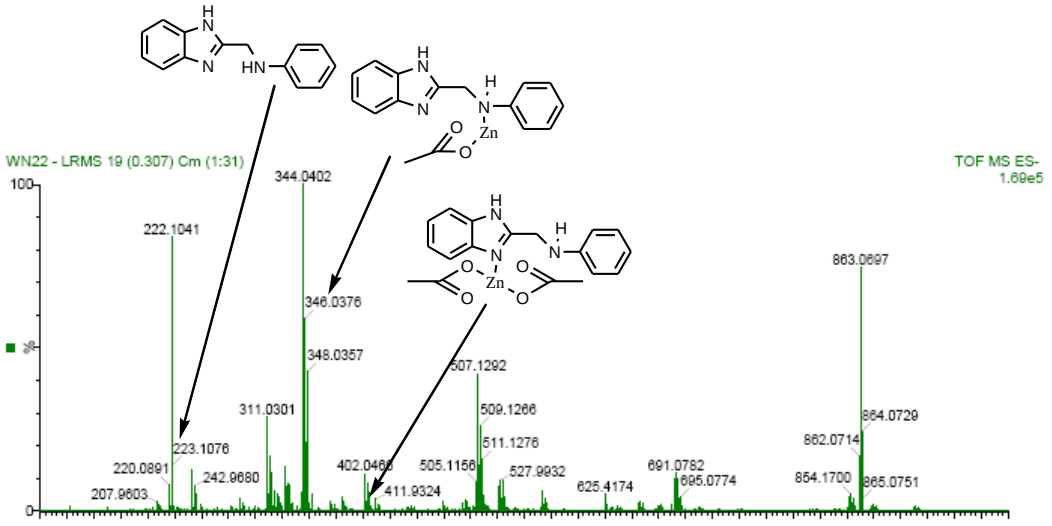

Figure 3.6: HR-MS spectrum of complex **7** showing m/z peak of the fragments

The characteristic absorption of the ligands and complexes in the infrared region of the electromagnetic spectrum was also used to deduce the chemical environments of the N–H and C=N functional groups and hence the formation of the complexes. The IR spectra of the ligands displayed a strong ν_{N-H} stretching band between 3427 to 3357 cm^{-1} and broad absorption bands ranging from 2916 to 3053 cm^{-1} which could be assigned to intermolecular hydrogen bonds.[26] The bands associated with $\nu_{C=N}$ stretching of the benzimidazole were between 1604 to 1594 cm^{-1} comparable to other literature results of 1600 to 1633 cm^{-1}.[27] A useful feature in the elucidation of complex formation was the significant shifts in the $\nu_{C=N}$ bands from lower frequencies (in the ligands) to higher frequencies in the complexes (Table 3.1). For example, the frequency of C=N vibration in **L3** shifted from 1595 cm^{-1} to 1687 cm^{-1} in the corresponding complex **3** (Figure 3.7). This indicates the binding of the metals to the unsaturated nitrogen atom of benzimidazole which is in agreement with most benzimidazole complexes.[28] The disappearance of the sharp N–H band in the complex could be due to inter- or intramolecular H-bond interaction.

Table 3.1 C=N stretching band for complexes (ligands)[a]

Complexes	$\nu_{C=N}$ /cm^{-1}	Complexes	$\nu_{C=N}$ /cm^{-1}
1	1700 (1604)	**4**	1705 (1604)
2	1604 (1602)	**5**	1682 (1604)
3	1687 (1595)	**6**	1679 (1602)

[a] $\nu_{C=N}$ of ligands in brackets

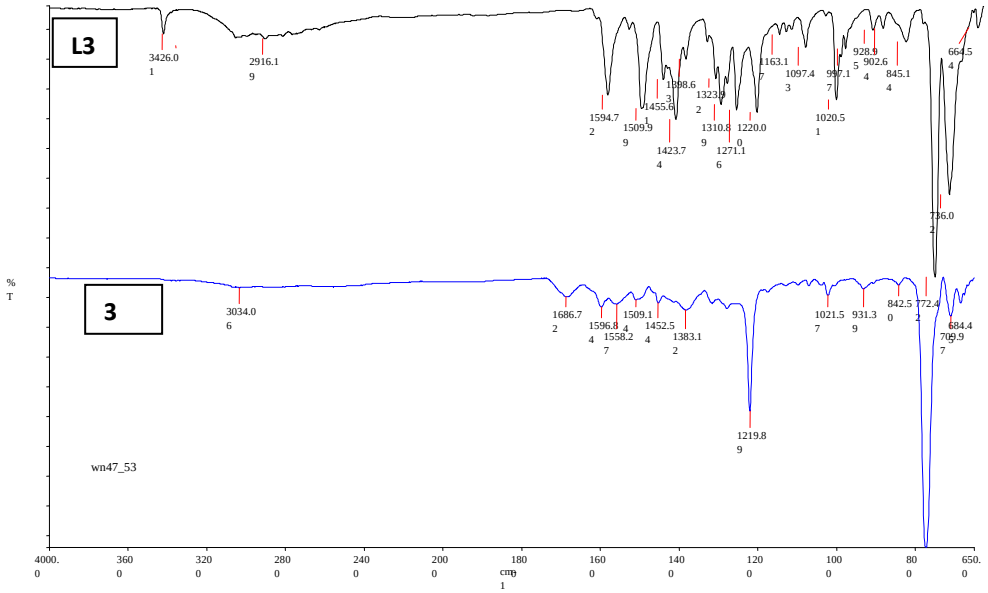

Figure 3.7: IR spectrum of **L3** and **3** showing the shift in $\nu_{C=N}$

The measured room temperature magnetic moment for **5**, **6** and **9** were obtained as 1.85, 1.86 and 2.12 BM respectively. These observed magnetic moments are similar to other literature reports where complexes with Cu-Cu interaction exhibited lower magnetic moments of about 1.53 BM.[29] However, the magnetic moment of Cu(II) ion ranges between 1.73 -3.00 BM and that of $CuAc_2{\cdot}2H_2O$ is 1.34 BM (289.3K) and 1.40 BM (320.7K).[12] A marked change from the reference value of the starting material, $CuAc_2{\cdot}2H_2O$, thus indicates complex formation between the metal acetate and the ligand. Furthermore, the complexes exhibited magnetic moments that are within the ranges of Cu(II) ion in d^9 electronic configuration, hence, the results indicate the presence of Cu atom in the compounds.

Microanalyses of all the complexes were performed to ascertain their purity and consistency with the proposed structures (Schemes 3-2 and 3-3). From the data obtained, the empirical formulae of complexes **1**-**6** and **9** were consistent with one metal centre, one ligand unit and two acetate or benzoate units [$ML(OR)_2$] while those of compounds **7** and **8** agreed with one metal centre, two ligand units and two acetate units [$ML_2(OR)_2$]. The measured C, H and N values for compounds **1**, **6** and **8** were within the acceptable range. However, the N content of **3**, **4**, **5** and **7** deviated from the acceptable range. The deviation could be due to instrument calibration of the N atom since the respective C and H contents were within the acceptable purity range. The measured C, H, N values for complexes **2** and **9** deviated slightly from the acceptable range possibly due to the *in situ* generation of the metal benzoate before reacting with the ligand. This is likely to generate acetic acid as an impurity/by-product. Attempts to purify these two compounds to the required levels have so far been unsuccessful.

3.3.2 Solid state structures of complexes 3, 6 and 8

Single crystals of **3**, **6** and **8** suitable for X-ray diffraction analyses were obtained from slow evaporation of a methanol solution of **3** and **6** and dichloromethane solution of **8** at room temperature. A summary of crystallographic data and structural refinement parameters are presented in Table 3.2 whilst Tables 3.3 to 3.5 contain selected bond lengths and angles for the complexes.

Table 3.2 Crystal data for complexes **3, 6** and **8.**

Crystal data	**3**	**6**	**8**
Chemical formula	$C_{56}H_{44}Br_2N_6O_8Zn_2.2CH_3OH$	$C_{56}H_{44}Br_2Cu_2N_6O_8 \cdot 2CH_3OH$	$C_{32}O_4ZnBr_2N_6H_{30}$
Mr	1283.62	1279.96	787.81
Crystal system	Triclinic	Triclinic	Triclinic
space group	P-1	P-1	P-1
Temperature (K)	100	100	173
a, b, c (Å)	10.7836 (15), 11.6897 (16), 11.6997 (16)	10.5718 (7), 11.6594 (7), 11.6631 (7)	9.4041(6), 12.1658(8) , 14.7332(9)
α, β, γ (o)	74.925 (8), 82.395 (8), 75.853 (8)	75.481 (3), 75.859 (3), 82.766 (3)	103.670(3) , 102.615(3), 94.692(3)
V (Å3)	1377. 2 (3)	1346.32 (14)	1582.42(17)
Z	2	1	2
Radiation type	$M_o K_\alpha$	$M_o K_\alpha$	$M_o K_\alpha$
μ (mm^{-1})	2.39	2.34	
Crystal size (mm)	0.38 × 0.35 × 0.25	0.20 × 0.20 × 0.15	0.10 × 0.10 × 0.10
Data collection			
Diffractometer	Bruker Apex II Duo diffractometer	Bruker Apex II Duo diffractometer	Bruker Apex II Duo diffractometer
Absorbtion correction	Multi-scan Bruker SADABS	Multi-scan Bruker SADABS	Multi-scan Bruker SADABS
T_{min}, T_{max}	0.464, 0.587	0.652, 0.720	
No of measured, independent and observed [I> 2σ(I) reflections	11291, 4843, 4391	23779, 6531, 5905	611,323,107
R_{int}	0.021	0.018	
Refinement			
$R[F^2>2\sigma(F^2)]$, $wR(F^2)$, *S*	0.023, 0.052, 1.05	0.034, 0.094, 1.07	
No. of reflections	4843	6531	23107
No. of parameters	358	365	424
No. of restraints	0	0	0

The solid state structures of the **3** and **6** as revealed from the single crystal X-ray analysis showed that the complexes are binuclear and exhibit inverted symmetries. Each asymmetric unit of the complexes comprises of only one metal centre, two benzoate ligands and one benzimidazolyl ligand. For each molecule, the two metal centres are bridged by two pairs of benzoate ligands to form a paddle-wheel structure. Complex **8** on the other hand is mononuclear with no inverted symmetry. The asymmetric unit consists of a metal centre, two ligand units and two acetate groups.

In the molecular structure of **3** (Figure 3.8), each Zn(II) atom of the binuclear compound is coordinated equatorially by four O-atoms of the benzoate and one axial N-atom from the

ligand, **L3**, to give a five-coordinate geometry. The ligand, **L3**, coordinates in a monodentate fashion *via* the benzoimidazolyl N-atom. The protonated benzimidazole N-atom is non-coordinative but interacts with the O-atom of the solvent molecule (CH_3OH) *via* hydrogen bonding. The Zn–O bond lengths in the equatorial plane are in the range of 2.0269 (14) – 2.1164 (14) Å while the axial Zn–N bond length is 2.0195 (16) Å which are similar to other reported Zn(II) complexes.[30] The Zn–N bond length of complex **3** compares well with 2.02 Å reported for a single N-atom coordinated axially[31] but shorter than the average Zn–N bond length of 2.10-2.11 Å reported for a four-coordination[32] and six-coordinated zinc atoms with bond length in the rage of 2.15-2.19 Å.[33] The relatively shorter Zn–N bond length could be due to the high number of coordination of the metal centre.[34] The bond angles of N–Zn–O range from 98.5 (6) ^{o} to 102.9 (6) ^{o}, a deviation from a regular square pyramidal geometry of 90^{o} which could be due to steric hindrances from the bulky ligand units. The Zn$\cdots$Zn distance between the two Zn atoms bridged by the four carboxylate groups is 3.0311 (6) Å, similar to literature reports of other dimeric Zn(II) complexes.[35] The observed metal-metal distance is greater than the sum of the van der Waal radii of Zn (1.39 Å)[36] and thus suggest the absence of Zn–Zn interatomic metal bond. Each Zn-atom is therefore five-coordinated and adopts a distorted square pyramidal geometry.

Table 3.3 Selected bond length (Å) and bond angle (^{o}) of **3**

Zn1—Zn1^{i}	3.0311 (6)	O1^{i}—Zn1—Zn1^{i}	71.44 (4)	O4—Zn1—O1^{i}	87.40 (6)
Zn1—O1^{i}	2.1164 (14)	O2—Zn1—Zn1^{i}	87.04 (4)	O4—Zn1—O2	85.94 (6)
Zn1—O2	2.0856 (14)	O2—Zn1—O1^{i}	158.43 (5)	N3—Zn1—Zn1^{i}	169.62 (5)
Zn1—O3	2.0269 (14)	O3—Zn1—Zn1^{i}	81.43 (4)	N3—Zn1—O1^{i}	98.51 (6)
Zn1—O4	2.0274 (14)	O3—Zn1—O1^{i}	90.37 (6)	N3—Zn1—O2	102.91 (6)
Zn1—N3	2.0195 (16)	O3—Zn1—O2	87.84 (6)	N3—Zn1—O3	101.64 (6)
O1—Zn1^{i}	2.1164 (14)	O3—Zn1—O4	157.03 (6)	N3—Zn1—O4	101.30 (6)
		O4—Zn1—Zn1^{i}	76.18 (4)		

[i] the symmetry transformation used to generate equivalent atoms; -*x*+1, -*y*+1, -*z*+2.

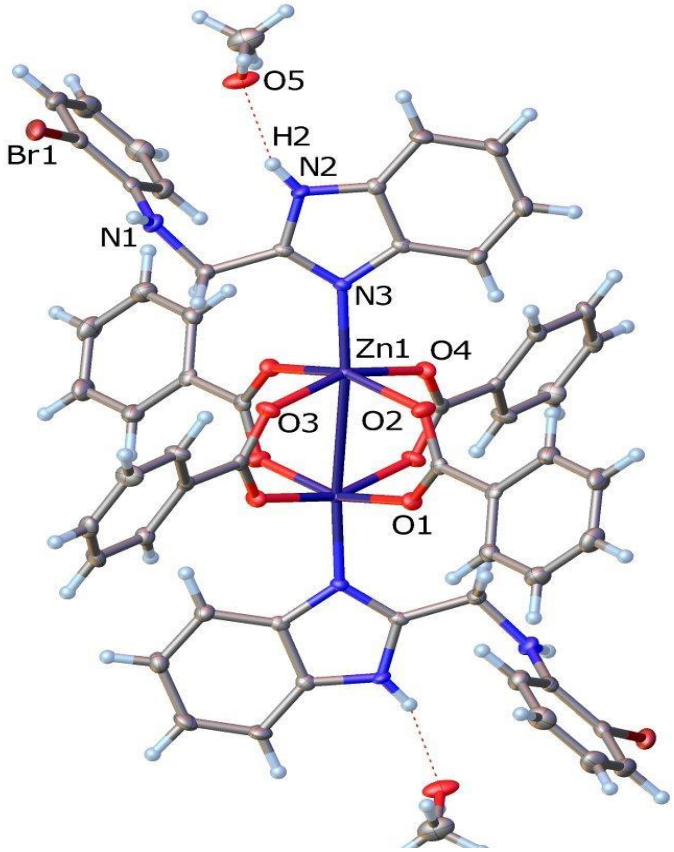

Figure 3.8: ORTEP view of the solid-state structure of **3** with thermal ellipsoid drawn at 50 % probability level.

In the binuclear structure of **6** (Figure 3.9), each Cu atom is also bonded to four oxygen atoms of the carboxylate equatorially with Cu–O bond length ranging from 1.9549 (16) Å to 1.9970 (16) Å. The N-atom of the monodentate benzimidazole ligand is bonded axially to Cu(II) to record Cu–N bond length of 2.1390 (19) Å. The basal plane O–Cu–O bond angles range from 88.00 (8)^{o} to 166.94 (7)^{o} and deviates from a regular octahedral suggesting the geometry around each copper atom is a slightly distorted octahedral. The average Cu–O and Cu–N bond lengths of 1.9759 and 2.1390 (19) Å respectively compares favorably to other related Cu(II) complexes.[37] The Cu–Cu bond distance of 2.6946(5) Å (Table 3.4) is within the normal range of 2.40 - 2.70 Å reported for related complexes.[38]

Table 3.4 Selected bond lengths (Å) and bond angles (^{o}) of **6**

Cu(1)-O(3)	1.9549(16)	O(3)-Cu(1)-O(1)	166.48(7)
Cu(1)-O(1)	1.9624(16)	O(1)-Cu(1)-O(2)	90.64(7)
Cu(1)-O(4)	1.9891(17)	O(4)-Cu(1)-O(2)	166.94(7)
Cu(1)-O(2)	1.9970(16)	O(3)-Cu(1)-N(1)	96.84(7)
Cu(1)-N(1)	2.1390(19)	O(1)-Cu(1)-N(1)	96.62(7)
		O(4)-Cu(1)-N(1)	98.56(7)
Cu(1)-Cu(1)^{i}	2.6946(5)	O(2)-Cu(1)-N(1)	94.47(7)

^{i} The symmetry transformation used to generate equivalent atoms; *-x*+1, *-y*, *-z*+2.

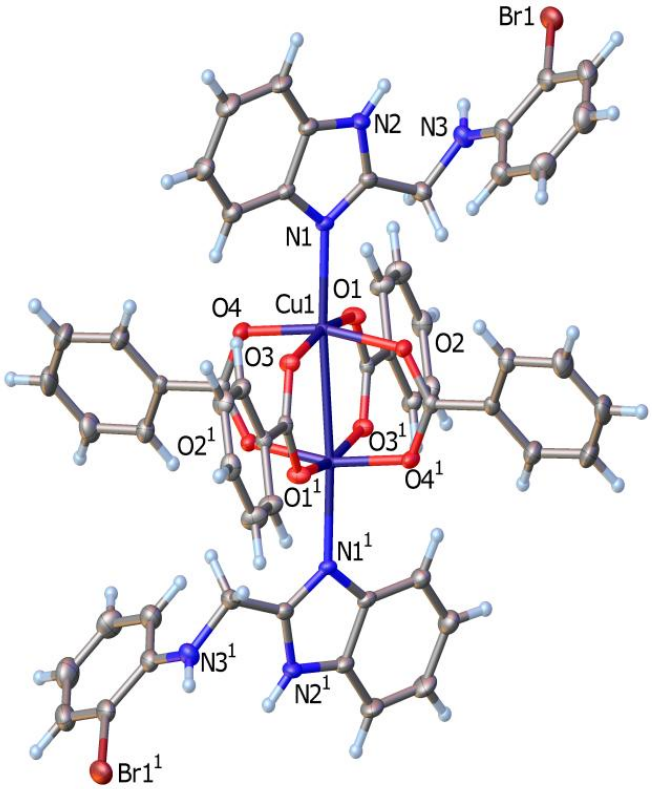

Figure 3.9: ORTEP view of the solid state structure of **6** with thermal ellipsoid drawn at 50 % probability level.

Solid state structure of the acetate Zn(II) complex **8** confirmed the formation of a mononuclear species (Figure 3.10) in which the Zn atom consists of two monodentate ligand **L3** units and two monodentate acetate groups to complete a four-coordination environment. Each ligand is coordinated to Zn(II) atom *via* the benzoimidazolyl nitrogen atom as observed in the solid state structures of complexes **3** and **6**. The Zn-N and Zn-O bond lengths observed (Table 3.5) compares well with other complexes with similar geometry where Zn-N were around 2.015 (2) to 2.047(2) Å and Zn-O bond lengths were in the range of 1.96 (2) to 1.98

(2) Å.[39] The bond angles deviate from the regular tetrahedron of 109.5°, hence the four coordinated Zn(II) atom exhibits a distorted tetrahedral geometry.

Table 3.5 Selected bond lengths (Å) and bond angles (°) of **8**

Zn1-O3	1.9708(13)	O1-Zn1-O3	117.84(6)
Zn1-N4	2.0346(16)	O1-Zn1-N4	105.66(6)
Zn1-N1	2.0277(17)	O1-Zn1-N1	118.81(6)
Zn1-O1	1.9493(14)	N1-Zn1-N4	100.27(7)

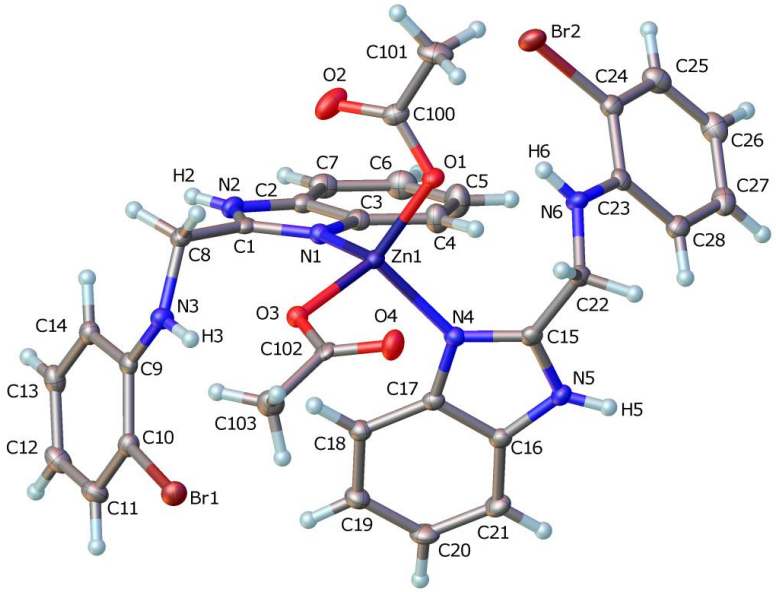

Figure 3.10: ORTEP view of the solid-state structure of **8** with thermal ellipsoid drawn at 50 % probability level.

The protonated N-atom of the benzimidazole moiety is non-coordinating but is involved in intra and intermolecular hydrogen bonding with the O-atom of the acetate. The intramolecular H-bonding is between the N-H of the benzoimidazolyl ligand and the O-atom of the acetate within the same molecule while the intermolecular H-bonding interaction is between the N-H of the benzimidazole ligand and adjacent O-atom of the acetate (Figure 3.11). This intermolecular H-bonding results in the formation of 1-D system.

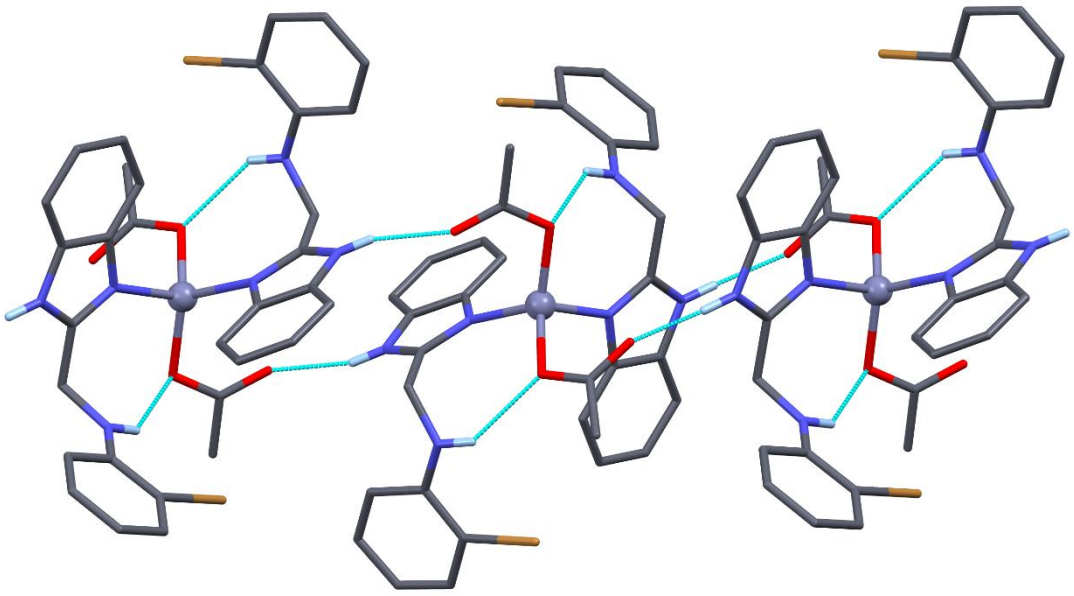

Figure 3.11: Packing diagram of **8** showing the N-H···O hydrogen bonding

3.3.3 Electron Paramagnetic Resonance (EPR) Analysis

Structural characteristics of paramagnetic copper complexes **5** and **6** in solid and solution states were investigated using EPR spectroscopy at room temperature. The solution and solid state X-band EPR spectra of complexes **5** and **6** are shown in Figure 3.12. The measured EPR spectra parameters are presented in Table 3.6.

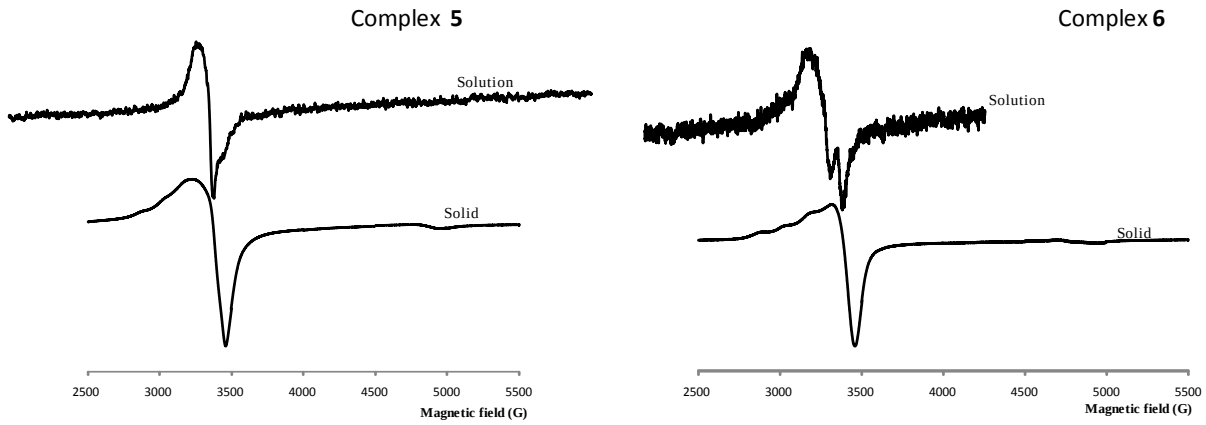

Figure 3.12: Solution and powdered-state X-band EPR spectra of complex **5** & **6** at room temperature

The observed spectra of the complexes in solid and solution-state indicates a non-coupling interaction of the unpaired copper electrons in the dimer. The non-interaction of the two Cu centres could be ascribed to the larger separation which is evident in the Cu–Cu bonds of 2.69 Å determined by single crystal X-ray of complex **6.** This Cu–Cu distance is longer than the estimated bond distances of 1.6 Å that allows electron spin–spin coupling to make the complexes magnetically dilute.

The solid-state spectra of both complexes exhibited four hyperfine splitting in the parallel region and a weak up-field absorbance (around 4900 G) attributed to the dimer signal (g_x). The weak resolution of the hyperfine splitting in the spectrum is due to the spin coupling exchange between the oxygen molecule and the Cu(II) ion[40] and also the longer spin-lattice relaxation times. Nevertheless, these observed hyperfine coupling is typical of Cu(II) complexes where the unpaired electron occupies the $3dx^2$-y^2 orbital of copper.[41] Both complexes display a rhombic tensor spectra in which the ground state electron occupy the $3dx^2$-y^2 orbital.

The g_{av}, $g_{\parallel}$ and $g_{\perp}$ values measured from the spectra compares well with other binuclear copper carboxylate compounds[42] which points to the existence of similar coordination environment around each Cu(II) centre in the complexes. The coordination of Cu metal by four equatorial oxygen atoms from the carboxylate and an axial nitrogen atom in a distorted square pyramidal geometry similar to complexes **5** and **6** gives g_{av} in the range of 2.10 – 2.20 while an equatorial coordination sphere of four N–atoms ranges between 2.08 – 2.10.[43]

The similarity in the first derivative curve (Figure 3.12) and similar $g_{\perp}$ values [$g_{\perp}$ = 2.15 (**5)** and $g_{\perp}$= 2.09 (**6**)] of the complexes in solid and liquid state reveal the retention of the

binuclear structures in solution. Retention of the binuclear paddle-wheel structure is consistent with other literature reports[44] and could be attributed to the ability of carboxylate ligands to form stronger bridging system compared to halides. We were unable to determine $g_{\parallel}$ in solutions due to poor spectra resolution at room temperature.

Table 3.6 Solid-state X-Band EPR parameters of **5** and **6**

Complex	$g_{\parallel}$ (cm^{-1})	$g_{\perp}$ (cm^{-1})	g_{av}	$A_{\parallel}$ (G)
5	2.380	2.081	2.181	150.8
6	2.327	2.076	2.160	150.8

3.4 Conclusion

In conclusion, four benzoimidazolyl ligand derivatives were synthesized and reacted with Zn(II) and Cu(II) carboxylate salts to form the corresponding Zn(II) and Cu(II) complexes. Two of the synthesized ligands, **L3** and **L4**, are new likewise all the reported complexes. The complexes were fully characterized by mass spectrometry, IR spectroscopy and microanalyses. In addition, diamagnetic zinc compounds **1**-**4, 7** and **8** were characterized by ^{1}H and ^{13}C NMR spectroscopy while paramagnetic complexes **5**, **6** and **9** were further characterized by magnetic moment measurements. The X-ray diffraction analyses of compounds **3**, **6** and **8** revealed that benzoimidazolyl ligands are monodentate and coordinates to metals *via* the benzoimidazolyl N-atom while the protonated N-atom of the imidazole is non-coordinative but involved in interatomic or intermolecular H-bonding. Compounds **3** and **6** are binuclear with the carboxylate ligand bridging the two metal centers to form a paddle-wheel structure. However, compound **8** exists as a mononuclear complex consisting of two benzoimidazolyl ligand units and two monodentate acetate groups. EPR investigation of the copper complexes confirmed the retention of the binuclear paddle-wheel structures in solution.

References

[1] (a) O'Keefe, B. J.; Breyfogle, L. E., Hillmyer, M. A.; Tolman, W.B. *J. Am. Chem. Soc.* **2002**, *124*, 4384-4393. (b) Chen, H.-Y.; Tang, H.-Y.; Lin, C.-C. *Macromolecules* **2006**, *39*, 3745-3752. (c) Williams, C. K.; Breyfogle, L. E.; Kyung Choi, S.; Nam, W. ; Young Jr. V. G.; Hillmyer, M. A.; Tolman, W. B. *J. Am. Chem. Soc.* **2003**, *125*, 11350 – 11359. (d) Dijkstra, P. J.; Du, H.; Feijen, J. *Polym. Chem.* **2011**, *2*, 520–527.

[2] (a)Chen, H.-Y.; Huang, B.-H.; Lin, C.-C. *Macromolecules* **2005**, *38*, 5400-5405 (b) Cheng, M.; Moore, D. R.; Reczek, J. J.; Chamberlain, B. M.; Lobkovsky, E. B.; Coates, G.W. *J. Am. Chem. Soc.* **2001**, *123*, 8738-8749 (c) Williams, C. K.; Breyfogle, L. E.; Choi, S. K.; Nam, W.; Young, Jr., V. G.; Hillmyer, M. A.; Tolman, W. B. *J. Am. Chem. Soc.* **2003**, *125*, 11350-11359. (e) Azor, L.; Bailly, C.; Brelot, L.; Henry, M.; Mobian, P.; Dagorne, S. *Inorg. Chem.* **2012**, *51*, 10876-10883. (f) Jensen, T. R.; Schaller, C. P.; Hillmyer, M. A.; Tolman, W. B. J. *Organomet. Chem.* **2005**, *690*, 5881–5891.

[3] Liu, Z.; Gao, W.; Zhang, J.; Cui, D.; Wu, Q.; Mu, Y. *Organometallics* **2010**, *29*, 5783–5790.

[4] Radano, C.P.; Baker, G.L.; Smith, M.R. *J. Am. Chem. Soc.* **2000**, *122*, 1552-15553.

[5] (a) Li, K.; Darkwa, J.; Guzei, I.A.; Mapolie, S.F. *J. Organomet. Chem.* **2002**, *660*, 108-115. (b) Chamberlain, B.M.; Cheng, M.; Moore, D.R.; Ovitt, T.M.; Lobkovsky, E.B.; Coates, G.W. *J. Am. Chem. Soc.* **2001,** *123,* 3229-3238.

[6] Sun, W.-H.; Shao, C.; Chen, Y.; Hu, H.; Sheldon, R.A.; Wang, H.; Leng, X.; Jin X. *Organometallics* **2002,** *21*, 4350-4355.

[7] Craigo, W.A.; LeSueur, B.W.; Skibo, E.B. *J. Med. Chem.* **1999**, *42*, 3324-3333.

[8] Storey, R.F.; Sherman, J.W. *Macromolecules* **2002,** *35,* 1504-1512.

[9] Chisholm, M.H.; Gallucci, J.; Phomphari, K. *Chem. Commun.* **2003**, 48.

[10] (a) Ejfler, J; Kobylka, M.; Jerzykiewicz, L.B.; Sobota, P. *Dalton Trans.* **2005,** 2047-2050. (b) Chisholm, M.H.; Eilerts, N.W.; Huffman, J.C.; Iyer, S.S.; Pacold, M.; Phomphrai, K. *J. Am. Chem. Soc.* **2000**, *122*, 11845-11854.

[11] Zhang, J.; Jian, C.; Gao, Y.; Wang, L.; Tang, N.; Wu, J. *Inorg. Chem.* **2012**, *51*, 13380−13389.

[12] Arrowsmith, R.L.; Pascu, S.I.; Smugowski, H. *Organomet. Chem.* **2012**, *38*, 1–35 and references therein.

[13] Gowda, R.R.; Chakraborty, D. *J. Mol. Catal. A: Chem.* **2010**, *333*, 167–172.

[14] Williams, C.K.; Brooks, N.R.; Hillmyer, M. A.; Tolman, W. B. *Chem. Commun.* **2002**, 2132-2133.

[15] Drouin, F.; Oguadinma, P.O.; Whitehorne, T. J. J.; Prud'homme, R. E.; Schaper, F.; *Organometallics* **2010**, *29*, 2139–2147.

[16] Garces, A.; Sanchez-Barba, L. F.; Alonso-Moreno, C.; Fajardo, M.; Fernandez-Baeza, J.; Otero, A.; Lara-Sanchez, A.; Lopez-Solera, I.; Marıa Rodrıguez, A. *Inorg. Chem*. **2010**, *49*, 2859–2871.

[17] John, A.; Katiyar, V.; Pang, K.; Shaikh, M.M.; Nanavati, H.; Ghosh, P. *Polyhedron* **2007,** *26*, 4033-4044.

[18] Bhunora, S.; Mugo, J.; Bhaw-Luximon, A.; Mapolie, S.;Van Wyk, J.; Darkwa, J.; Nordlander, E. *Appl. Organometal. Chem.* **2011**, *25*, 133–145.

[19] Sun, J.; Shi, W.; Chen, D.; Liang, D. *J. Appl. Polym. Sci.* **2002,** *86*, 3312–3315.

[20] Bruker-AXS, Madison, Wisconsin, USA, **2009.**

[21] (a) Sheldrick, *Acta Cryst*. **2008**, *A64*, 112. (b) SADABS Area-Detector Absorption Correction; Siemens Industrial Automation, Inc.: Madison,WI, **1996**. (c) SAINT Area-Detector integration Softeware. Siemens Industrial Automation, Inc.: Madison,WI, **1995**.

[22](a)Achar, K.C.S.; Hosamani, K.M.; Seetharamareddy, H.R. *Eur. J. Med. Chem.* **2010**, *45*, 2048-2054. (b) Skolnik, H.; Day, A.R.; Miller, J.G.; *J. Am. Chem. Soc.* **1943**, *65*, 1858–1862.

[23] Silverstein, R. M.; Webster, F. X.; Kiemle, D.J. *Spectrometric Identification of Organic compounds*, John Wiley & Sons Inc, **2005**.

[24] (a) Neuvonen, H.; Neuvonen. K. *J. Chem. Soc*., *Perkin Trans. 2*, **1999**, 1497–1502. (b) Hunt, P. A.; Straughan, B. P.; Ali, A.A.M.; Harris, R. K.; Say, B. J. *J. Chem. Soc*., *Dalton Trans.*, **1990**, 2131-2135.

[25] (a) Ye, B.-H.; Li, X.-Y.; Williams, I.D.; Chen, X.-M. *Inorg. Chem.*, **2002**, 41, 6426 – 6431. (b) Lin, S-J.; Hong, T.-N.; Tung, J.-Y.; Chen, J.-H. *Inorg. Chem.*, **1997**, *36*, 3886-3891.

[26] Teyssie, P.; Carette, J. J. *Spectrochim. Acta.* **1963**, *19*, 1407–1423.

[27] (a) Jiang, M.; Li, J.; Huo, Y.-Q.; Xi, Y.; Yan, J.-F.; Zhang, F.-X. *J. Chem. Eng. Data* **2011**, *56*, 1185–1190. (b) Liu, Q.-X.; Zhao, Z.-X.; Zhao, X.-J.; Yao, Z.-Q.; Li, S.-J.; Wang, X.-G. *Cryst. Growth Des.* **2011**, *11*, 4933–4942.

[28] Elder, M. S.; Melson, G.A.; Busch, D.H. *Inorg. Chem.* **1966**, *5*, 74 -77 and references therein.

[29] Devereux, M.; O'Shea, D.; O'Connor, M.; Grehan, H.; Connor, G.; McCann, M.; Rosair, G.; Lyng, F.; Kellett, A.; Walsh, M.; Egan, D.; Thati, B. *Polyhedron* **2007**, *26*, 4073–4084.

[30] (a) Das, S.; Bharadwaj, P.K. *Cryst. Growth Des.* **2006**, *6*, 187-192. (b) Chen, H.-Y.; Tang, H.-Y.; Lin, C.-C. *Macromolecules* **2006**, *39*, 3745-3752. (c) Jiang, T.; Zhang, X.-M. . *Cryst. Growth Des.* **2008**, *8*, 3077-3083.

[31] Qin, L.; Li, Y.; Guo, Z.; Zheng, H. *Cryst. Growth Des.* **2012**, *12*, 5783-5791.

[32] Roberts, C. C.; Barnett, B.R.; Green, D.B.; Fritsch, J.M. *Organometallics* **2012**, *31*, 4133−4141.

[33] Chaudhuri, P.; Stockheim, C.; Wieghardt, K.; Deck, W.; Gregrozik, R.; Vahrenkamp, H.; Nuber, B.; Weiss, J. *Inorg. Chem.* **1992**, *31*, 1451- 1462.

[34] Chen, X.-M.; Tong, Y.-X. *Inorg. Chem.* **1994**, *33*, 4586-4588.

[35] Qin, L.; Li, Y.; Guo, Z.; Zheng, H. *Cryst. Growth Des.* **2012**, *12*, 5783-5791. (b) Sreehari, N.; Varghese, B.; Manoharan, P.T. *Inorg. Chem*. **1990**, *29*, 4011-4015.

[36] Bondi, A. *J. Phys. Chem.* **1964**, *68*, 441−451.

[37](a) Bertolotti, F.; Forni, A.; Gervasio, G.; Marabello, D.; Diana, E. *Polyhedron* **2012**, *42*, 118–127. (b) Drozdzewski, P.; Brozyna, A.; Kubiak, M. *J. Mol. Struct.* **2004**, *707*,131-137.

[38] (a) Fan, M.; Yang, Q.; Tong, H.; Yuan, S.; Jia, B.; Guo, D.; Zhou, M.; Liu, D. *RSC Advances* **2012**, *2*, 6599–6605. (b) Rao, V.M.; Sathyanarayana, D.N.; Manohar, H. *J. Chem Soc. Dalton Trans.* **1983**, 2167-2173.

[39] (a) Singh, B.; Long, J.R.; Fabrizi de Biani, F.; Gatteschi, D.; Stavropoulos, P. *J. Am. Chem. Soc.* **1997**, 119, 7030-7047. (b) Kumar, U.; Thomas, J.; Nagarajan, R.; Thirupathi, N. *Inorg. Chim. Acta* **2011**, 372, 191-199.

[40] Bianca Ene, A.; Bauer, M.; Archipov, T.; Roduner, E. *Phys. Chem. Chem. Phys.* **2010**, *12*, 6520–6531.

[41] Stachova, P.; Melnik, M.; Korabik, M.; Mrozinski, V.; Koman, M.; Glowiak, T.; Valigura, D. *Inorg. Chim. Acta* **2007,** *360*, 1517–1522.

[42] (a) Kozlevcar, B.; Leban, I.; Turel, I.; Segedin, P.; Petric, M.; Pohleven, F.; White, A.J.P.; Williams, D.J.; Sieler, J. *Polyhedron*, **1999**, 18, 644-651. (b) Ross, P.K.; Allendorf, M.D.; Solomon, E.I. *J. Am. Chem. Soc.* **1989,** 111, 4009 – 4021.

[43] (a) Addison, A.W.; Carpenter, M.; Lau, L.K.M.; Wicholas, M. *Inorg. Chem.* **1978**, 17, 1545–1552. (b) Jotham, R.W.; Kettle, S.F.A.; Marks, J.A. *J. Chem. Soc., Dalton Trans.*, **1972**, 420 – 438.

[44] (a) Martin, R. L.; Whitley, A. *J. Chem. Soc.* **1958**, 1394-1402. (b) Rigamonti, L.; Carlinoa, S.; Halibi, Y.; Demartina, F.; Castellanoa, C.; Ponti, A.; Pievo, R.; Pasini, A. *Polyhedron*, 2013, 53, 157–165.

Chapter Four

Ring opening polymerization of ε-caprolactone and lactide mediated by (Benzoimidazolylmethyl)amine Zn(II) and Cu(II) complexes

4.1 Introduction

Plastic materials have become integral to our daily lives and hence essential domestic and industrial commodities. Majority of these plastic materials are obtained from petroleum-based raw materials and are non-degradable. However, relative low cost of production has made these non-degradable commodity plastics dominate the market. Consequently, the huge environmental challenges of managing the wastes generated from these conventional plastics in addition to the rising cost of crude oil as oil reserves get depleted[1] have necessitated the need to search for alternative polymers that are biodegradable and also obtained from renewable sources. Polylactide (PLA) and Polycaprolatone (PCL) and their copolymers are envisaged as potential substituents to conventional polymers. These polyesters have attracted significant interest in both industry and academia due to their biodegradability and biocompatibility, thus, making them versatile in the food packaging, pharmaceutical and biomedical fields.[2]

The convenient method of synthesizing these polyesters is by ring opening polymerization (ROP) using heteroleptic metal complexes as catalysts to afford high molecular weight polymers with good molecular weight distribution.[3] This has led to the design of many complexes based on tin[4], aluminum,[5] titanium,[6] zirconium,[7] iron,[8] zinc,[9] copper,[10] rare earth,[11] alkali[12] and alkaline earth[13] metals as catalysts/ initiators for the ROP of lactides and ε-caprolactone. However, the application of these polyesters in health and other biological systems has necessitated the search for relatively non-toxic or biologically compatible metal complexes to substitute the currently used tin-based complexes which are toxic and difficult

to remove from the polymers after syntheses.[2e] In this regard, zinc, copper, calcium, magnesium and alkali metal complexes are being studied for possible application.[13b] We report herein the polymerization of lactides and ε-caprolactone using (benzoimidazolylmethyl) amine zinc and copper complexes previously reported in Chapter three.

4.2 Experimental

4.2.1 Materials and instrumentations

All reactions were carried out under dry nitrogen gas facilitated by a standard Schlenk line technique. Glassware used in the polymerization was oven-dried at 120 ^{o}C overnight. The monomers, ε-caprolactone (ε-CL) and lactide were purchased from Sigma Aldrich Co. ε-CL was dried over CaH_2, vacuum distilled and stored under inert conditions prior to use while the lactides were purified by crystallization from dry toluene and stored under P_2O_5. $CDCl_3$ was also bought from Sigma Aldrich and dried over activated alumina. Toluene and methanol were purchased from Merck chemicals. Toluene was distilled from sodium while methanol was purified by distillation from magnesium. The zinc and copper complexes used in the polymerization were prepared as described in Chapter three. NMR spectra were recorded on Bruker 400 UltraShield NMR (400 MHz for ^{1}H and 100 MHz for ^{13}C) spectrometer. All the chemical shifts were recorded in δ units relative to tetramethylsilane. The ^{1}H and ^{13}C spectra are referenced using residual $CDCl_3$ solvent peaks. The mass spectra of the polymers were obtained using micromass LCT premier mass spectrometer while the number average molecular mass (M_n) and the molecular weight distribution of the polymers were determined using Gel Permeation Chromatography (GPC) at the University of Stellenbosch.

4.2.2 General procedure for ε-caprolactone and lactide polymerization.

Polymerization of ε-caprolactone was carried out in bulk at 110 ^{o}C. In a typical bulk polymerization, 0.54 μmol of the complex was weighed into a pre-heated Schlenk tube equipped with a magnetic stirrer and ε-CL (0.60 ml, [M]/[I] = 100/1) was added. The Schlenk tube was immersed in silicon oil bath at the set temperature and the reaction mixture stirred until completion of polymerization. The extent of monomer conversions was monitored by taking aliquots at regular intervals and percentage conversions determined by ^{1}H NMR spectroscopy. In the case of lactides, (0.36 g, [M]/[I] = 100/1) were added to a rapidly stirring solution of 0.25 μmol complex in toluene (1 ml) and the reaction mixture stirred at 110 ^{o}C. The reactions were monitored to completions (as in ε-CL) by ^{1}H NMR spectroscopy.

4.2.3 Polymerization Kinetics.

For kinetic studies, aliquots of the polymer were taken at regular time intervals and quenched (frozen) in liquid nitrogen. The quenched aliquots were dissolved in $CDCl_3$ and analyzed by ^{1}H NMR spectroscopy. For ε-CL polymerization, the ratio of initial monomer concentration to monomer concentration at time, t, $[CL]_o/[CL]_t$, was determined based on the relative peak intensities of ε-CL to PCL from the ^{1}H NMR spectrum.[7d] The signals around 4.2 ppm and 4.0 ppm correspond to ε-CL and PCL respectively. The ratio $[CL]_o/[CL]_t$, was calculated according to equation 4.1.

$$\frac{[CL]_o}{[CL]_t} = \frac{I_{4.2} + I_{4.0}}{I_{4.2}} \qquad (4.1)$$

$I_{4.2}$ = integral of monomer, ε-CL

$I_{4.0}$ = integral of polymer, PCL

For lactide polymerization, the peak intensities around 4.8 ppm and 5.4 ppm corresponding to monomer ([LA]) and polymer ([PLA]) respectively were used to compute for the monomer to polymer ratio $[LA]_o/[LA]_t$, according to the equation 4.2;

$$\frac{[LA]_o}{[LA]_t} = \frac{I_{4.8} + I_{5.4}}{I_{4.8}} \qquad (4.2)$$

Where $I_{4.8}$ = integral of monomer, LA

$I_{5.4}$ = integral of polymer, PLA

The apparent rate constants of the reaction were obtained from the gradient of the line of best-fit of the plot of $In[M]_o/[M]_t$ versus time.

4.2.4 Polymer characterization

The molecular weight (M_w) and number average molecular mass (M_n) of the polymers were determined by Size Exclusion Chromatography (SEC) at Stellenbosch University. The SEC instrument consist of Waters 1515 isocratic HPLC pump, Waters 717plus auto-sampler, Waters 600E system controller (run by Breeze version 3.30 SPA), a Waters in-line Degasser AF and a Waters 2414 differential refractometer (operated at 30^{o}C) in series with a Waters 2487 dual wavelength absorbance UV/Vis detector operating at variable wavelength. The polymers were dissolved in a BHT stabilized THF (2 mg/ ml), filtered through a 0.45 μm nylon filters and eluted through two sets PLgel (Polymer laboratories) 5 μm Mixed-C (300x7.5 mm) column and a precolumn (PLgel 5 μm Guard, 50x7.5 mm) at a flow rate of 1 ml/min. The column oven was kept at 30^{o}C and injection volume was 100 μl. THF (HPLC grade stabilized with 0.125% BHT) was used as the eluent. Narrow polystyrene standards ranging from 580 to 2 x 10^6 g/mol was used for calibration hence molecular weights were measured as polystyrene equivalents.

4.3 Results and Discussions

4.3.1 Polymerization of ε-CL and LA

The ring opening polymerization reaction of ε-caprolactone (ε-CL), $_{D,L}$-lactide ($_{D,L}$-LA) and $_{L}$-lactide ($_{L}$-LA) was investigated using selected Zn(II) and Cu(II) complexes synthesized as described in Chapter three (Scheme 4-1). The polymerization of ε-caprolactone and lactides was carried out at 110 ^{o}C in bulk and in toluene respectively. Preliminary investigations under these conditions are summarized in Table 4.1. The initial results attest to the fact that the complexes exhibited significant catalytic activities towards the ROP of ε-CL and LA achieving maximum conversion of 98% between 48-96 h (Figures 4.1 and 4.2). Hence, further mechanistic and kinetics of the polymerization reactions were investigated in addition to the effects of reaction conditions on the catalyst performance and the polymer characteristics.

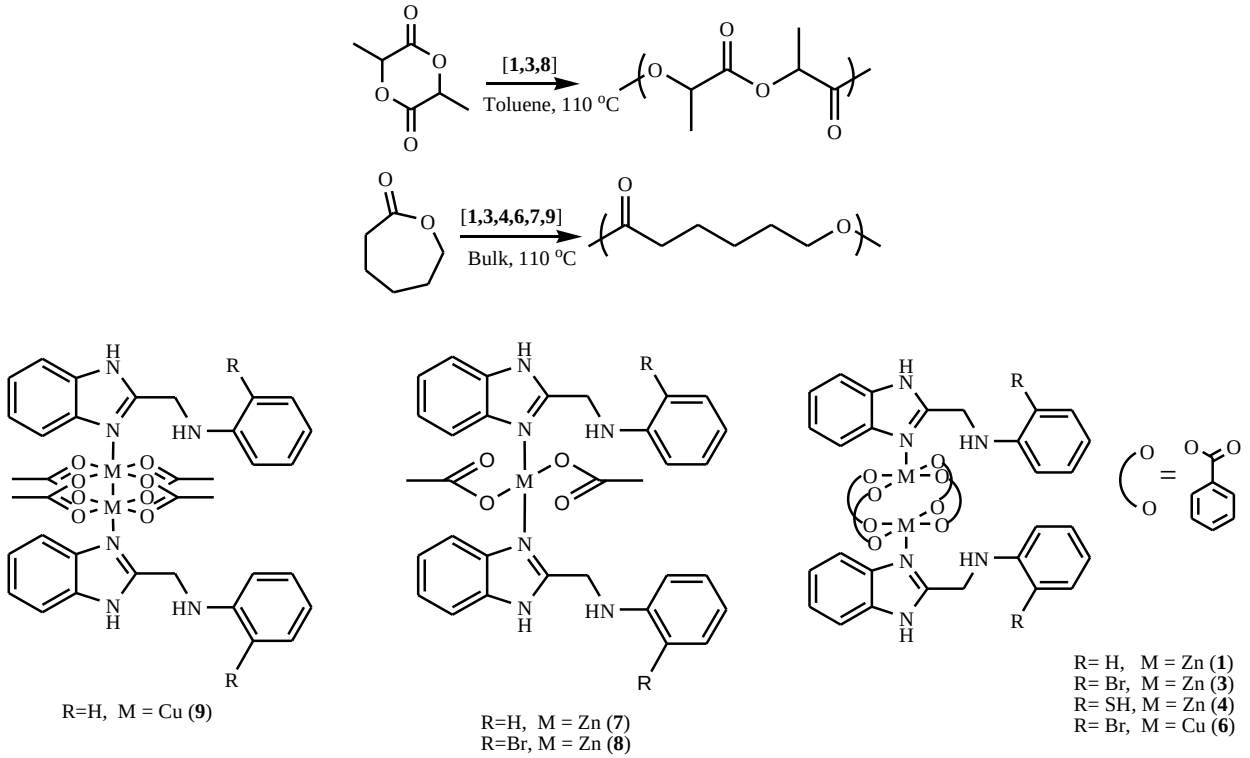

Scheme 4-1

Table 4.1: ROP of ε-CL, $_{D,L}$-LA and $_{L}$-LA catalyzed by **1**, **3**, **4**, **6-9**[a]

Entry	Catalyst	Monomer	t (h)	conv (%)	Mn_{NMR}[b]	Mn_{GPC}[c]	PDI[c]	I*[d]
1	**1**	ε-CL	36	96	10906	6609	1.52	0.61
2	**1**	$_{D,L}$-LA	32	95	13731	2917	1.45	0.21
3	**1**	$_{L}$-LA	33	96	13780	3131	1.37	0.23
4	**3**	ε-CL	48	95	10857	7131	1.50	0.66
5	**3**	$_{D,L}$-LA	50	95	13532	2601	1.41	0.19
6	**4**	ε-CL	32	96	10960	4823	1.43	0.44
7	**6**	ε-CL	52	95	10843	8212	1.49	0.76
8	**7**	ε-CL	32	97	11078	8104	3.64	0.73
9	**8**	$_{D,L}$-LA	95	95	13506	3026	1.48	0.22
10	**9**	ε-CL	48	96	10983	5440	2.29	0.50

[a] Condition:110 [o]C. [M]:[I]=100, $[LA]_o$ = 2.5 mmol, $[\varepsilon\text{-CL}]_o$ = 5.41 mmol, polymerization of ε-CL in bulk and LA in toluene. [b]Calculated from Molecular weight of monomer x[M]/[I] x %Conv. [c]Measured by GPC. [d]Initiator efficiency = Mn_{GPC}./Mn_{NMR}

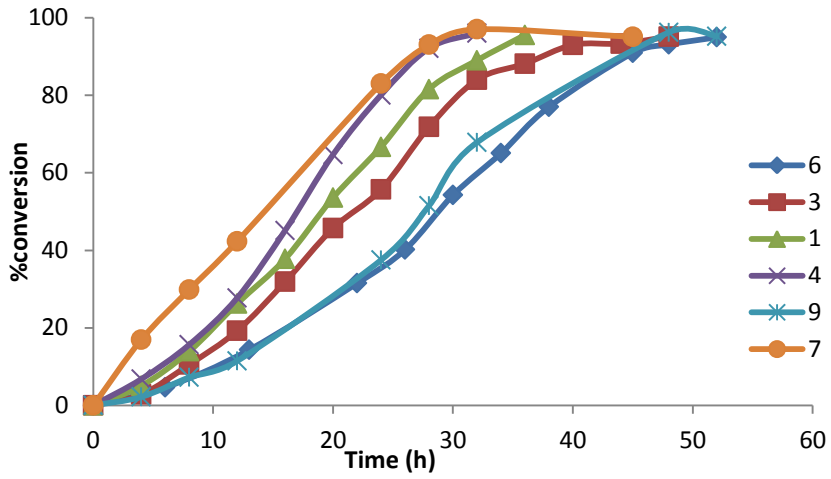

Figure 4.1: Plot of conversion (%) vs time (h) for PCL

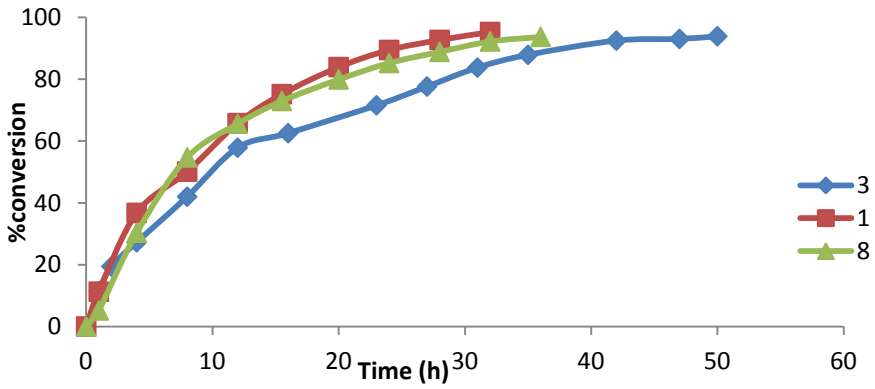

Figure 4.2: Plot of conversion (%) vs time (h) for LA

4.3.2 Kinetics of ε-CL polymerization

The kinetics of ε-caprolactone polymerization using **1**, **3**, **4**, **6**, **7** and **9** at 110 ^{o}C in bulk were investigated by monitoring ^{1}H NMR spectra of sampled aliquots until conversion was almost complete (>95%). The aliquots were periodically taken and the percentage conversions of ε-CL to PCL were determined by comparing the relative peak intensities at 4.2 ppm and 4.0 ppm respectively from the ^{1}H NMR spectrum. The rates of the reaction were determined by plotting a semi-logarithm graph of $\ln[CL]_o/[CL]_t$ versus time as shown in Figures 4.3 and 4.4. In all cases, there was an induction period ranging between *ca* 8–26 h depending on the nature of the catalyst. Induction periods are usually associated with structural rearrangement/ aggregation of the reacting species to form the actual active sites.[14] The copper complexes exhibited longer induction periods compared to the zinc complexes.

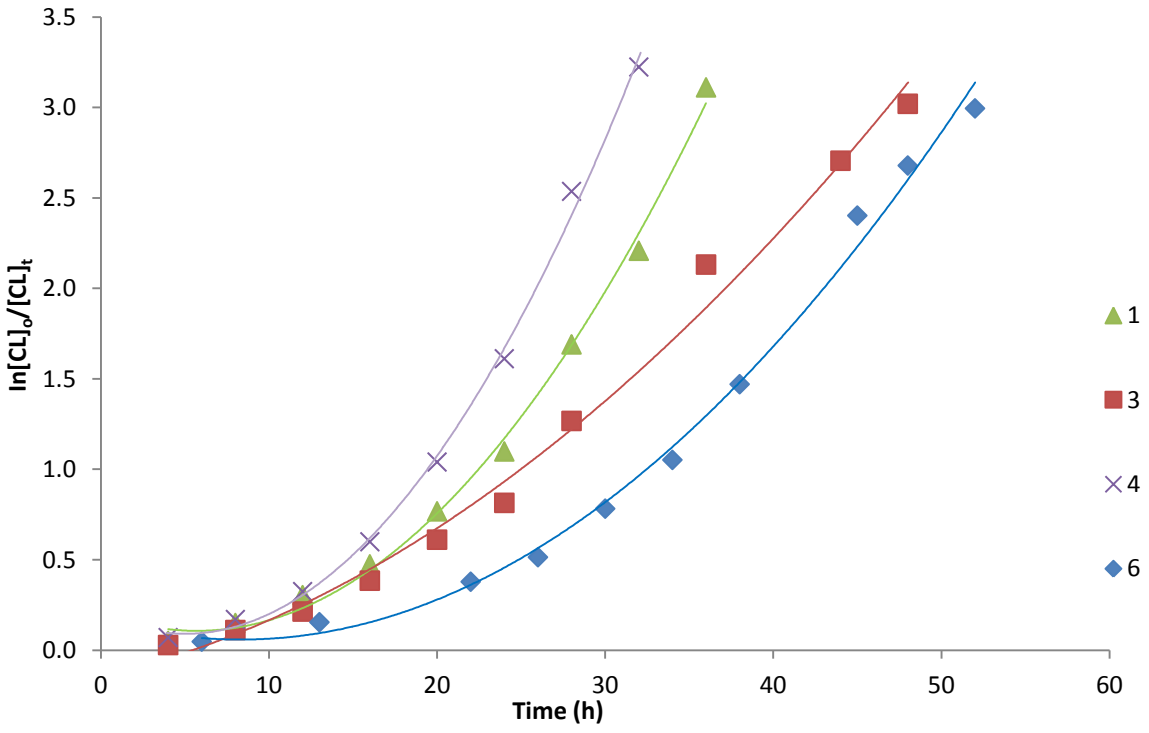

Figure 4.3: Plot of $\ln[CL]_o/[CL]_t$ vs time showing induction period for **1,3,4** and **6**

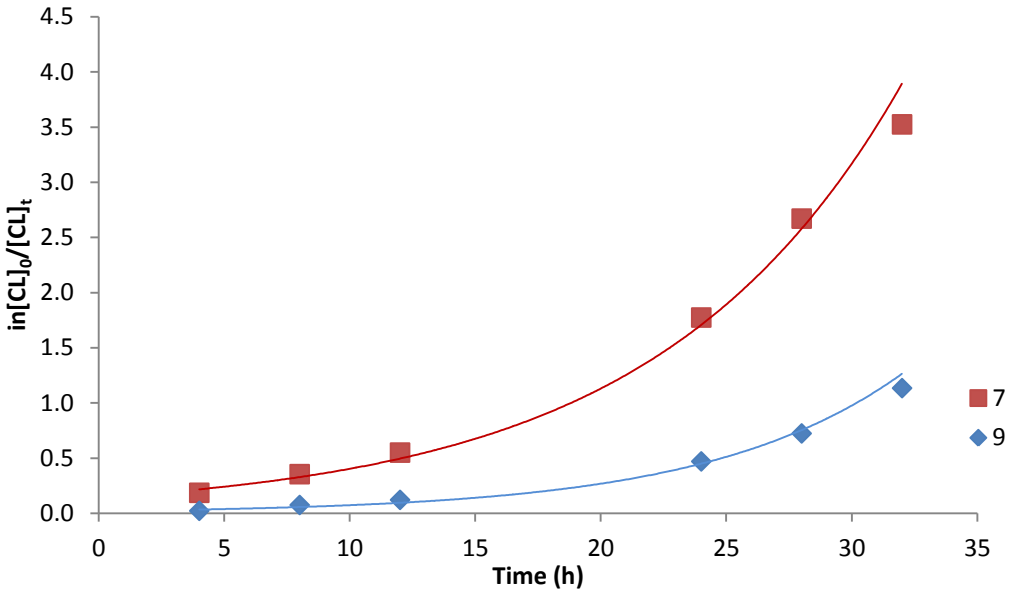

Figure 4.4: Plot of ln[CL]o/[CL]t vs time showing induction period for **7** and **9**

However, linear relationships consistent with a pseudo-first order reaction with respect to the monomer (ε-CL) were observed after the induction period (Figures 4.5 and 4.6). This implied that the generated active sites remained the same until completion of the reaction. Thus, the rate of ε-CL polymerization after induction proceeded according to equation 4.3.

$$-\frac{d[CL]}{dt} = k_{app}[CL] \qquad (4.3)$$

where $k_{app} = k_p[I]^x$, and where k_p is the chain propagation rate constant.

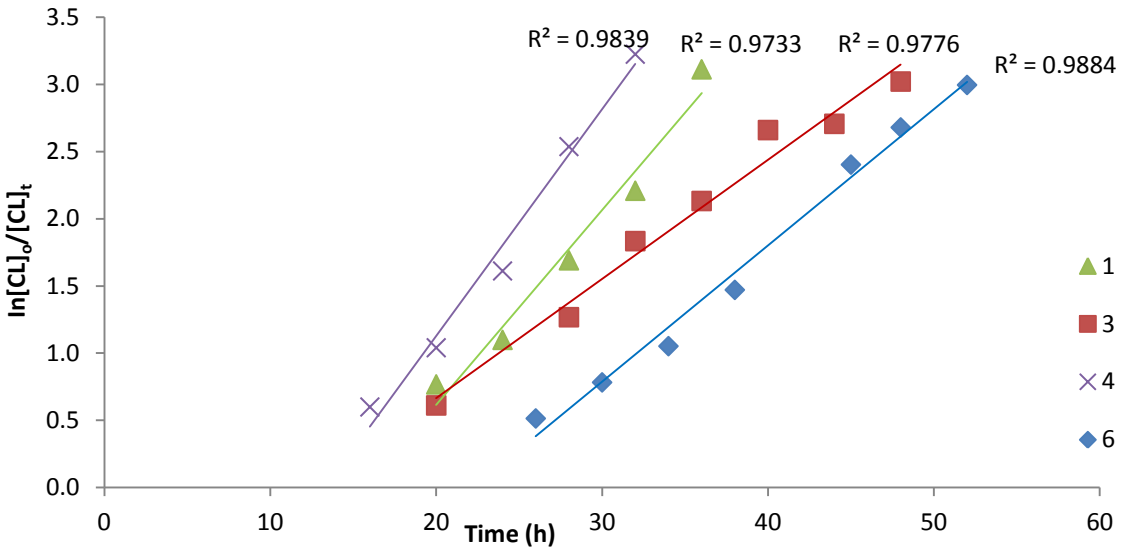

Figure 4.5: Plot of $\ln[CL]_o/[CL]_t$ vs time showing the linear fit after induction period for **1,3,4** and **6**

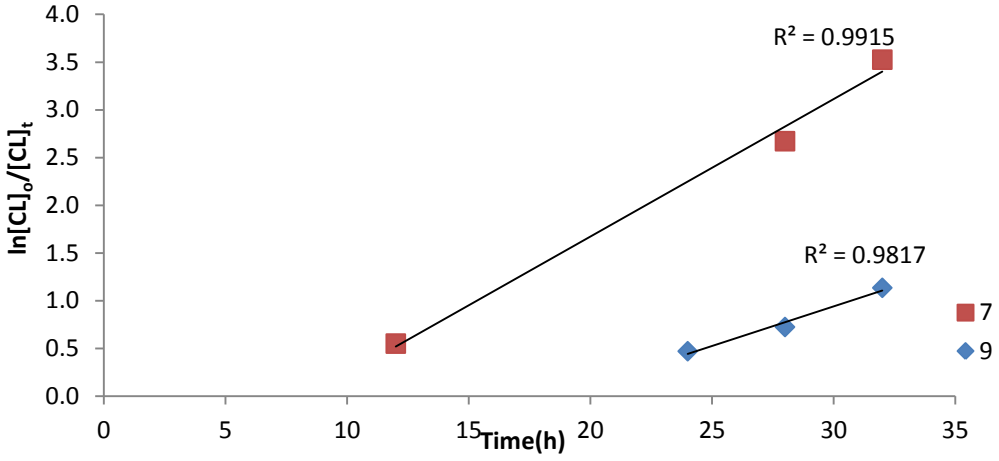

Figure 4.6: Plot of $\ln[CL]_o/[CL]_t$ vs time showing the linear fit after induction period for **7** and **9**

The apparent rate constants of **1**, **3**, **4**, **6**, **7** and **9** extracted from the plot of $In[CL]_o/[CL]_t$ versus time taking into account the induction period were 0.0624 h^{-1}, 0.0537 h^{-1}, 0.0762 h^{-1}, 0.0447 h^{-1}, 0.0922 h^{-1} and 0.0268 h^{-1}, respectively (Figures 4.3 and 4.4). These results revealed higher catalyst activities in Zn(II) complexes compared to Cu(II) complexes. For example, the zinc-based complex **3** (0.0537 h^{-1}) was higher in activity than its analogous

copper-based complex **6** (0.0447 h^{-1}). These observed higher catalytic activities of zinc complexes over copper complexes towards the polymerization of ε-CL had been reported by Ojwach *et al.*[15] In their report, the zinc complexes exhibited rates that were about twice that of their corresponding copper complexes. The higher catalytic activities of Zn(II) metals relative to their corresponding Cu(II) metals could be due to its electropositive nature which makes it more electrophilic and hence easy coordination to the monomers. This could account for the high activities of zinc complexes in the ROP of lactides and lactones.

We also observed increased catalytic activities of the complexes bearing electron-donating groups on the ligand motifs as compared to complexes with electron-withdrawing groups. For instance, complex **4** (0.0762 h^{-1}) containing –SH group was more active compared to its analogous complex **3** (0.0447 h^{-1}) bearing electron-withdrawing group –Br. The two-fold drop in the reaction rate constant is similar to reports by Chisholm *et al.*[16] where replacement of a ^{t}Bu group with electron-withdrawing -CF_3 group on the pyrazole ligand resulted in a decrease in the rate of reaction. Similar observations were also made by Alcazar-Roman *et al.*[17] where the rate of polymerization of ε-caprolactone by the complex containing electron-withdrawing groups exhibited lower rate constant of 3.57 x 10^{-3} Ms^{-1} compared to 19.80 x 10^{-3} Ms^{-1} displayed by the complex bearing electron-donating groups. Similar trends have been reported by O'keefe *et al.*[3c] We also observed higher rate of reactions with the acetate complexes compared to the corresponding benzoate catalysts. For instance, complex **7** showed a higher rate constant of (0.0922 h^{-1}) compared to the analogous complex **1** (0.0624 h^{-1}) which has the benzoate group. The decrease in activity could be attributed to steric factors imposed by the bulky benzoate groups.

Comparatively, the observed rate constants for the complexes were lower than literature reports of other zinc complexes.[18,19] For instance, Huang *et al.*[20] reported 0.031 s^{-1} apparent polymerization rate constant for ε-CL polymerization by zinc complexes which is one of the fastest reported in literature. Also, titanium alkoxide reported by Cayuela *et al.*[21] exhibits rate of 0.0183 s^{-1} in ε-CL polymerization. However, the activity of the complexes towards ε-CL polymerization is similar to the zinc complex reported by Chamberlain *et al.*[22] (0.126 h^{-1}) and more active than the aluminum alkoxide catalyst investigated by Zhong *et al.*[23] that recorded a rate constant of 0.067 day^{-1}. The presence of alkoxide groups on the active metal centre may be responsible for the high catalytic activities of these reported complexes. Studies have shown alkoxides are more efficient initiators for polymerization reaction compared to carboxylates due to their high nucleophilicity.[2e,24]

To gain insight into the order of reaction with respect to the catalyst/initiator and the subsequent overall order of the reaction, further kinetic studies were done using complex **1**. This was performed at different catalyst concentrations at constant monomer concentration. A graph of In k_{app} versus In[**1**] was plotted to obtain the order with respect to the catalyst which was deduced from the gradient of the line of best fit (Figure 4.7).

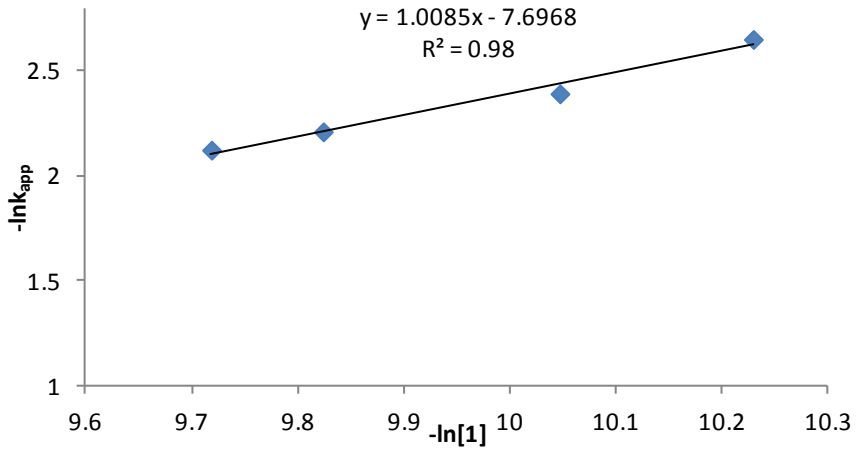

Figure 4.7: Plot of $-\ln k_{app}$ vs $-\ln$[**1**]

From Figure 4.7, the order of the reaction with respect to the catalyst **1** was obtained as 1.0085 ≈ 1. Therefore the overall order of reaction (sum of the orders) with respect to the monomer and the catalyst/complex, **1**, is 2. The rate equation for the polymerization reaction could thus be expressed as depicted in equation 4.4.

$$-\frac{d[CL]}{dt} = k_p[CL][\mathbf{1}] \qquad (4.4)$$

4.3.3 Kinetics of lactide polymerization

Kinetic studies were also conducted to establish the order of reaction with respect to the monomer and complex for the polymerization of *meso*-lactide ($_{D,L}$-LA) and $_{L}$-lactide ($_{L}$-LA) using Zn(II) complexes **1**, **3** and **8**. Cu(II) complexes were not tested due to the low activities observed in ε-CL polymerization. The order of reaction with respect to the monomer for the polymerization reactions was also obtained by plotting $\ln[LA]_o/[LA]_t$ versus time (Figure 4.8). The plots exhibited a pseudo-first order reaction with respect to the monomer in all cases due to the linearity of the plots.

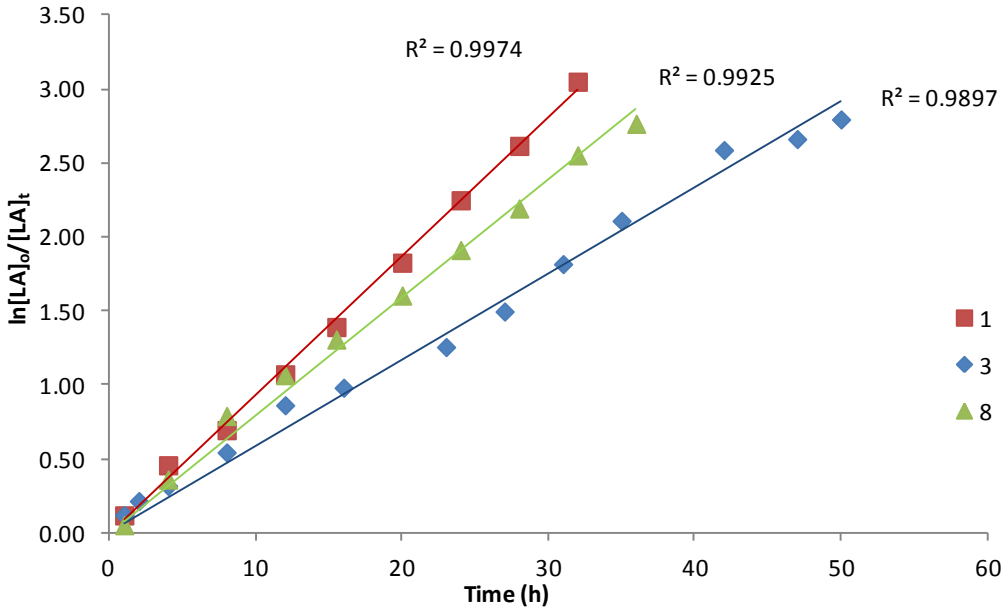

Figure 4.8: Plot of $\ln[LA]_o/[LA]_t$ vs time for $_{D,L}$-lactide polymerization in toluene

Interestingly, no induction period was observed in the polymerization of LA as opposed to the ε-CL reactions. This behavior could be attributed to the high basicity of the LA monomer due to the presence of two carbonyl groups.[19] The general rate law for the $_{D,L}$-LA polymerization reaction can hence be written as shown in equation 4.5.

$$-\frac{d[LA]}{dt} = k_{app}[LA] \qquad (4.5)$$

where $k_{app} = k_p[I]^x$, and where k_p is the chain propagation rate constant.

The recorded apparent rate constants (k_{app}) for **1**, **3** and **8** were 0.0934, 0.0582 and 0.0796 h^{-1} respectively. Complexes bearing the electron-withdrawing –Br group recorded lower rates of polymerization. Thus complex **3** (0.0582 h^{-1}) exhibited lower catalytic activity compared to complex **1** (0.0934 h^{-1}) which has –H atom. The electronic effect of ligands on the activities of complexes in LA polymerization was consistent with trends reported in the polymerization of ε-CL.

Consistent with the trends observed for the ε-CL polymerization reactions, binuclear benzoate Zn(II) complexes exhibited lower catalytic activities compared to the corresponding mononuclear acetate complexes. For instance, the binuclear complex **3** exhibited a lower rate constant of 0.0582 h^{-1} compared to the rate constant of 0.0796 h^{-1} reported for the corresponding mononuclear benzoate complex **8**. This trend contrasts the expected results where most multinuclear complexes gave rise to higher catalytic activities.[25] In this scenario, the difference in catalytic activities could be ascribed to the steric crowding around the active metal centre by the bulkier bridging benzoate groups compared to the smaller acetate groups, thus hindering coordination of the monomer to the metal centre. Reduction of the rate of polymerization as a consequence of crowding around the active site has also been reported by Carpentier and co-workers.[26]

Compared to other published reports,[27] these complexes showed lower catalytic activities. For instance the zinc complex by chamberlain *et al.*[28] polymerized *rac*-lactide at the rate of 0.054 min^{-1} at 25 ^{o}C when the [LA]/[Zn] ≈ 490. Other highly active zinc complexes with phenomenal activities were reported by Chisholm *et al.*[29] (>93% lactide conversion within 1 h at 25 ^{o}C) and Wheaton and Hayes[30] (>90% conversion in 50 min at 25 ^{o}C). However, the catalytic activities of **1, 3** and **8** are comparable and/ or higher than aluminum alkoxide (90% lactide conversion within 96 h at 100 ^{o}C), tin methoxide (95% lactide conversion within 24 h at100 ^{o}C), titanium butoxide (90% lactide conversion within 24 h at100 ^{o}C) and zinc alkoxide (90% lactide conversion after 6 day 1 h at 25 ^{o}C).[16] The factors that improve catalytic activities of the complexes reported in literature have been discussed in the polymerization of ε-CL.

To determine the order of reaction with respect to the catalyst, the dependence of k_{app} on catalyst concentration was analyzed using **1**. A plot of -lnk_{app} vs -ln[**1**] gave a linear graph with a non-integer gradient of 0.49 (Figure 4.9).

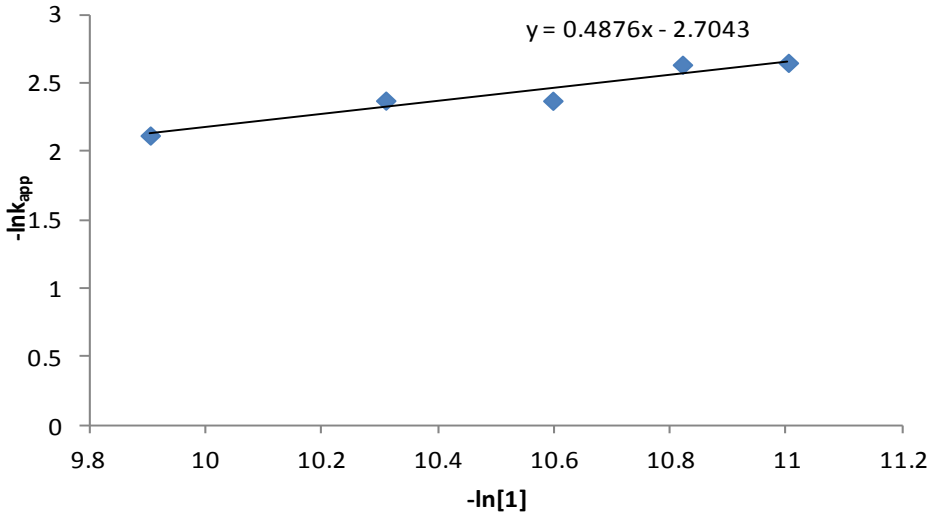

Figure 4.9: Plot of -lnk_{app} vs –ln[**1**] for *meso*-lactide polymerization.

The gradient denotes the order with respect to the catalyst thus the rate equation can be represented as shown in equation 4.6.

$$-\frac{d[LA]}{dt} = k_p[LA][\mathbf{1}]^{0.49} \qquad (4.6)$$

Such fractional orders with respect to catalysts have being observed for the polymerization of lactides by zinc complexes[20,31] and ε-caprolactone by triyttrium complex[22] and have been attributed to the aggregation of the active species during polymerization.

4.3.4 The number of active centers (n)

Our attempts to determine the number of active sites in these complexes were unsuccessful. The number of active initiating sites in **1** for the polymerization of both $_{D,L}$-LA and ε-CL was studied by plotting the degree of polymerization (DP) at a fixed conversion against [M]/[**1**]. The degree of polymerization is the number of repeated units in the polymer chain and obtained by dividing the molecular weight of the polymer by the molar mass of the monomer (Table 4.2). The dependence of DP on varying [M]/[I] ratio is essential in evaluating the number of active sites of a catalyst which is calculated as inverse of the gradient of the plot.[14b] Using **1** for the polymerization of LA and ε-CL, the degree of polymerization was interestingly found to be independent of the [M]/[I]. This contrasts reports by Dubois *et al.*[32] and could be attributed to the inability of the expected initiator (acetate group) to initiate the polymerization (*vide supra*). At this stage, we are unable to unambiguously account for this observation.

Table 4.2. Determination of the number of active initiating sites in **1**[a]

Entry	Monomer	[M]/[**1**]	Conv(%)	Mn[b]	DP
1	ε-CL	50	95	6226	55
2	ε-CL	75	95	7119	62
3	ε-CL	100	96	6609	58
4	ε-CL	125	95	8562	75
5	ε-CL	150	95	6449	57
6	$_{D,L}$-LA	50	95	2472	17
7	$_{D,L}$-LA	75	95	2571	18
8	$_{D,L}$-LA	100	96	2917	20
9	$_{D,L}$-LA	125	95	1920	13
10	$_{D,L}$-LA	150	95	2404	17

[a] Polymerization of LA and ε-CL in toluene and in bulk respectively at 110 ^{o}C. [b] GPC determined molecular weight of polymers (≥95% conversion)

4.3.5 Stability of Initiator 1 and 9

The stability or immortality of the catalysts was investigated through sequential addition of an equivalent amount of the monomer without addition of the catalyst. Thus, after complete consumption of the monomer in the first cycle ([LA]/[**1**] = 50 and [ε-CL]/[**9**] = 100), an additional 50 and 100 equivalent of LA and ε-CL respectively were added without the addition of catalyst **1** and **9**. It was observed that the polymerization proceeded to near completion, achieving 96% conversion after 30 h (LA) and 98% after 49 h (ε-CL). The recorded k_{app} for the polymerization of the second LA equivalent was 0.0919 h^{-1}, a 24% drop in activity from the 1st cycle (0.1204 h^{-1}) (Figure 4.10). On the other hand, the catalytic activity of **9** towards ε-CL polymerization dropped from 0.1163 h^{-1} (1st cycle) to 0.0725 h^{-1} (2nd cycle) corresponding to 38%. From this data, it can then be concluded that though the complexes remain active during the reaction, a significant loss of catalyst activities occurred. This indicates some degree of catalyst deactivation which can be speculated to emanate from build-up of monomer impurities and/ or complex decomposition at the high temperatures of the reaction.

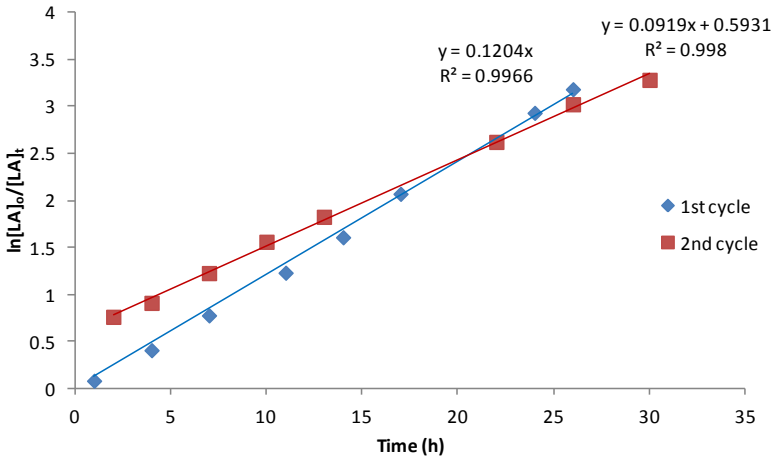

Figure 4.10: Kinetic plot for the polymerization of two equivalent amount of LA by complex **1**

4.3.6 Effect of temperature and solvent on the polymerization

The influence of temperature on the catalytic activities of the complexes in the polymerization of LA and ε-CL were evaluated by carrying out the reactions at 60, 90 and 110 ^{o}C (Table 4.3) using **3**, **6** and **8**. It is evident that as the temperature decreases, the rate of polymerization reaction in both LA and ε-CL also decreases. The duration of induction period was also observed to be temperature dependent with lower temperatures giving rise to longer induction periods. For instance at 90 ^{o}C, an induction period of *ca* 40 h was observed while a much longer induction period of 123 h was recorded at 60 ^{o}C (Figure 4.11). There was also a marked dropped in the apparent rate constant from 0.0906 h^{-1} (90 ^{o}C) to 0.0164 h^{-1} (60 ^{o}C) in ε-CL polymerization. Similar observations were recorded in LA polymerization at low temperature (Figure 4.12).

Table 4.3 Temperature and solvent effect on the polymerization of $_{D,L}$-LA and ε-CL[a]

Entry	[M]	[I]	Solvent	Temp (^{o}C)	Induction time (h)	k_{app} (h^{-1})
1	ε-CL	**3**	Bulk	110	16	0.0560
2	ε-CL	**3**	Bulk	90	48	0.0298
3	ε-CL	**3**	Bulk	60	144	0.0071
4	ε-CL [b]	**6**	Bulk	110	26	0.0447
5	ε-CL	**6**	Toluene	110	20	0.0534
6	ε-CL	**6**	Methanol	110	4	0.1473
7	$_{D,L}$-LA	**8**	Toluene	110	None	0.0796
8	$_{D,L}$-LA	**8**	Methanol	110	None	3.0000
9	$_{D,L}$-LA	**8**	Toluene	90	None	0.0385

[a] Condition: [M]/[I] = 100, [ε-CL] = 4.4 mmol, [$_{D,L}$-LA] = 2.5 mmol. [b] [ε-CL] = 5.3 mmol. [c] k_{app} for the whole reaction (including the induction period)

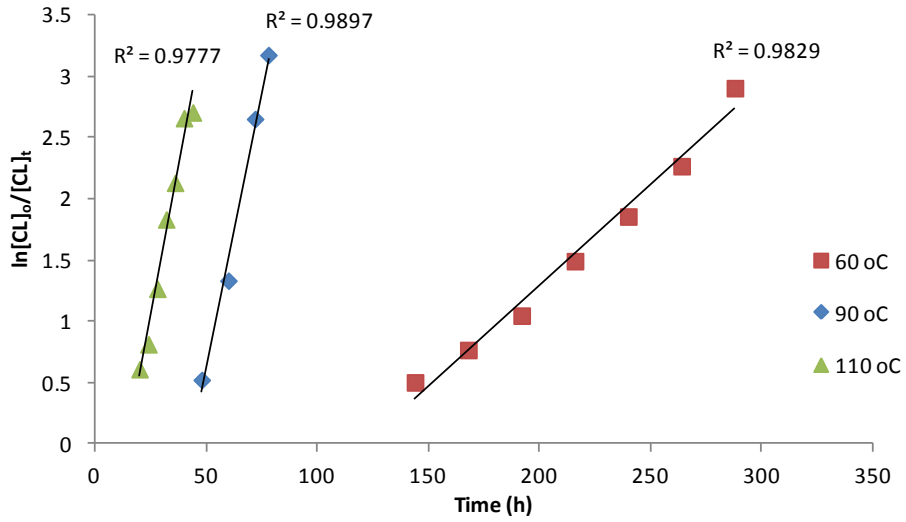

Figure 4.11: Kinetic plots for the polymerization of ε-CL by **3** at 60, 90 and 110 ^{o}C after induction period.

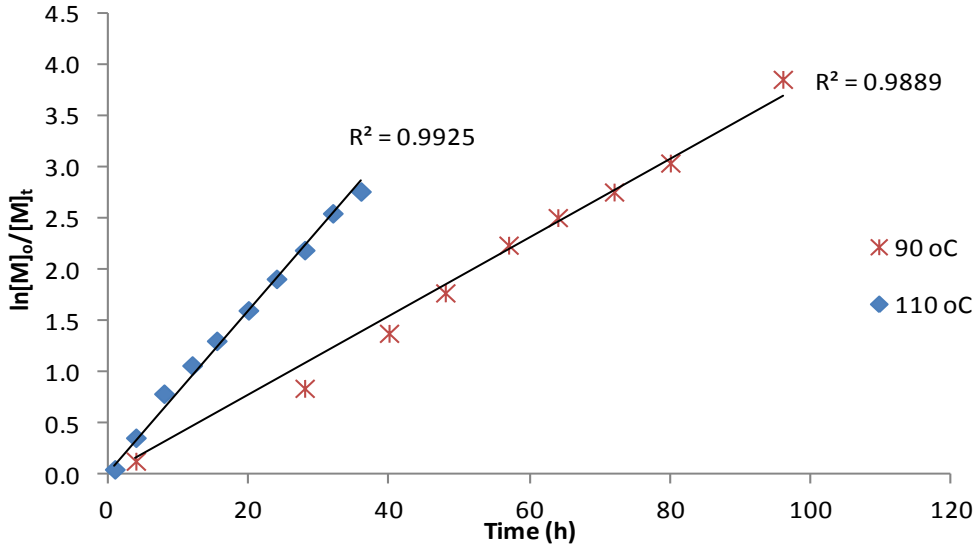

Figure 4.12: Kinetic plots for the polymerization of $_{D,L}$-lactide by **8** at 110 ^{o}C and 90 ^{o}C.

The effect of solvents on the activity of the catalysts was also investigated by carrying out the polymerization in bulk, toluene and methanol for ε-CL while lactide polymerization was performed in toluene and methanol. The apparent rate constant of ε-CL polymerization increased significantly from 0.1014 h^{-1} (bulk) to 0.1912 h^{-1} when methanol was used (Figure 4.13). Furthermore, there was virtually no induction period in the methanol reaction and maximum conversion was achieved within 16 h compared to about 60 h in bulk and toluene reactions (Figure 4.13). While a comparatively shorter induction period was observed in toluene as compared to bulk polymerization, the rate of polymerization were relatively similar. The significant increase in the catalytic activity of **8** in the presence of methanol could be due to *in situ* generation of metal alkoxide which are known to be highly active in the polymerization of lactides and lactones as compared to their metal acetate analogues.[2e] This was also demonstrated by Song *et al.*[27c] where the addition of isopropanol to zinc silylamido complexes resulted in marked increase in the rate of lactide polymerization at room temperature. For instances, 99% LA conversion was attained within 30 min on addition of the isopropanol compared with 98% conversion within 120 min in the absence of isopropanol.

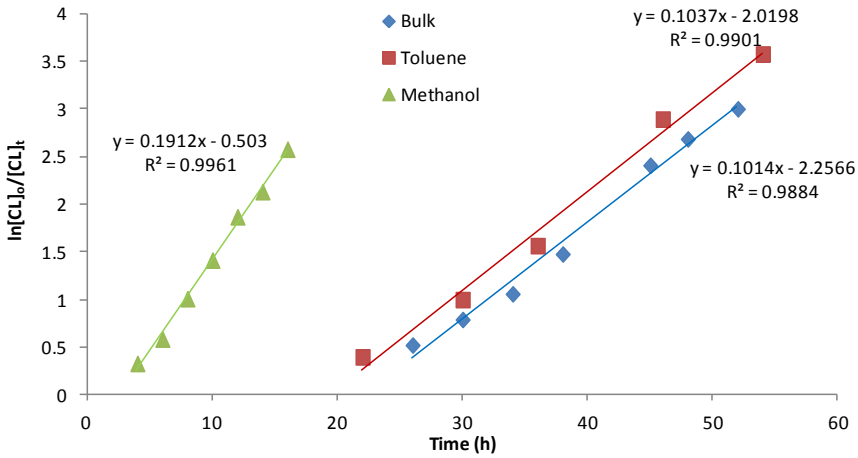

Figure 4.13: Kinetic plot for ε-CL polymerization in different solvents at 110 ^{o}C

Lactide polymerization with complex **8** in toluene and methanol (Figure 4.14) exhibited similar characteristics as observed in the polymerization of ε-CL. The k_{app} of 0.0796 h^{-1} recorded for polymerization in toluene increased significantly to 3.00 h^{-1} in methanol solvent. This significant increase in the catalytic activity of the complex in methanol could be due to the formation of metal alkoxide.[27c]

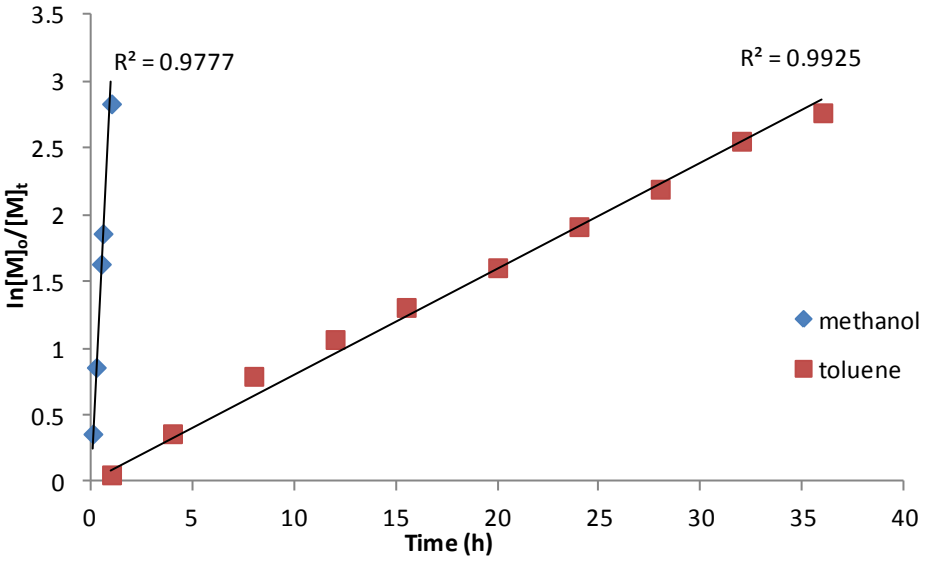

Figure 4.14: Kinetic plot for $_{D,L}$-LA polymerization in different solvents at 110 ^{o}C.

4.3.7 Mechanism of LA and ε-CL polymerization

The polymerization of ε-CL and LA using heteroleptic Zn(II) and Cu(II) complexes is likely to proceed through either coordination-insertion mechanism (CIM) or activated-monomer mechanism (AMM). In the CIM route, the polymer end chain bears the nucleophile (acetate in this case) on one end and the metal centre (Zn(II) or Cu(II) complex) on the other end. However, chain transfer agents (water or alcohols) in the system might promote hydrolysis of the metal end to form an –OR end group. On the other hand, polymerization through AMM route would result in the polymer bearing the proton and alkoxide from an external nucleophile (water or alcohols).[33] To establish the mechanism of lactide and ε-caprolactone

polymerization by **7**, ^{1}H NMR spectroscopy and ESI-MS spectra of the synthesized polymers were analyzed. The ^{1}H NMR spectra of all the polymers revealed the absence of methyl protons peaks which is characteristic of the acetate as the initiating group in CIM. For instance the ^{1}H NMR spectra of polymers sampled after 8 and 32 h of polymerization ([ε-CL]/[**7**]) revealed only peaks associated with the polymers while the methyl protons associated with the acetate group were not observed (Figure 4.15). Similar observations were made in the ^{1}H NMR spectrum of poly(*meso*-LA) (Figure 4.16).

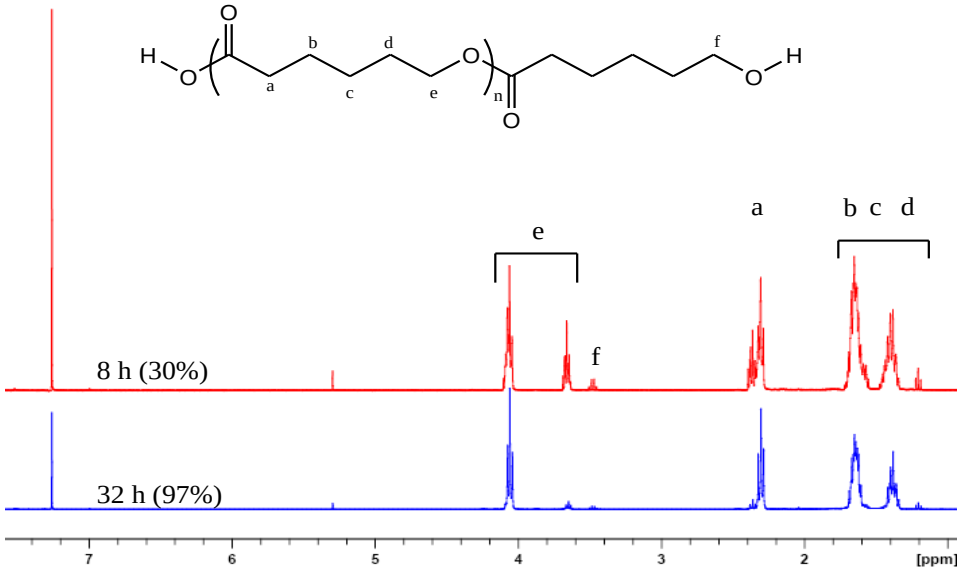

Figure 4.15: ^{1}H NMR spectrum of polycaprolactone ([ε-CL]/[**7**]) after 8 and 32 h

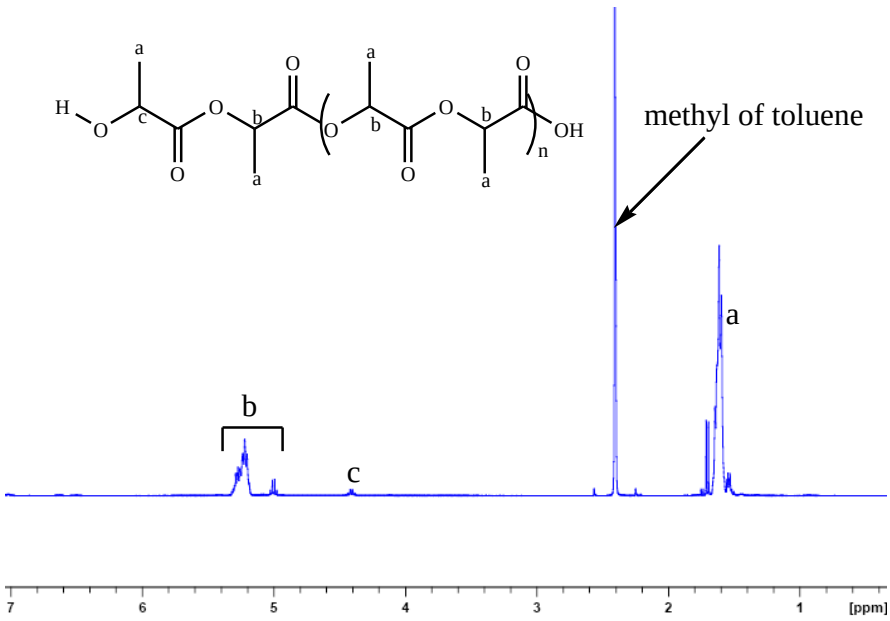

Figure 4.16: ^{1}H NMR spectrum of poly($_{D,L}$-lactide) polymerized in toluene at 110 ^{o}C after 95% conversion

Analysis of the ESI-MS spectra of these polymers supported ^{1}H NMR spectra analyses as no *m/z* fragments corresponding to the complexes were observed. The ESI-MS spectra of poly(ε-caprolactone) ([ε-CL]/[**7**]) and poly($_{D,L}$-lactide) exhibited signals corresponding to $HO(C_6H_{10}O)_nH{\cdot}Na^+$ and $HO(C_6H_8O_4)_nH{\cdot}Na^+$ respectively (Figure 4.17 and 4.18). The presence of –OH end group could be due to the presence of adventitious water molecules that are capable of initiating reactions. Furthermore, carboxylates are relatively weaker nucleophiles; hence, the more reactive –OH nucleophile is likely to initiate the reaction at the expense of the acetate group. This phenomenon has been reported by Pilone *et al.*[34]and Bourissou *et al.*[35]From this data, the reaction can thus be said to proceed through an activated-monomer mechanism. The proposed reaction mechanism is shown in Scheme 4-2.

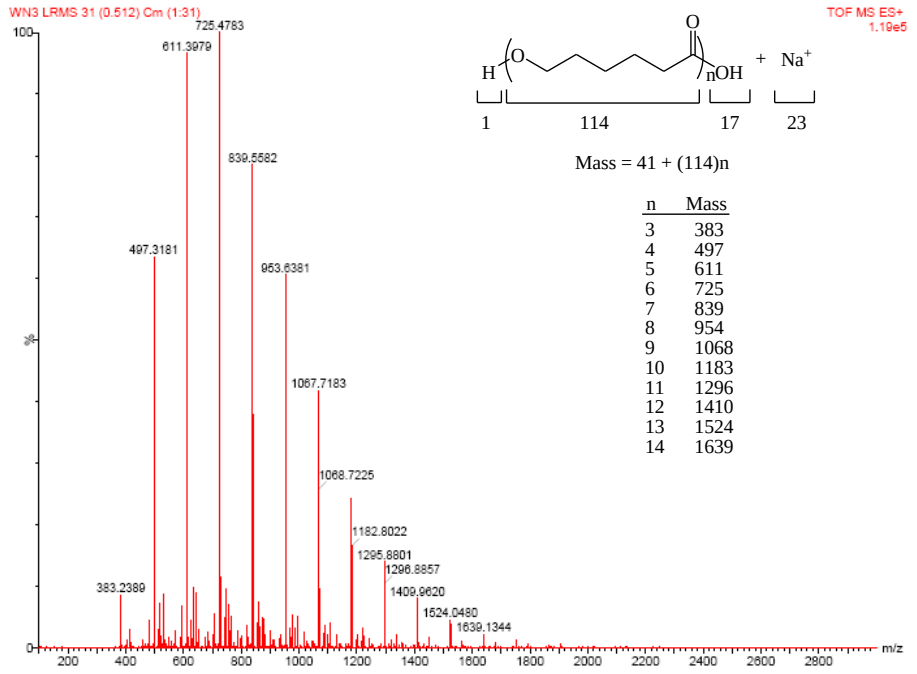

Figure 4.17: ESI spectrum of crude PCL after 8 h of reaction between ε-CL and complex **7** ([ε-CL]/[**7**] = 100:1) at 110 ^{o}C.

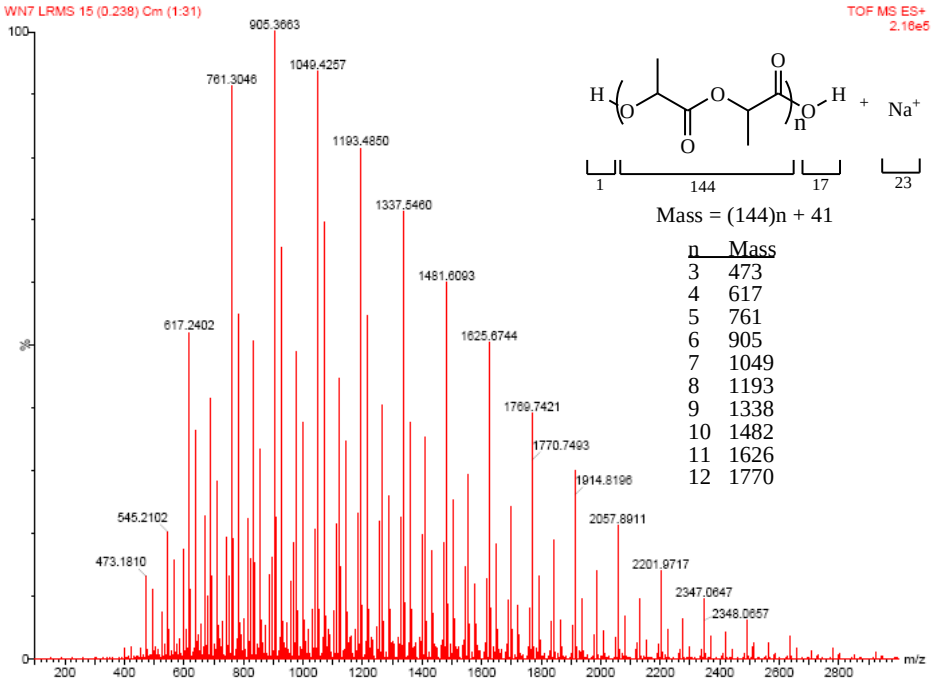

Figure 4.18: ESI spectrum of crude PLA ([$_{D,L}$-LA]/[**3**] = 100:1) polymerized at 110 ^{o}C.

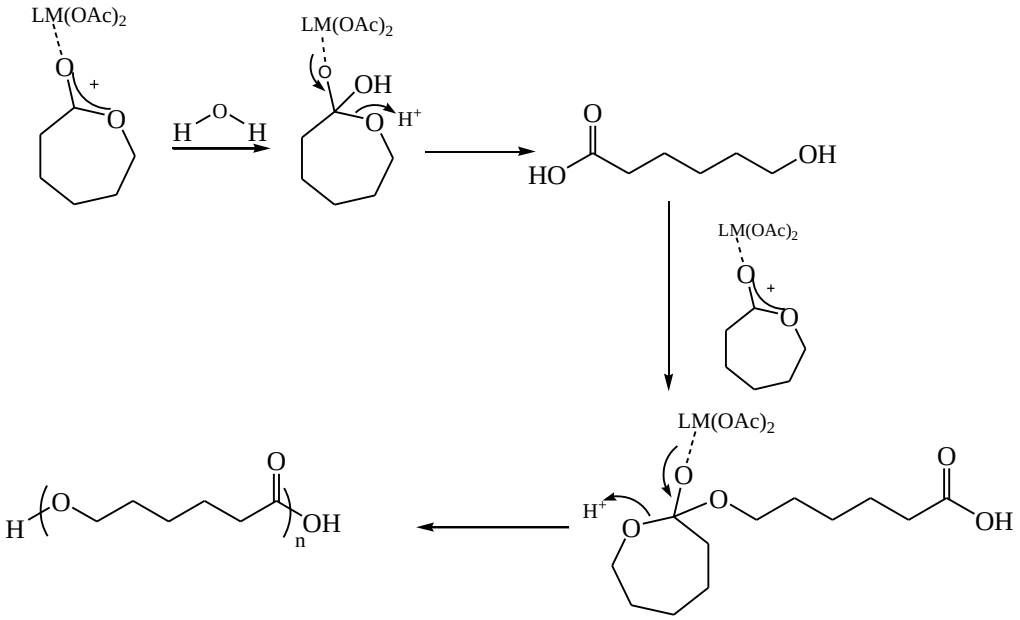

Scheme 4-2

4.3.8 Molecular weight and molecular weight distribution of PLA and PCL

The molecular weights and molecular weight distribution (PDI) for PCL and PLA obtained using **1, 3, 4**, **6, 7, 8** and **9** were determined by GPC analyses and compared with their corresponding theoretical values computed from ^{1}H NMR spectroscopy. Figure 4.19 shows a typical GPC trace obtained for both PCL and PLA at different time. The molecular weights obtained range from 3 299 g/mol to 8 104 g/mol. These values were much lower than the expected theoretical values of about 10 000 g/mol. For instance in the polymerization of ε-CL by **7**, the observed molecular weight at 97% ε-CL conversion was 8 104 g/mol compared to the expected molecular weight of 11 078 g/mol. This translates to 73% initiator efficiency (IE). Similar lower molecular weights of PLAs relative to the expected molecular weights were also measured. For instance, the expected molecular weight of PLA using **1** at [M]/[I] ratio of 50:1 after 96% conversion is 6 908 g/mol but the observed molecular weight was 2 472 g/mol corresponding to 36% initiator efficiency (IE).

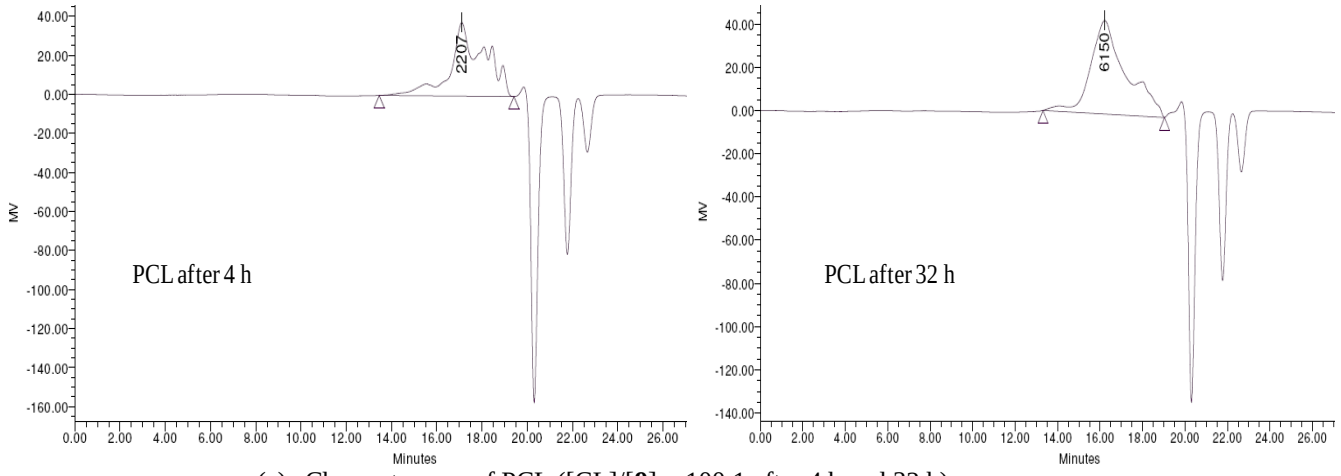

(a) Chromatogram of PCL ([CL]/[**9**] = 100:1 after 4 h and 32 h)

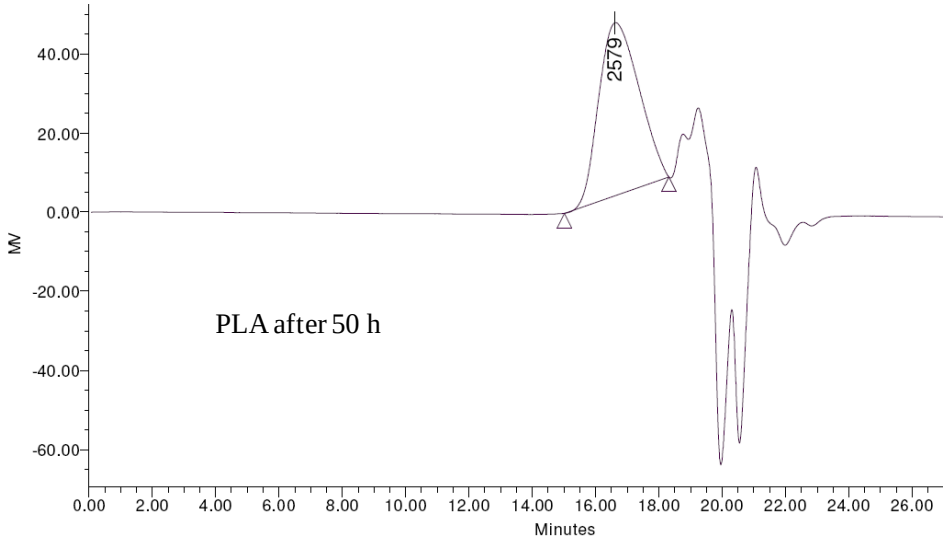

(b) Chromatogram of PLA ([*meso*-LA]/[**3**]) = 100:1 after 50 h

Figure 4.19: Typical GPC trace of PLA and PCL obtained at different times.

The polymers also exhibited moderate to high PDI values in the range of 1.29 to 3.97. The broadening of PDI values and low polymer molecular weights could be due to the existence of transesterification reaction during the polymerization as observed in other literature reports.[36] Transesterification occurs due to lack of control in the polymerization reaction leading to the random breakage of the polymer chains (Scheme 4.3).

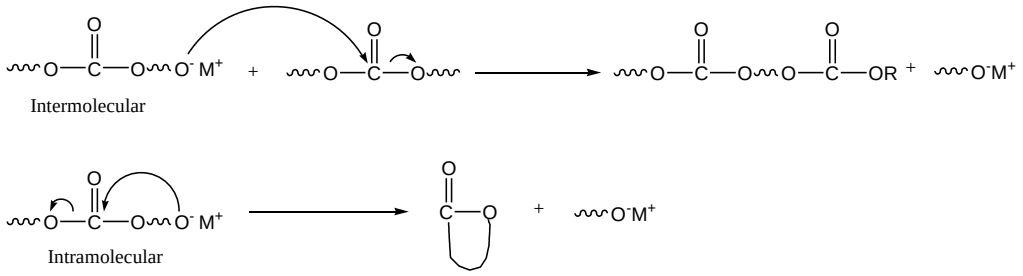

Scheme 4.3

To established the possibility of intermolecular and/ or intramolecular transeterification controlling the broad PDI, the ES-MS spectra of PCL ([CL]/[**7**]=100:1, 32 h) was analyzed as an example (Figure 4.20). The mass distribution of the polymers corresponds to the formula ($nCL+Na^+$+17) consistent with –OH end-cap. For example the *m/z* peak at 725 corresponds to (6 x 114.14+23+17). Evident in the spectrum are also smaller *m/z* peaks corresponding to ($nCL+Na^+$). For instance the *m/z* peak at 1164 corresponds to (10 x 114.14 + 23). This offset *m/z* peaks could be due to the possible formation of cyclic oligomers with loss of the water. The presence of oligomers indicates the occurrence of transesterification reaction giving rise to the broad PDI.

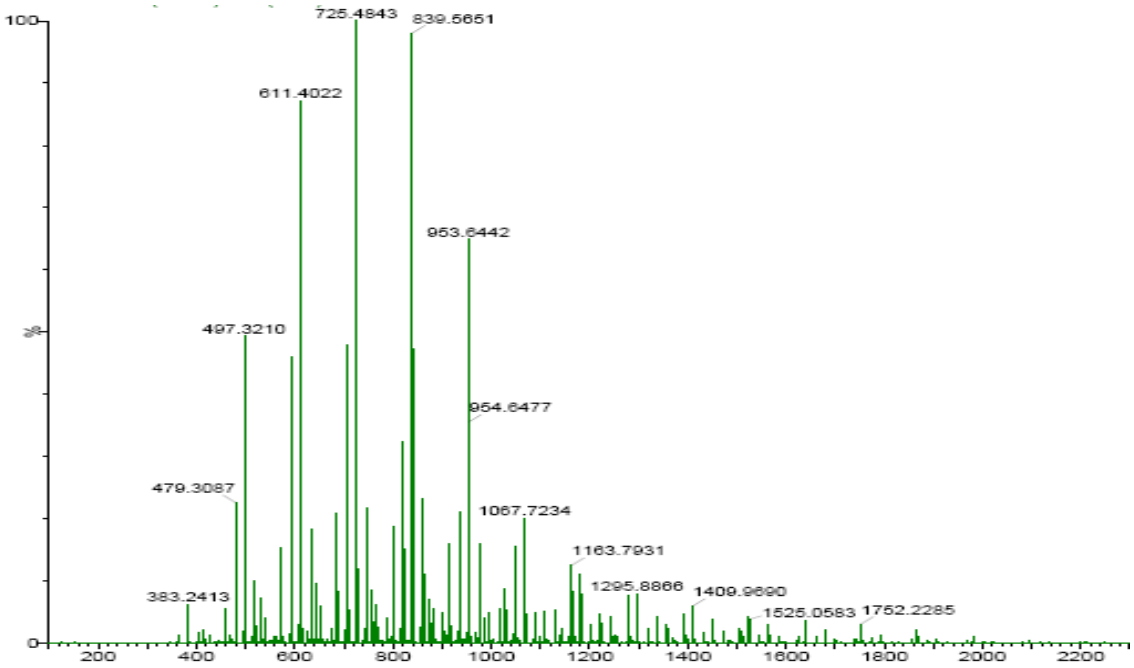

Figure 4.20: Mass spectrum of PCL ([CL]/[**7**]=100:1) after 32 h

The poor initiating tendencies of carboxylate groups as compared to alkoxides could also account for the low molecular weight and the broad molecular weight distribution of the polymers.[29] However, the reactions showed living polymerization characteristics as depicted in the linearity of the plots of experimental molecular weight vs % conversion (Figure 4.21).

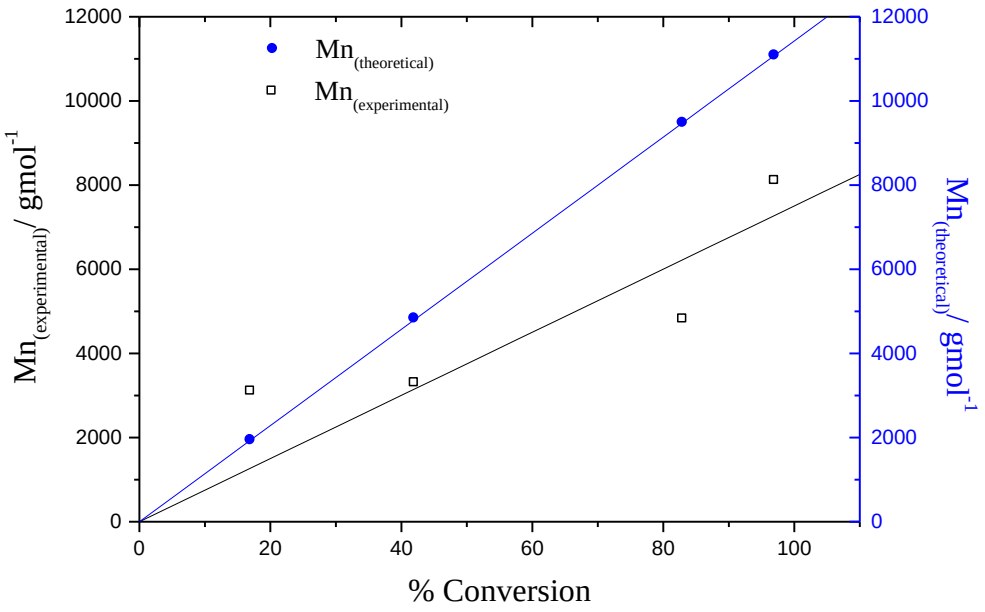

Figure 4.21: Plot of Mn^{GPC} vs % conversion showing living polymerization of PCL

4. 3.9 Microstructural analyses of Polylactides

The stereochemistry and polymer tacticity of the synthesized poly(*meso*-lactide) and poly($_L$-lactide) were determined by homonuclear decoupled ^{1}H NMR and ^{13}C NMR spectroscopy. The methine region of the homonuclear decoupled ^{1}H NMR of poly(*meso*-lactide) and poly($_L$-lactide) are presented in Figure 4.22 while their respective ^{13}C NMR spectra are shown in Figure 4.23. The single resonance peak observed in the homonuclear decoupled ^{1}H NMR spectrum of poly($_L$-lactide) obtained from catalyst **1** at [M]/[I]=100 is characteristic of *iii* signal.

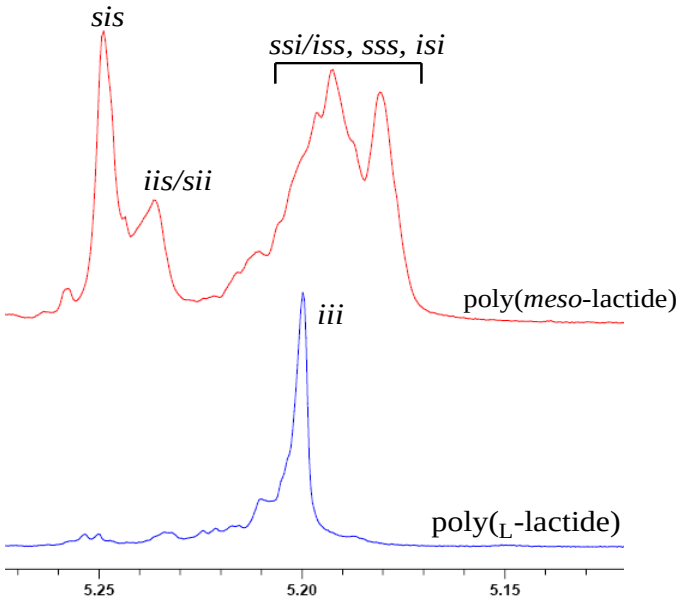

Figure 4.22: Methine resonance in homonuclear decoupled ^{1}H NMR spectra of PLAs prepared from respective monomer with **1** at 110 ^{o}C

Similarly, single resonance peak was also observed in the corresponding ^{13}C NMR spectrum. These observations connote the polymerization of $_{L}$-lactide by **8** to give predominantly isotactic polylactide which is in tandem with the reports of Jiang *et al.*[37] and Dove *et al.*[38] The observation of a single resonance peak, *ii* or *iii*, is due to the identical chiral centers in the monomer hence during polymerization, this configuration is maintained (Scheme 4-4).[39]

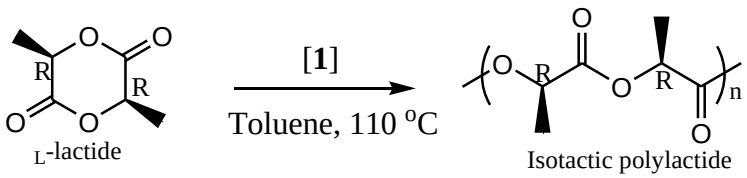

Scheme 4-4

The poly(*meso*-lactide) on the other hand exhibited five tetrads, *sss*, *ssi*, *iss*, *sis* and *isi*, in the homonuclear decoupled ^{1}H NMR spectrum (Figure 4.22). The tacticity of the polymers were also determined by comparing and assigning peaks in the methine region according to other

literature results[40] taking into account the peak intensities since they enable the prediction of the preferred mode of monomer addition to the growing chain end.[41]

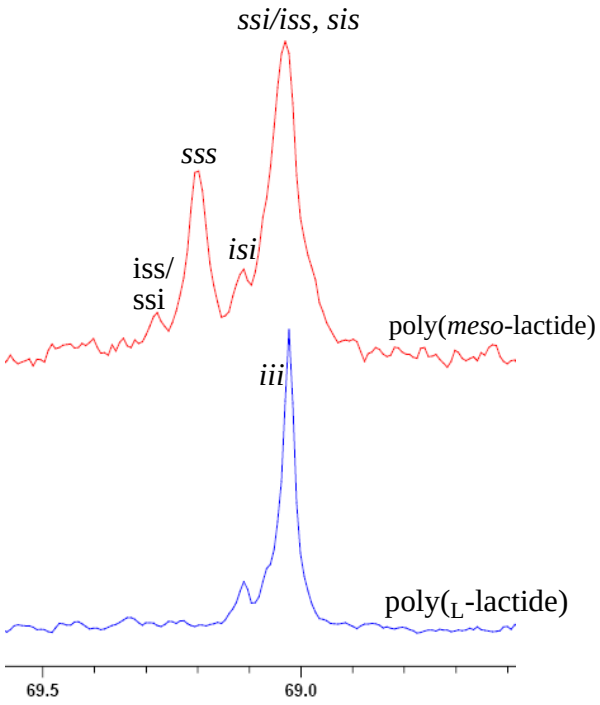

Figure 4.23: Methine carbon signals in the ^{13}C NMR spectra of PLAs prepared from respective monomer with **1** at 110 ^{o}C

The intensities of the *iss/ssi* tetrads relative to *sss* and *sis* peaks in the spectra points to the production of atactic PLA. For instance in a heterotactic and sydiotactic poly(*meso*-lactide) reported in literature, only two (2) well resolved *sss* and *sis* tetrads are normally observed.[40,42] The formation of atactic PLAs from *meso*-lactide is due to the random nature and the lack of stereoselectivity of the catalyst towards the $_{D,L}$-LA monomer. Control of polymer stereochemistry and stereo regularity can be achieved by employing chiral catalysts. This was demonstrated by using optical N-heterocyclic carbene catalysts in the polymerization of *meso*-lactic to give predominantly heterotactic PLA.[38] Ovitt and Coates also reported the use chiral aluminum and yttrium alkoxide to produce heterotactic and syndiotactic PLAs from *meso*-lactide.[43]

4.4 Conclusion

In conclusion, the synthesized complexes formed active catalysts towards the ROP of LA and ε-CL of which the zinc-based complexes showed higher catalytic activities compared to their copper analogues. The ligand architecture was also found to influence the catalytic activities of the complexes. Complexes bearing electron-withdrawing groups exhibited lower catalytic activities toward the LA and ε-CL polymerization compared to corresponding complexes bearing electron-donating groups. We have also shown that mononuclear complexes were more active than the corresponding binuclear catalysts. This suggest that less crowding around the metal centre by the less bulky acetate group could be enhancing monomer coordination to the metal centre. The nature of the monomer also affected the activities of the complexes. LA monomer showed higher reactivity compared to the ε-CL in polymerization reaction.

The polymerization of LA and ε-CL proceeds *via* a pseudo-first order reaction with respect to the monomers and the polymerization mechanism was found to be activated-monomer pathway with adventitious water initiating the reaction. The rate of polymerization reactions was influenced by the type of solvent and temperature. A significant change in the rate of polymerization was observed on using methanol as solvent for the polymerization reaction.

The polymers produced had molecular weights ranging between 2 000 to 12 700 g/mol which were lower than the expected molecular weights. The molecular weight distributions of the polymers were also broad ranging from 1.29 to 3.64. The low molecular weight and broad polydispersity indices were as a result of the poor nature of the carboxylate initiators. The polymerization of $_{L}$-lactide and $_{D,L}$-lactide produced isotactic and atactic polylactides

respectively. The formation of atactic polylactide from $_{D,L}$-lactide implied the complexes lacked control of polymer stereochemistry.

References

1 (a) Luckachan, G.E.; Pillai, C. K. S. *J. Polym. Environ.* **2011,** *19*, 637–676. (b) Crabtree, G.W.; Dresselhaus, M.S.; Buchanan, M.V. *Phys. Today* **2004**, *54*, 39 – 44.

[2](a) Azor, L.; Bailly, C.; Brelot, L.; Henry, M.; Mobian, P.; Dagorne, S. *Inorg. Chem*. **2012,** *51*, 10876-10883. (b) Tian, H.;Tang, Z.; Zhuang, X.; Chen, X.;Jing, X. *Prog. Polym Sci*, **2012**, *37*, 237– 280. (c) Davidson, M.G.; O'Hara, C.T.; Jones, M.D.; Keir, C.G.; Mahon, M.F.; Kociok-Kohn, G. *Inorg. Chem*. **2007**, *46*, 7686-7688. (d) Chiellini, E.; Solaro, R. *Adv. Mater.*, **1996**, *8*, 305-313. (e) Albertsson, A.-C.; Varma, I.K. *Biomacromolecules*, **2003**, *4*, 1466-1486.

[3] (a) Wu, J.; Pan, X.; Tang, N.; Lin, C.-C. *Eur. Polym. J.* **2007**, *43*, 5040 – 5046 and references therein. (b) Wu, J.; Yu, T.-L.; Chen, C.-T.; Lin, C.-C. *Coord. Chem. Rev.* **2006**, *250*, 602 – 626. (c) O'Keefe, B. J.; Hillmyer, M. A.; Tolman, W. B. *J. Chem. Soc., Dalton Trans* **2001**, 2215–2224. (d) Labet, M.; Thielemans, W. *Chem. Soc. Rev.* **2009**, *38*, 3484–3504.

[4] (a) Aubrecht, K. B.; Hillmyer, M. A.; Tolman, W. B. *Macromolecules* **2002**, *35*, 644 - 650. (b) Kowalski, A.; Libiszowski, J.; Duda, A.; Penczek, S. *Macromolecules* **2000**, *33*, 1964 - 1971. (c) Dove, A. P.; Gibson, V. C.; Marshall, E. L.; Rzepa, H. S.; White, A. J. P.; Williams, D. J. *J. Am. Chem. Soc.* **2006**, *128*, 9834 - 9843. (d) Celiz, A. D.; Scherman, O. A. *Macromolecules*, **2008**, *41*, 4115–4119. (e) Degirmenci, M.; Izgin, O. Yagci, Y. *J. Polym. Sci., Part A: Polym. Chem.* **2004**, *42*, 3365–3372.

[5] (a) W. Yao, Y. Mu, A. Gao, Q. Su, Y. Liu and Y. Zhang, *Polymer* **2008**, *49*, 2486–2491. (b) Huang, C.-H.; Wang, F.-C.; Ko, B.-T.; Yu, T.-L.; Lin, C.-C. *Macromolecules* **2001**, *34*, 356–361. (c) Montaudo, G.; Montaudo, M. S.; Puglisi, C.; Samperi, F.; Spassky, N.; Borgne, A. L.; Wisniewski, M. *Macromolecules* **1996**, *29*, 6461- 6465. (d) Liu, Y. C.; Ko, B. T.; Lin, C. C. *Macromolecules* **2001**, *34*, 6196 - 6201.

[6] (a) Davidson, M. G.; Jones, M. D.; Lunn, M. D.; Mahon, M. F. *Inorg. Chem.* **2006**, *45*, 2282–2287. (b) Chmura, A. J.; Davidson, M. G.; Jones, M. D.; Lunn, M. D.; Mahon, M. F. *Dalton Trans.* **2006**, 887–889. (c) Gregson, C. K.; Blackmore, I. J.; Gibson, V. C.; Long, N. J.; Marshall, E. L.; White, A. J. P. *Dalton Trans*. **2006**, 3134- 3140. (d) Kim, S. H.; Kim, D. J.; Go, M. J.; Ko, Y. S.; Lee, J.; Kim, Y. *Dalton Trans.* **2012**, *41*, 11619 - 11628.

[7] (a) Chmura, A. J.; Davidson, M. G.; Jones, M. D.; Lunn, M. D.; Mahon, M. F.; Johnson, A. F.; Khunkamchoo, P.; Roberts, S. L.; Wong, S. S. F. *Macromolecules* **2006**, *39*, 7250–7257. (b) Jones, M. D.; Davidson, M. G.; Kociok-Kohn, G. *Polyhedron* **2010**, *29*, 697-700. (c) Whitelaw, E. L.; Jones, M. D.; Mahon, M. F.; Kociok-Kohn, G. *Dalton Trans.* **2009**, 9020-9025. (d) Ning, Y.; Zhang, Y.; Rodriguez-Delgado, A.; Chen, E. Y.-X. *Organometallics* **2008**, *27*, 5632 – 5640.

[8] (a) Gorczynski, J. L.; Chen, J.; Fraser, C. L. *J. Am. Chem. Soc.* **2005**, *127*, 14956-14957. (b) O'Keefe, B. J.; Breyfogle, L. E.; Hillmyer, M. A.; Tolman, W. B. *J. Am. Chem. Soc.* **2002**, *124*, 4384- 4393.

[9] (a) Chen, C.T.; Chan, C.Y.; Huang, C.A.; Chen, M.T.; Peeng, K.F. *Dalton Trans.* **2007**, 4073 - 4078. (b) Gao. A.-H.; Yao, W.; Mu, Y.; Gao, W.; Sun, M.-T.; Su, Q. *Polyhedron* **2009**, *28*, 2605 - 2610. (c) Zhang, C.; Wang, Z.-X. *J. Organomet. Chem.* **2008**, *693*, 3151-3158. (d) Bunge, S. D.; Lance, J. M.; Bertke, J. A. *Organometallics* **2007**, *26*, 6320-6328. (d) Lian, B.; Thomas, C. M.; Casagrande Jr, O. L.; Lehmann, C. W.; Roisnel, T.; Carpentier, J.-F. *Inorg. Chem.* **2007**, *46*, 328-340. (e) Jensen, T. R.; Schaller, C. P.; Hillmyer, M. A.; Tolman, W. B. *J. Organomet. Chem.* **2005**, 5881-5891.

[10] (a) John, A.; Katiyar, V.; Pang, K.; Shaikh, M. M.; Nanacati, H.; Hemant, G.; Ghosh, P. *Polyhedron* **2007**, *26*, 4033-4044 (b) Whitehorne, T. J. J.; Schaper, F. *Chem. Commun.* **2012**, *48*, 10334–10336.

[11] (a) Mazzeo, M.; Tramontano, R.; Lamberti, M.; Pilone, A.; Milione, S.; Pellecchia, C. *Dalton Trans.* **2013**, *42*, 9338–9351. (b) Agarwal, S.; Karl, M.; Dehnicke, K.; Seybert, G.; Massa, W.; Greiner, A. *J. Appl. Polym. Sci.* **1999**, *73*, 1669–1674.

[12] (a) Zhang, J.; Jian, C.; Gao, Y.; Wang, L.; Tang, N.; Wu, J. *Inorg. Chem.* **2012**, *51*, 13380−13389. (b) Chang, Y.-N.; Liang, L.-C. *Inorg. Chim. Acta* **2007**, *360*, 136 - 142.

[13](a) Rong, G.; Deng, M.; Deng, C.; Tang, Z.; Piao, L.; Chen, X.; Jing, X. *Biomacromolecules* **2003**, *4*, 1800–1804. (b) Ejfler, J.; Kobylka, M.; Jerzykiewicz, L. B.; Sobota, P. *Dalton Trans.* **2005**, 2047 – 2050.

[14] (a) Mata-Mata, J.L.; Gutierrez, J. A.; Paz-Sandoval, M. A.; Madrigal, A. R.; Martinez-Richa, A. *J. Polym. Sci., Part A: Polym. Chem.* **2006**, *44*, 6926-6942. (b) Dubois, Ph.; Jacobs, C.; Jerome, R.; Teyssie, Ph. *Macromolecules* **1991**, *24*, 2266-2270.

[15] Ojwach, S.O.; Okemwa, T.T.; Attandoh, N.W.; Omondi, B. *Dalton Trans.* **2013**, *42*, 10735–10745.

[16] Chisholm, M. H.; Eilerts, N.W.; Huffman, J.C.; Iyer, S.S.; Pacold, M.; Phomphrai, K. *J. Am. Chem. Soc.* **2000**, *122*, 11845-11854.

[17] Alcazar-Roman, L. M.; O'Keefe, B. J.; Hillmyer, M. A.; Tolman, W. B. *Dalton Trans.* **2003**, 3082 – 3087.

[18] Chen, H.-Y.; Huang, B.-H.; Lin, C.-C. *Macromolecules* **2005,** *38*, 5400-5405.

[19] Darensbourg, D. J.; Karroonnirun, O. *Macromolecules* **2010**, *43*, 8880–8886.

[20] Huang, Y.; Wang, W.; Lin, C.-C.; Blake, M.P.; Clark, L.; Schwarz, A.D.; Mountford, P. *Dalton Trans.* **2013**, *42*, 9313–9324.

[21] Cayuela, J.; Bounor-Legare, V.; Cassagnau, P.; Michel, A. *Macromolecules* **2006**, *39*, 1338-1346.

[22] Chamberlain, B.M.; Jazdzewski, B.A.; Pink, M.; Hillmyer, M.A.; Tolman, W.B. *Macromolecules* **2000,** *33*, 3970-3977.

[23] Zhong, Z.; Dijkstra, P.J.; Feijen, J. *J. Am. Chem. Soc.* **2003**, *125*, 11291 - 11298

[24] Pilone, A.; Lamberti, M.; Mazzeo, M.; Milione, S.; Pellecchia, C. *Dalton Trans.* **2013**, *42*, 13036–13047.

[25] Williams, C.K.; Brooks, N.R.; Hillmyer, M.A.; Tolman, W.B. *Chem. Commun.* **2002**, 2132–2133.

[26] Bouyahyi, M.; Ajellal, N.; Kirillov, E.; Thomas, C. M.; Carpentier, J. F. *Chem.–Eur. J.* **2011**, *17*, 1872–1883.

[27] (a) Sung, C.-Y.; Li, C.-Y.; Su, J.-K.; Chen, T.-Y.; Lin, C.-H.; Ko, B.-T. *Dalton Trans.* **2012**, *41*, 953–961. (b) Wang, L.; Ma, H. *Dalton Trans.* **2010**, *39*, 7897–7910. (c) Song, S.; Zhang, X.; Ma, H.; Yang, Y. *Dalton Trans.* **2012**, *41*, 3266–3277. (d) Sarazin, Y.; Liu, B.; Roisnel, T.; Maron, L.; Carpentier, J.-F. *J. Am. Chem. Soc.* **2011**, *133*, 9069–9087.

[28] Chamberlain, B.M.; Cheng, M.; Moore, D.R.; Ovitt, T.M.; Lobkovsky, E.B.; Coates, G.W. *J. Am. Chem. Soc.* **2001**, *123*, 3229-3238.

[29] Chisholm, M. H.; Gallucci, J.; Phomphrai, K. *Inorg. Chem.* **2002**, *41*, 2785−2794.

[30] Wheaton, C. A.; Hayes, P.G. *Chem. Commun.* **2010**, *46*, 8404–8406.

[31] Williams, C.K.; Breyfogle, L.E.; Choi, S.K.; Nam, W. *J. Am. Chem. Soc.* **2003**, *125*, 11350-11359.

[32] Dubois, Ph.; Ropson, N.; Jerome, R.; Teyssie, Ph. *Macromolecules* **1996,** *29*, 1965-1975

[33] Ajellal, N.; Carpentier, J.-F. Guillaume, C.; Guillaume, S.M.; Helou, M.; Poirier, V.; Sarazin, Y.; Trifonov, A. *Dalton Trans.* **2010**, *39*, 8363–8376.

[34] Pilone, A.; Lamberti, M.; Mazzeo, M.; Milione, S.; Pellecchia, C. *Dalton Trans.* **2013**, *42*, 13036–13047.

[35] Bourissou, D.; Martin-Vaca, B.; Dumitrescu, A.; Graullier, M.; Lacombe, F. *Macromolecules* **2005**, *38*, 9993-9998.

[36] (a) Song, S. Ma, H.; Yang, Y. *Dalton Trans.* **2013**, *42*, 14200–14211. (b) Petrus, R.; Sobota, P. *Dalton Trans.* **2013**, *42*, 13838–13844.

[37] Jiang, W.; Huang, W.; Cheng, N.; Qi, Y.; Zong, X.; Li, H.; Zhang, Q. *Polymer* **2012**, *53*,5476-5479.

[38] Dove, A.P. Li, H.; Pratt, R. C.; Lohmeijer, B.G.G.; Culkin, D.A.; Waymouth, R.M.; Hedrick, J.L. *Chem. Commun.* **2006**, *27*, 2881–2883

[39] Chisholm, M.H.; Iyer, S.S.; Matison, M.E.; McCollum, D.G.; Pagel, M. *Chem. Commum.* **1997**, *20*, 1999-2000.

[40] (a) Thakur, K. A. M.; Kean, R. T.; Zell, M. T.; Padden, B. E.; Munson, E. J. *Chem. Commun.* **1998**, 1913-1914. (b) Thakur, K. A. M.; Kean, R. T.; Hall, E. S.; Kolstad, J. J.; Munson, E. J. *Macromolecules* **1998**, *31*, 1487-1494.

[41] Thakur, K. A. M.; Kean, R. T.; Hall, E. S.; Kolstad, J. J.; Lindgren, T.A. *Macromolecules* **1997**, *30*, 2422-2428.

[42] (a) Kricheldorf, H.R. *Chemosphere* **2001**, *43*, 49-45. (b) Chamberlain, B. M.; Cheng, M.; Moore, D.R.; Ovitt, T.M.; Lobkovsky, E.B.; Coates, G.W. *J. Am. Chem. Soc.* **2001,** *123*, 3229-3238. (c) Kasperczyk, J.E. *Polymer* **1999**, *40*, 5455-5458.

[43] Ovitt, T.M.; Coates, G.W. *J. Am. Chem. Soc.*, **2002**, 1316-1326.

Chapter Five

Summary and future perspective

5.1 Summary

In conclusion, this work reports the syntheses and structural characterization of (benzoimidazolylmethyl)amine ligand derivatives and their respective Zn(II) and Cu(II) carboxylate complexes. The ligands form mononuclear and dinuclear Zn(II) and Cu(II) carboxylate complexes in which the ligand is monodentate and coordinates *via* the benzimidazole N-atom. The nature of the carboxylate anion influences the coordination chemistry of the resultant Zn(II) complexes. Whereas, the acetate complexes are mononuclear complex in which the Zn(II) metal is coordinated by two ligand units and two monodentate acetate anions, the benzoate compounds form binuclear paddle-wheel structures. EPR analyses of the copper complexes confirmed retention of the solid state dimeric paddle-wheel structures in solutions.

All the complexes were tested for the ring opening polymerization of lactides and ε-caprolactone and were observed to be active towards the polymerization of these cyclic monomers. The activities of the complexes are greatly influenced by the type of metal centre with zinc complexes showing higher catalytic activities compared to their analogous copper complexes. The ligand structure also affected the overall activity of the complexes. The catalytic activities of complexes with electron-withdrawing groups on the ligand motifs were comparatively lower than those bearing electron-donating groups. Steric conditions around the active metal centre were also observed to influence the catalytic activity of the complexes. The complexes with less sterically demanding acetate anions were more active than their analogous complexes containing bulkier benzoate groups. All the polymerization reactions proceeded via a pseudo-first order reaction pathway with respect to the monomer.

The complexes exhibited relatively lower initiator efficiencies. Moderate molecular weights ranging between 2000 to 12700 g/mol of the polymers were obtained. The lack of control of the polymerization reactions in addition to transesterification reactions resulted in polymers with broad molecular weight distributions (PDI=1.29-3.64). The complementary analysis of ^{1}H NMR and MS-ESI spectra of the polymers revealed that the polymerization of the lactides and ε-caprolactone proceeded via an activated monomer mechanism. The polymerization of *meso*-lactide gave rise to predominantly atactic polylactides whiles $_{L}$-lactide produced mainly isotactic polymers. It can be inferred from the tacticity of the poly(*meso*-lactide) that the complexes lack control of over the stereosequence of the polymers.

5.2 Recommendations for future work

This study revealed that biocompatible Zn(II) and Cu(II) complexes were active towards the ROP of lactides and lactones. However, the use of carboxylate initiators resulted in low initiator efficiency and low polymer molecular weights. With the catalytic activity increasing in the presence of alcohols, the design of complexes with an alkoxide initiating groups will go a long way in improving the catalytic efficiency and improving the molecular weight of the polymers. Therefore as part of the future research, we intend to design alkoxide complexes of zinc and copper and test their catalytic activities towards the ring opening polymerization of lactides and ε-caprolactone.